# PROBING NEUROCHEMISTRY WITH FAST-SCAN CYCLIC VOLTAMMETRY

Pavel Takmakov

A dissertation submitted to the faculty of the University of North Carolina at Chapel Hill in partial fulfillment of the requirements for the degree of Doctor of Philosophy in the Department of Chemistry

Chapel Hill
2011

Approved by:

R. Mark Wightman

Royce W. Murray

Nanncy L. Allbritton

Max L. Berkowitz

Gregory S. McCarty

© 2011
Pavel Takmakov
ALL RIGHTS RESERVED

## ABSTRACT

Pavel Takmakov

**PROBING NEUROCHEMISTRY WITH FAST-SCAN CYCLIC**

(under the direction of R. Mark Wightman)

"Fast-scan cyclic voltammetry (FSCV) with carbon-fiber microelectrodes is a prominent analytical technique for rapid and sensitive detection of electrochemically active analytes in mammalian brain. In recent years this technique became very popular among neuroscientists. However, many improvements for FSCV are possible. Chapter 1 introduces the technique and provides brief description of recent improvements in fast-scan cyclic voltammetry.

During voltammetric experiments, potential applied to electrodes changes carbon surface. Chapter 2 describes investigation of the changes induced by waveforms with anodic potential limits of 1.0 V, 1.3 V and 1.4 V. Instrumental methods of analysis such as XPS, AFM and SEM together with electrochemical studies were used. It was observed, that for waveforms with high anodic potential (1.3 V and 1.4 V) carbon electrode surface continuously oxidizes and etches away. Thus, the electrode surface which has surface groups that promote adsorption of catechols is constantly renewed. A benefit of surface renewal is sustainability to chemical fouling.

Carbon electrode surface has electrochemically active chemical groups which are oxidized and reduced during voltammetric potential ramps. Electrochemical reactions for these groups involve protons, thus changes in pH of solution generate characteristic cyclic voltammograms. Hence, FSCV can be used to sample rapid pH fluctuations in the brain that are associated with metabolism and changes in the cerebral blood flow. However, cyclic voltammograms for pH changes recorded in brain in vivo and in the flow cell have different shapes, which compromises the identity of pH signal. Chapter 3 describes investigation of the peaks in cyclic voltammogram for pH which led to the conclusion that adsorption of electrochemically inert species to electrode surface is responsible for the interference and the mismatch. Identity of pH signal in brain in vivo was confirmed by inducing acidosis by increasing concentration of carbon dioxide in breathing mixture (hypercapnia). Acidic pH shift with characteristic cyclic voltammogram was recorded with FSCV in hypercapnia.

Traditionally, FSCV experiments are done with a single carbon-fiber microelectrode. These electrodes are produced manually and they are very fragile. Chapter 4 describes alternative microfabricated microelectrode arrays (MEAs) which are more robust than glass-encased carbon fibers and can be produced using batch fabrication methods. Microelectrodes in MEAs are distant from each other, thus heterogeneity in analyte concentration such as difference in dopamine release in the

brain can be studied. Also, microelectrodes in the array are independently addressable which means that multiplexed detection of different analytes in brain can be performed simultaneously.

Instrumentation for FSCV experiments in freely moving animals is custom made which limits the dissemination of this technique. Chapter 5 describes instrumentation for FSCV experiments for combined electrochemical and electrophysiological measurements in details. All electronic components are documented and layouts of electronic circuits are provided in this chapter.

Recording of brain functions with multiple electrodes is beneficial in providing information about interconnections of different brain regions as well as synchronization of their activity. This approach was limited to electrophysiological recordings. Chapter 6 describes recordings of endogenous and pharmacologically induced activity of dopaminergic neurons in separate brain hemispheres of anesthetized rat. Synchronization of activity of dopaminergic neurons between two separate and symmetrical systems is observed. Possible link to slow wave oscillations that occur in brain cortex during sleep is discussed."

To My Family

**ACKNOWLEDGEMENTS**

Many people have contributed to my work. First, I would like to thank my PhD advisor, Dr. R. Mark Wightman, who guided me through my research endeavors and helped me to develop into a scientist. Dr. Wightman has always been available for advice and support. He was a great source of inspiration and I'm very grateful for his mentoring.

I want to thank my wife, Marina Krylova, for her continuous support and assistance. Marina has demonstrated a lot of patience towards my inclination to spend extra time in the lab instead of spending it with her at home.

I want to thank my immediate and extended family for being supportive during period of my study. I'm glad that they accepted the path that I chose and supported me all the way through.

I highly appreciate collaboration with many excellent people in the lab. First, I want to thank Dr. Richard B. Keithley and Dr. Matthew K. Zachek. I appreciate their contribution to my work and enjoyed many hours of inspirational discussions that we had. I want to thank Collin McKinney for providing me with valuable advices and helping me to learn more about circuits and electronics, as well as for helping with instruments for my experiments. I want to thank Dr. Jinwoo Park for his guidance and support in experiments with animals. I appreciate my collaboration with Dr. Gregory McCarty and his contribution to design of microfabricated devices that I used and his help with the publications.

I would like to thank postdoctoral fellows Dr. Parastoo Hashemi, Dr. Zoe McElligott-Kash and Dr. Nina Owesson-White for their support, advices and discussions.

Dr. Carrie Donley and CHANL facility members have been extremely helpful with instrumentation for surface analysis and consultations. I appreciate their contribution very much.

I want to thank my coworkers, Jenny Ariansen, Anna Belle, Elizabeth Bucher, Elyse Dankoski, Adam Dengler and Paul Walsh, for assistance with the experiments and support in and beyond the lab.

I would like to thank former Wightman Lab members who formed my extended "scientific family" and were "role models" for me: Dr. Nii Addy, Dr. Evgeny Budygin, Dr Michael Heien, Dr. Natalie Herr, Dr. Charlie Miller, Dr. Jelena Petrovic, Dr. Paul Phillips. I'm grateful for all insightful discussions that we had every year at Pittsburgh Conference and Society for Neuroscience meetings.

I want to thank faculty members at the Department of Chemistry and at University of North Carolina Neuroscience Center for answering many of my questions and dramatically expanding horizons of my knowledge.

Also, I want to thank my friends, Dr. Pavel Aronov (Stanford University) and Dr. Ivan Vlassiouk (Oak Ridge National Laboratory), for many valuable scientific discussions and advices.

I appreciate financial support from NIH, Eli Lilly and Eastman Chemical Company that made this work possible.

## TABLE OF CONTENTS

List of Figures……..xiii

List of Abbreviations and Symbols……...xv

Chapter 1. Advancements in Probing Neurochemistry with Fast-Scan cyclic Voltammetry.....1

Introduction.....1

Dynamic State of Carbon Surface and regeneration of Adsorption Sites .....8

Measurement of pH in Brain In Vivo and Interference from Adsorption.....12

Microelectrode Arrays for voltammetric Measurements in Brain In Vivo.....15

Dissertation Outline .....19

References.....20

Chapter 2. Carbon Microelectrodes with a Renewable Surface.....25

Introduction.....25

Materials and Methods .....27

Chemicals. .....27

Fabrication of Carbon Fiber Microelectrodes..…..28

Fabrication of PPF Electrodes.....28

Electrochemical Experiments.. .....29

Flow Injection Apparatus. .....31

Electrochemical Modification of PPF Electrodes.....31

XPS Analysis ..... 31

AFM Imaging ..... 32

Scanning Electron Microscopy ..... 33

Optical Microscopy ..... 33

Data Analysis ..... 33

Results and Discussion ..... 34

Effect of Applied Potential on Background Current of Carbon Microelectrodes ..... 34

Characterization of Surface Effects of Potential Cycling on PPF Electrodes ..... 37

Physical Changes Caused by Electrochemical Potential Limits ..... 40

Increased Adsorption of Catecholamines Resulting from Oxidative Etching of Carbon Fiber Microelectrodes ..... 46

Recovery of Fouled Carbon Microelectrodes by Overoxidative Surface Renewal. ..... 50

Conclusions. ..... 52

References ..... 54

Chapter 3. Characterization of Local pH Changes in Brain Using Fast-Scan Cyclic Voltammetry with Carbon Microelectrodes ..... 59

Introduction ..... 59

Materials and Methods ..... 63

Chemicals. ..... 63

Fabrication of Carbon Fiber Microelectrodes ..... 63

Electrochemical Experiments ..... 64

Flow Injection Apparatus.. ..... 65

Animal Experimentation ..... 65

Results and Discussion ..... 67

Characterization of the Peaks in Cyclic Voltammogram for pH change. ..... 67

Capacitive Contributions to the Cyclic Voltammogram for pH change. ..... 70

Background-subtracted Cyclic Voltammograms due to the Adsorption of Electrochemically Inert Species. ..... 72

Distortion of Cyclic Voltammograms for pH change due to Adsorption of Electrochemically Inert Species. ..... 78

Distortion of Cyclic Voltammogram for pH change from DOPAC. ..... 82

Verification of FSCV pH Signal with Acidosis Induced by verification of pH signal with Acidosis Induced by Hypercapnia. ..... 85

Conclusions ..... 88

References ..... 89

Chapter 4. Carbon Microelectrode Arrays Compatible with Fast-Scan Cyclic Voltammetry. ..... 94

Introduction ..... 92

Materials and Methods ..... 96

Chemicals and drugs ..... 96

Fabrication of PPF Miroelectrode Arrays of MEA 1.0 Generation. ..... 96

Fabrication of PPF Miroelectrode Arrays of MEA 2.0 Generation. ..... 97

Data Acquisition. ..... 98

Flow Injection Apparatus. ..... 99

Experiments in Animals. ..... 100

Results and Discussion ..... 100

Design of Microfabricated Microelectrode Arrays. ..... 100

Multiplexed Detection with Individually Addressable Microelectrode Arrays ..... 100

Microelectrode Arrays for Multisite Recording of Dopamine Release in Anesthetized Animals ..... 112

Conclusions ..... 114

References ..... 115

Chapter 5. Instrumentation for Fast-Scan Cyclic Voltammetry Combined with Electrophysiology for Behavioral Experiments in Freely Moving Animals. ..... 119

Introduction ..... 119

Design ..... 121

Overview of Setup for Combined Behavioral Experiments. ..... 121

Design of Potentiostat for In Vivo Voltammetry. ..... 125

Design of Headstage for Combined FSCV and Electrophysiological Measurements in Freely Moving Animals ..... 129

Design of the UEI Chassis. ..... 134

Conclusions ..... 141

References ..... 142

Chapter 6. Evidence of Contralateral Synchronization of Transient Dopamine Release in Nucleus Accumbens In Vivo ..... 145

Introduction ..... 145

Materials and Methods ..... 148

Chemicals and drugs ..... 148

Fast-Scan cyclic Voltammetry ..... 149

Experiments in Animals. ..... 149

Data Analysis. ..... 150

Results and Discussion ..... 153

Evidence of Connection between Dopaminergic Systems of Left and Right Hemisphere ..... 153

Synchronization of Endogenous Dopamine Transients between Hemispherres in Anesthetized Rats ..... 155

Synchronization of Pharmacologically Induced Dopamine Transients between Hemispherres in Anesthetized Rat ..... 157

Conclusions ..... 161

References ..... 162

## LIST OF FIGURES


| Figure | | Page |
|---|---|---|
| 1.1 | Schematic representation of the mainstream techniques used to measure local brain activity……..... | 4 |
| 1.2 | Effect of oxidative etching on the surface of carbon electrodes…….. | 11 |
| 1.3 | Cyclic voltammograms for pH recorded in brain and in flow cell…….. | 14 |
| 1.4 | Measurement of dopamine transients in nucleus accumbens of both hemispheres in anesthetized rat after pharmacological alteration wit raclopride and cocaine……..…….... | 18 |
| 2.1 | Cyclic voltammograms in PBS buffer recorded at carbon fiber electrodes (A - C) and PPF electrodes (D - I)…….....……. | 36 |
| 2.2 | XPS spectra of PPF electrode surfaces…….. | 39 |
| 2.3 | AFM images of the PPF electrode surface morphology after different treatment conditions……. | 41 |
| 2.4 | Images of PPF electrodes after prolonged treatment with the extended waveforms……. | 43 |
| 2.5 | Images of carbon fiber microelectrodes after prolonged treatment with the extended waveform……..... | 45 |
| 2.6 | Application of the extended waveforms facilitates adsorption of catechols with different functional groups…….. | 48 |
| 2.7 | Sensitivity of carbon fiber towards 500 nM dopamine fouled by polymerization of tyramine is recovered by brief application of the extended waveform……. | 51 |
| 3.1 | Background subtracted cyclic voltammograms of pH shifts…… | 69 |
| 3.2 | Capacitive peak identification……...……. | 72 |
| 3.3 | Adsorption of electrochemically inert species at carbon-fiber microelectrodes……. | 77 |
| 3.4 | Interference from adsorptive species to background subtracted cyclic voltammograms for pH……..…….. | 81 |
| 3.5 | The effect of DOPAC adsorption on the background-subtracted pH change cyclic voltammogram……..……. | 84 |
| 3.6 | Monitoring of brain acidosis induced by hypercapnia in vivo with FSCV on | 87 |

carbon-fiber microelectrode…….

4.1 Microfabricated array of different generations……... 103

4.2 Detection of dopamine in flow cell with MEA 1.0……..……. 105

4.3 Simultaneous detection of dopamine using FSCV and amperometry.……. 108

4.4 Simultaneous detection of dopamine and oxygen…….……... 111

4.5 Simultaneous monitoring of electrically excited dopamine release in vivo…… 113

5.1 Setup for combined freely moving Echem/Ephys experiments…….…….. 122

5.2 Block diagram for UEI potentiostats and headstage……. 124

5.3 Schematic circuitries for headstages with iontophoresis, analog background subtraction and multiple electrodes recordings…….. 128

5.4 Photo of miniaturized headstage used for combined Echem/Ephys freely moving experiments adjacent to a U.S. dime…….. 132

5.5 Circuitry for headstage used for combined Echem/Ephys freely moving experiments…….. 133

5.6 Circuitry for switching control module…… 136

5.7 Circuitry for electrochemical amplifier with variable gain…….……. 138

5.8 Circuitry for neural spike amplifier……..…….. 140

6.1 Carbon-fiber microelectrodes placement for dual contralateral recordings…… 152

6.2 Contralateral stimulation induces dopamine release in nucleus accumbens…. 154

6.3 Recording of dopamine transients in nucleus accumbens core in the left and right hemispheres……..……..... 156

6.4 Dopamine transients in the nucleus accumbens core in left and right hemispheres..... 158

6.5 Spectral analysis of dopamine transients……. 160

## LIST OF ABBREVIATIONS AND SYMBOLS

| | |
|---|---|
| 5-HT | 5-hydroxytryptamine |
| 4MC | 4-methylcatechol |
| Å | angstrom |
| AFM | atomic force microscopy |
| ADC | analog to digital converter |
| AMPH | amphetamine |
| AP | anterior-posterior |
| BOLD | blood oxygenation level dependence |
| C | capacitance |
| C | concentration |
| C | coulomb |
| CE | capillary electrophoresis |
| CMOS | complimentary metal-oxide semiconductor |
| Coc | cocaine |
| CP | caudate putamen |
| CV | cyclic voltammogram |
| D | diffusion coefficient |
| DA | dopamine |
| DAC | digital to analog converter |
| DAT | dopamine transporter |
| DC | direct current |
| DOPAC | 3,4-dihydroxyphenylacetic acid |
| DV | dorsal-ventral |

| | |
|---|---|
| E | applied potential |
| Echem | electrochemical measurements |
| Ephys | electrophysiological measurements |
| EDTA | ethylenediaminetetraacetic acid |
| FSCV | fast-scan cyclic voltammetry |
| fMRI | functional magnetic resonance imaging |
| HPLC | high pressure liquid chromatography |
| Hz | hertz |
| i | current (A) |
| I/E | current to voltage conversion |
| i.p. | intraperitoneal injection |
| kg | kilogram |
| L | distance |
| L | left |
| LED | light emitting diode |
| M | molar |
| MFB | medial forebrain bundle |
| mg | milligram |
| min | minutes |
| mL | milliliter |
| ML | medial-lateral |
| mm | millimeter |
| mM | millimolar |
| ms | millisecond |

| | |
|---|---|
| NMR | nuclear magnetic resonance |
| µA | microamperes |
| µm | micrometer |
| MSN | medium spiny neuron |
| MEA | microelectrode array |
| METH | methamphetamine |
| MFB | medial forebrain bundle |
| MRI | magnetic resonance imaging |
| MS | Microsoft |
| nA | nanoamperes |
| NAc | nucleus accumbens |
| NAcc | nucleus accumbens (core) |
| NI | National Instruments |
| nM | nanomolar |
| RMS | root mean square |
| pA | picoampere |
| PAA | phenylacetic acid |
| PBS | phosphate buffered saline |
| PEA | β-phenylethylamine |
| PECVD | plasma enhanced chemical vapor deposition |
| PEEK | polyether ether ketone |
| PET | positron emission tomography |
| pF | picofarad |
| PPF | pyrolyrzed photoresist film |

| | |
|---|---|
| psi | pounds per square inch |
| Q | charge |
| R | resistance |
| R | right |
| Ra | raclopride |
| RIT | ritalin (methylphenidate) |
| s | seconds |
| SEM | scanning electron microscopy |
| SN | substantia nigra |
| SO | small outline |
| t | time |
| SW | switch |
| $t_{1/2}$ | time required for signal to decay 50% |
| TRIS | tris(hydroxymethyl)aminomethane buffer |
| UV | ultra violet |
| UEI | universal electrochemical instrument |
| V | applied potential |
| V | volts |
| VTA | ventral tegmental area |
| XPS | x-ray photoelectron spectroscopy |

# Chapter 1

# Advancements in Probing Neurochemistry with Fast-Scan Cyclic Voltammetry.

## INTRODUCTION

The human brain is a sophisticated organ that emerged as a result of several billions of years of evolution. [1] The evolutionary advantage of its complexity is the ability of humans to adapt to various environments and even change their environment to be made more compatible for human life and these traits eventually made *Homo Sapiens* the dominant species.

However, the weakness of this complex system is its susceptibility to malfunctions. There are many neurological disorders that currently cannot be efficiently controlled because the causes of these diseases are not fully understood. Among them there are several widespread diseases associated with the dysfunctions of dopaminergic neurons such as Parkinson's disease, schizophrenia and substance abuse that affect one, two and twenty two millions of people in the United States, respectively. [2] Better understanding of the dopaminergic system is needed for development of effective therapies.

Investigation of the mind has evolved as a rigorous science relatively recently and within a career span of some of our contemporaries. [3] Complete understanding of brain functions is still a far reaching goal; however a lot of knowledge was acquired about neurons on subcellular, cellular and intercellular levels. One of the reasons for

these advancements is developments in physics and chemistry that brought new technologies suitable for quantitative biological experiments. Excellent examples of this export are innovations in electronics and radar technology that facilitated discovery of electrical conductance in axons [4] and development of Falck-Hillarp histochemical fluorescent method (condensation of monoamines with formaldehyde) that was used to describe the anatomy of catecholamine-containing neurons. [5]

Experiments on isolated neurons and brain slices greatly contributed to the mechanistic understanding of the separate elements of brain circuits. One of the strength of these experiments is their relative simplicity. However, neurons themselves are spatially delocalized cells and they sent their projections many centimeters away from their cell bodies and link together different brain regions. [6] This means that a focus on distinct neurons or their subdivisions might be an oversimplification that does not represent the entire brain accurately. This suggests that study of the intact brain is the best way to access its functions.

Initial attempts to study the functioning brain had limited success due to lack of knowledge about the basic elements and lack of the quantitative techniques available for neuroscientist. [3] Nowadays, there is a great variety of methods for a scientist to choose from. The mainstream techniques that are used to measure local brain activity in vivo are summarized on **Figure 1.1**.

The simplest and the oldest method is electrophysiological measurement with microelectrodes. In this technique, changes in electrical field arising from neurons firing action potentials are sampled. Activity of single firing neuron can be recorded [7] and arrays of hundreds of microelectrodes can be used to sample multiple neurons

simultaneously. [8] The advantage of the technique is simplicity, excellent spatial and temporal resolution and compatibility with many behavioral paradigms.

Neural activity is a very energy demanding process. To provide an adequate energy supply, an extensive network of blood vessels and capillaries exists in the brain that provides neurons with glucose and oxygen and removes carbon dioxide and the products of metabolism. [9] Local changes in neural activity cause changes in both metabolite and nutrient concentrations as well as change in the blood flow and blood oxygenation level. Several spectroscopic techniques such as magnetic resonance imaging (MRI) and positron emission tomography (PET) were developed that can trace localized changes in the blood flow or visualize transport of metabolites, glucose or specific markers. [10] This information provides assessment of local neural activity. These techniques are noninvasive so they can be routinely used in experiments with humans. Also they can sample integral activity of the entire brain and have good temporal and spatial resolution.

Neurons communicate with each other through synaptic connections. Arrival of action potential to the terminal of a presynaptic neuron triggers release of a neurotransmitter (**Figure 1.1**). The neurotransmitter diffuses through the synaptic cleft and binds to receptors on a postsynaptic neuron and causes either polarization or depolarization of the neuron and changes its probability to fire action potential. Some neurotransmitters such as monoamines (dopamine, norepinephrine and 5-hydroxytryptamine) also diffuse away from the synaptic cleft in the extracellular space and bind to receptors on multiple adjacent neurons. Increase in concentration of neurotransmitters in extracellular space associated with the release can be detected using tools of analytical chemistry.

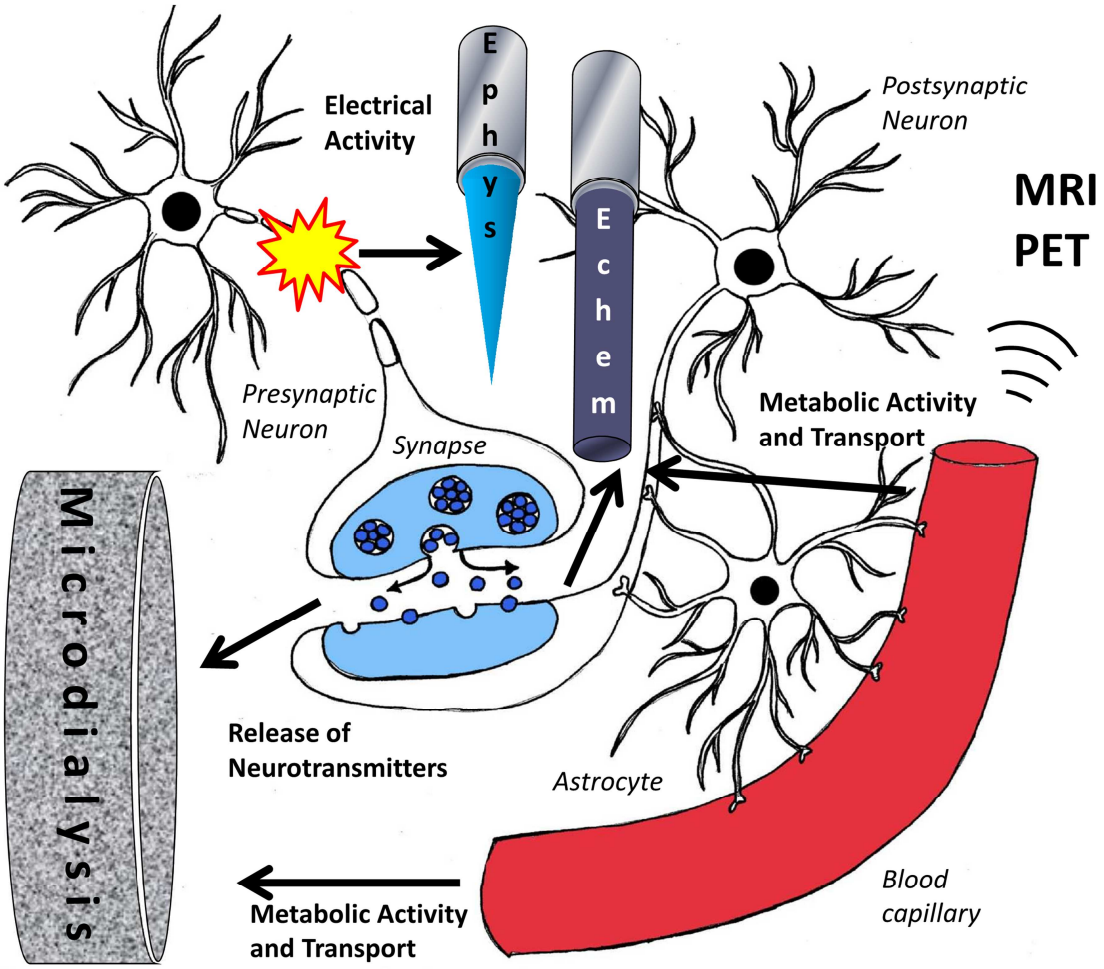


**Figure 1.1.** Schematic representation of the mainstream techniques used to measure local brain activity.

Brain consists of interconnected neurons, astrocytes and blood capillaries (labeled). Electrical activity of neurons can be assessed with microelectrodes by measuring transient changes in electrical field generated during firing of action potentials (microelectrode labeled “Ephys”). Metabolic activity and transport of oxygen, glucose and other species with blood flow associated with local neural activity and can be detected as the change in concentration of these species with noninvasive imaging techniques such as MRI and PET (labeled). Finally, release of neurotransmitters as well as change in concentration of certain analytes related to metabolism and blood flow can be detected with implantable biosensors based on electrochemical measurements (microelectrode labeled “Echem”) or by continues sampling of extracellular fluid with further external analysis with HPLC (probe labeled “Microdialysis”). Drawing courtesy of Marina Krylova.

A probe with semipermeable membrane is lowered in the brain and extracellular fluid is continuously extracted with its following chemical analysis using classical analytical techniques such as HPLC or CE. [10] This technique has an excellent limit of detection and excellent chemical resolution that allows establishing identity of the activated neurons. [11] Furthermore, multiple neurotransmitters and metabolites can be sampled simultaneously.

Alternatively, neurotransmitters in the extracellular space can be detected with an electrochemically based biosensor that is placed next to the release cite. Coincidently, many of neurotransmitters and metabolites are electrochemically active and can be oxidized at moderate potential and detected electrochemically. [12] In its most successful and popular form, this technique is known as fast-scan cyclic voltammetry (FSCV) or in vivo voltammetry. In this method, consecutive triangular ramps at scan rate of 200-1000 V/sec and various potential limits are applied at frequency of 10 Hz to a carbon-fiber microelectrode. The resulting current is recorded and analyzed. Background current before the chemical events of interest is removed using either digital or analog [13] background subtraction. [14]

Instrumentation for FSCV is portable and can be designed so that it does not restrict movement of an animal and it can be used with any experimental paradigm in behavioral chambers. Furthermore, successful attempts have been made to develop wireless FSCV systems that can provide additional “degrees of freedom” for behavioral experiments animals and possible application of FSCV in humans to verify placements of deep brain stimulation electrodes. [15] Although instrumentation for FSCV not very complex and can be readily assembled by someone who is familiar with electronics according to recently published schematics [16], the lack of adequate commercial

suppliers of instruments might discourage the wide spread use of FSCV, especially by research and development divisions in commercial organizations.

FSCV is an invasive technique; however it is typically used with carbon-fiber microelectrodes. The carbon fiber itself is very small (~5 μm in diameter) and does not cause substantial damage to the brain. No gliosis or disruption of blood vessels is observed for carbon-fiber probe after histochemical evaluation of the implantation site, and this differs from the substantial damage that is usually induced by microdialysis probe. [17] Also, no gliosis was observed after a month of chronic implantation. [18]

In FSCV voltammograms are collected at frequency of 10 Hz. This time resolution is sufficient to study neurotransmitter functions and observe the relation between animal behavior and neurotransmitter release. FSCV is comparable in temporal resolution to other techniques and much faster than temporal resolution of microdialysis (10 minutes). [11] One disadvantage of FSCV is background drift which limits the single differential measurement to about 100 seconds. Analog background subtraction has been employed to account for this shift and increase the recording time to 60 minutes. [13]

FSCV was developed for detection of catecholamines and the limit of detection for dopamine has been lowered to the subnanomolar range. [19] However, the number of molecules that can be detected with FSCV in vivo is growing. Detection of norepinephrine [20], 5-hydroxytryptamine [21], pH [22, 23], oxygen [22] and adenosine [24] in the brain were reported in literature in recent years. Unfortunately, electrochemically inert neurotransmitters and metabolites are still out of reach for FSCV. However it is possible to measure glucose and glutamate through auxiliary enzymatic reaction with further FSCV detection of hydrogen peroxide. [25]

There are many electrochemically active species in the brain extracellular fluid and it is tricky to have god selectivity for with FSCV. However, during several decades of development and improvement of the technique, principles for selectivity for in vivo biosensors were established. [26] According to these guidelines, five criteria including the electrochemical identity (voltammogram), anatomical and physiological verification, pharmacological verification and independent chemical identification need to be satisfied to establish identity of the voltammetric signal in vivo.

FSCV detection of neurotransmitters is the most popular in vivo electrochemical technique. Around 30 labs around the world are using in vivo voltammetry and the majority of them focus on psychology and behavioral neuroscience which involves FSCV experiments in freely moving rats. The fact that there are so many groups using FSCV means that the technique is mature enough to be transferred to the hands of biologists and non-electrochemists. However, there are still some challenges to overcome and improvements to make that require knowledge of electrochemistry, surface science and proficiency in development of instrumentation. These directions were taken and successfully explored in this work.

## DYNAMIC STATE OF CARBON SURFACE AND REGENERATION OF ADSORPTION SITES

High sensitivity and low limit of detection for fast-scan cyclic voltammetry are achieved by adsorption and preconcentration of catecholamines at the electrode surface. [27, 28] Apparently, the adsorption of catecholamines on carbon is very specific for catechols and aromatic species in comparison to gold where interferants such as proteins adsorb as well. [29] The chemical structure of the adsorption sites on carbon is unknown. Part of the problem is the multitude of surface active groups that exist on the surface and also the variety in carbon materials that used for the fabrication of the electrodes as well as variation in the pretreatment procedures for the electrode surfaces. [30, 31] An additional challenge is the small size of carbon-fiber microelectrodes which severely limits number of techniques that can be used for surface analysis. Furthermore, during FSCV experiment voltage ramps are continuously applied to the electrode and, as was shown earlier, the higher potential limits led to an increase in dopamine adsorption, [32, 33] which means that the electrochemical experiment itself in certain cases affects the surface integrity and changes the composition of the surface active groups. With this being said, standard procedure of surface analysis such as turning off the potential ramps and taking an electrode from the solution to the high vacuum chamber of XPS instrument are unlikely to provide adequate representation of dynamic composition of carbon surface during electrochemical experiment.

In this work, the effect of different voltage ramps on the surface chemistry of carbon-fiber microelectrodes was investigated with a variety of techniques such as XPS, AFM, SEM and electrochemistry. XPS and AFM was challenging with samples of such small area. Therefore, microfabricated pyrolyzed photoresist film (PPF) electrodes, that has similar properties [34] were used.

It was discovered that the application of extended potential ramps (up to 1.3 V and 1.4 V), which are traditionally used for FSCV experiments in freely moving animals, led to oxidative etching of the carbon surface. Complete etching and disappearance of carbon-fiber microelectrodes were observed after prolonged (days and weeks) cycling of microelectrodes with the extended waveforms. This observation suggests that adsorption sites on the carbon surface are continuously created and destroyed (regenerated) and the chemical composition of the carbon surface in FSCV experiments with the extended waveform is a result of dynamic equilibrium. This discovery brings new insights into carbon surface chemistry and its dynamic nature and provides routes to explore for improvement in electrochemical sensing.

Oxidative electrochemical etching associated with application of the extended waveform prevents electrode fouling by irreversibly adsorbed species. It was confirmed by purposeful fouling of carbon-fiber microelectrode with products of electrochemical oxidation of tyramine, which tend to form polymer that adsorbs on the electrode surface. [35] Complete recovery of electrode sensitivity was achieved after use of the extended waveform. The concept of renewable surface of electrode surface provides an excellent way to prevent chemical fouling. However, resurfacing of carbon electrodes also means that modification of carbon surface is not very useful with the extended waveform. Covalently attached molecules on carbon electrodes are expected to etch away during electrochemical oxidation of the surface (**Figure 1.2**).

Regeneration of dopamine adsorption sites on the surface during electrochemical etching implies that they exist in a dynamic equilibrium that is a function of the applied waveform. As was shown, anodic potential limit defines the structure and number of the adsorption sites on the carbon surface. [36] The other important parameter is a time period for which certain potential is applied. There is less time for oxidation and etching

to occur with faster scan rates. Hence, the dynamic equilibrium at the carbon surface is shifted and either structure or number of adsorptions sites on the surface is altered. This means that simple increase in the scan rate will not lead to a stable increase in the current according to the textbook equations. [37] The concept of dynamic carbon surface provides a route to the design of unusually shaped waveforms that combine fast scanning with sufficient time spent at high potentials. This promotes oxidative etching and regeneration of dopamine adsorption sites. [19] Consecutively, ability to use faster scan rate increases dopamine oxidation current and decreases signal to noise ratio which brings limit of detection for dopamine to subnanomolar range. [19] Low limit of detection is useful for exploring dopamine release in vivo in regions with sparse dopamine innervation, such as prefrontal cortex. [38] Dopamine in prefrontal cortex plays role in executive functions and short term memory and deficiencies of dopaminergic neurotransmission there were linked to schizophrenia. [39] This is an excellent example of how the discovery in electrochemistry (surface renewal and regeneration of adsorption sites) leads to improvement of analytical tools that can be used to study biology.

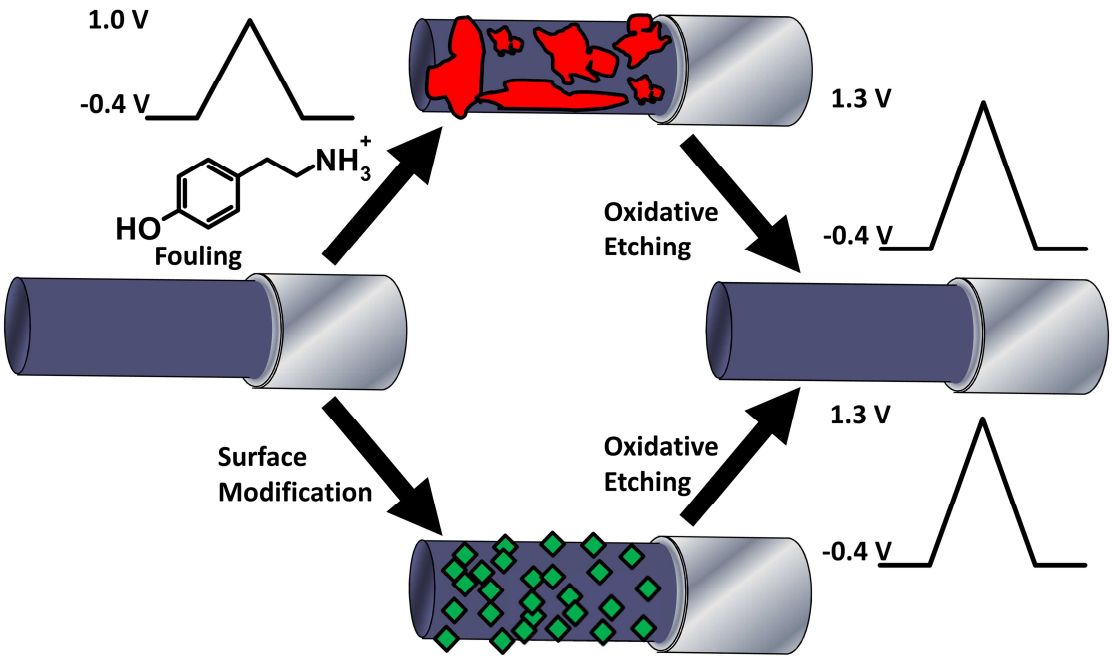


**Figure 1.2.** Effect of oxidative etching on the surface of carbon electrodes.

Electrochemical oxidation of tyramine on the carbon-fiber microelectrode leads to formation of polymer on the surface which fouls electrode (red plaques). However, further use of 1.3 V extended ramp removes the polymer and restore adsorption sites on the carbon surface. Similarly, any modification of the carbon electrode surface (green diamonds) will not be stable when used with 1.3 V waveform due to oxidative etching.

## MEASUREMENT OF PH IN BRAIN IN VIVO AND INTERFERENCE FROM ADSORPTION

Some chemical groups on the surface of carbon-fiber microelectrodes participate in electrochemical reactions that involve protons. [40] Thus in FSCV experiment change in solution pH leads to shift in the electrode background current and characteristic cyclic voltammogram for pH can be obtained after background subtraction. This pH effect was initially considered as interference for dopamine detection. [41] Though, later it was adopted for detection of fast pH changes in the brain. [22] However, the cyclic voltammograms recorded in brain in vivo did not accurately match the cyclic voltammograms recorded in the flow cell (**Figure 1.3**, **A** and **B**).

Carbon surface is rich in surface active groups that form adsorption site for many chemical species. [30, 31] Also, to facilitate preconcentration of dopamine, which is positively charged at physiological pH of 7.4, carbon-fiber microelectrode is held at potential of -0.4 V. Obviously, any other molecules and ions, especially aromatic and positively charged with affinity to carbon surface, adsorb at the electrode as well. Even if these species are not electrochemically active themselves, they interfere with the electrochemical detection of adsorptive analytes. They compete with dopamine for adsorption sites on the surface. [42] Furthermore, they disturb double layer and alter its capacitance. [37] FSCV is a background subtraction technique; hence electrochemically inert species that adsorb to the electrode surface produce distinct voltammograms related to the alteration of the double layer capacitance. [23]

Classification of peaks in cyclic voltammogram for pH change with the further investigation of their nature led to the conclusion that there are two reasons for the mismatch of pH signal in vivo and in the flow cell. First, since TRIS (tris(hydroxymethyl)aminomethane) that is used as a buffer, is also an amine that

positively charged at pH 7.4, it adsorbs on the surface and suppresses C-peak in the cyclic voltammogram for pH (**Figure 1.3**, **B** and **C**). Second, the dopamine metabolite, DOPAC (3,4-dihydroxyphenylacetic acid), is present in the brain extracellular fluid at a concentration of 20 µM. [43] DOPAC is electrochemically active and oxidation and reduction of DOPAC involves protons. The concentration of DOPAC does not change appreciably on the fast timescale at which FSCV measurements are done. Thus DOPAC does not interfere with background-subtracted detection of dopamine. However, since DOPAC electrochemistry is pH dependent, alterations in pH lead to appearance of extra peaks associated with shift in oxidation and reduction potentials of DOPAC. Traditionally, DOPAC is not present in calibration buffer and this cause the discrepancy in cyclic voltammograms for in vivo and flow cell pH shifts (**Figure 1.3**, **C** and **D**). [23]

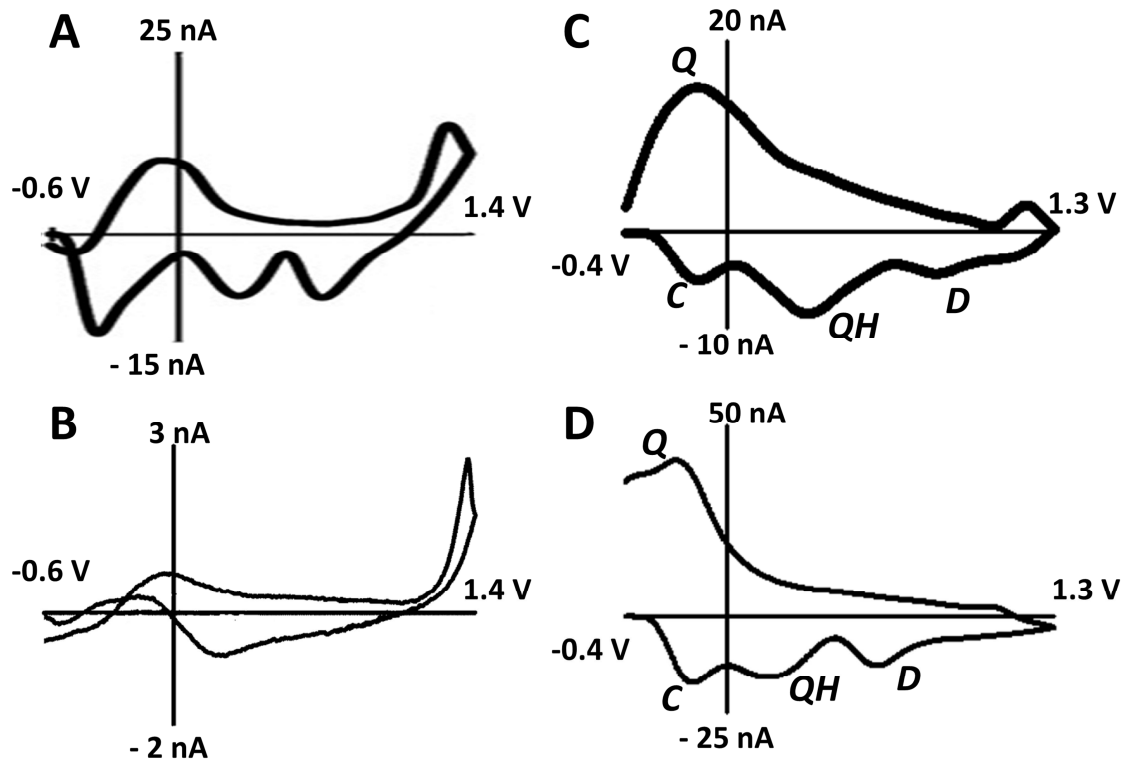


**Figure 1.3.** Cyclic voltammograms for pH recorded in brain and in flow cell.

Cyclic voltammogram for a pH change recorded in vivo (adapted from [44]) after electrical stimulation (A) is very different from the cyclic voltammogram recorded for pH 0.1 in TRIS buffer in flow cell (adapted from [33]) (B). In PBS buffer with addition of 20 µM of DOPAC peaks between cyclic voltammograms recorded in brain after electrical stimulation (C) and in flow cell for 0.25 pH change (D) were similar and labeled as C-peak, QH-peak, Q peak and D-peak.

## MICROELECTRODE ARRAYS FOR VOLTAMMETRIC MEASUREMENTS IN BRAIN IN VIVO

FSCV with carbon fiber microelectrodes provides excellent spatial resolution due to small diameter of carbon fibers (5 µm). However, the volume of the brain that is sampled with single carbon fiber is also very small. Average diffusion distance for dopamine in the brain is around 6 µm, [45] thus only dopamine in a volume of 20000 $\mu m^3$ is detected. Average concentration of dopaminergic synapses is 0.1 $\mu m^{-3}$, [46] thus there are only 2000 synapses that are sampled with a carbon-fiber microelectrode. However, there are roughly 22000 dopaminergic cells in nigrostriatal and mesolimbic dopamine systems [47] in each of two hemispheres and every dopamine neuron makes thousands of synaptic connections. [48] It means that just 0.005% of dopaminergic system is sampled with a single carbon-fiber microelectrode! What happens with the rest 99.995% of dopaminergic neurons during freely moving voltammetry experiments, when animals perform behavioral tasks is not known very well.

There are many other neurotransmitters and metabolites besides dopamine that can be detected with FSCV and monitoring of their concentration could bring new insights in understanding of brain functions. However, each of these analytes has distinct electrochemical properties. Thus they can be detected with best sensitivity and selectivity only under certain electrochemical conditions with certain electrode modification and with a waveform that tailored for the specific neurotransmitter. For instance, detection of 5-hydroxytryptamine with FSCV requires coating of microelectrode with Nafion (to prevent fouling by 5-hydroxiacetic acid) and non-triangular waveform with anodic potential of +1.0 V and scan rate of 1000 V/sec. [21] Voltammetric detection of oxygen is optimal with a cathodic sweep to -1.4 V and a scan rate of 200 V/sec. [34]

The challenges described above provide excellent opportunities for improvement of in vivo voltammetry. Microelectrode arrays (MEAs) compatible with FSCV would be an exceptionally powerful tool for sampling concentration of neurotransmitters in spatially different locations as well as for sampling different neurotransmitters simultaneously.

Microelectrode arrays have been used to measure neural electrophysiological activity for more than four decades, [8, 49] and it was adapted for electrochemical measurements much later, after advantages of microelectrodes were realized. [50, 51] However, implementation of MEAs compatible with FSCV has not happened until invention of pyrolyzed photoresist film (PPF) [34, 52] which provided a convenient route for microfabrication of MEAs and development of instrumentation that allowed independent control of the electrodes in the array. [16]

Several different designs for FSCV compatible microelectrode arrays were explored. [34, 53, 54] The desired MEAs should be suitable for measurement of neurotransmitters in brain in vivo. This goal imposes many limiting criteria that were never fulfilled by any electrochemical MEAs that were described in the literature earlier. First, MEAs should have carbon microelectrodes since this material has the best surface chemistry suitable for dopamine detection in vivo. [29, 36] Second, microelectrodes in the MEA should be decoupled electronically from each other thus independent control of the applied potential is possible. [34] Third, the MEA probes should be small enough to prevent damage of the nerve terminals in the brain. [53] Fourth, the packaging and mounting of the MEAs should be suitable for the experiments in freely moving animals. Fifth, hardware (potentiostats) and software designed for multichannel recordings in freely moving animals should be developed. [16, 34] Many principles from this list were successfully realized in the past four years. [16, 34, 53, 54] The future challenge is to perform FSCV recordings with MEAs in freely moving animals.

Nevertheless, the great potential of multielectrode recordings for exploring brain can be accessed with experiments in anesthetized animals. Previously it was reported, that combination of dopamine D2 autoreceptor blockers (raclopride, haloperidol) with dopamine transporter inhibitors (nomifensine, cocaine) can cause spontaneous transient dopamine release in nucleus accumbens of anesthetized rats. [55, 56] Previously, only measurements with a single carbon-fiber microelectrode were done thus nothing was known about the spatial distribution of these transients as well as about their timing between different brain regions. Recordings with two microelectrodes implanted in both hemispheres demonstrated synchronization in dopamine transients in nucleus accumbens between hemispheres (**Figure 1.4**). Cross correlation of dopamine concentration time traces shows almost perfect synchrony that slightly disturbed by noise with lag of -0.1 seconds and maximum at 0.87. Interestingly, there is no direct dopaminergic connection between dopaminergic systems of both hemispheres. [57] Therefore the observed synchronization between hemispheres implies that dopamine neurons follow some slow oscillatory tone that synchronizes their firing. [58] This instance demonstrates that sampling of dopamine even in just two separate brain locations can provide a new insight in dopamine function which was not accessible for traditional single microelectrode measurements.

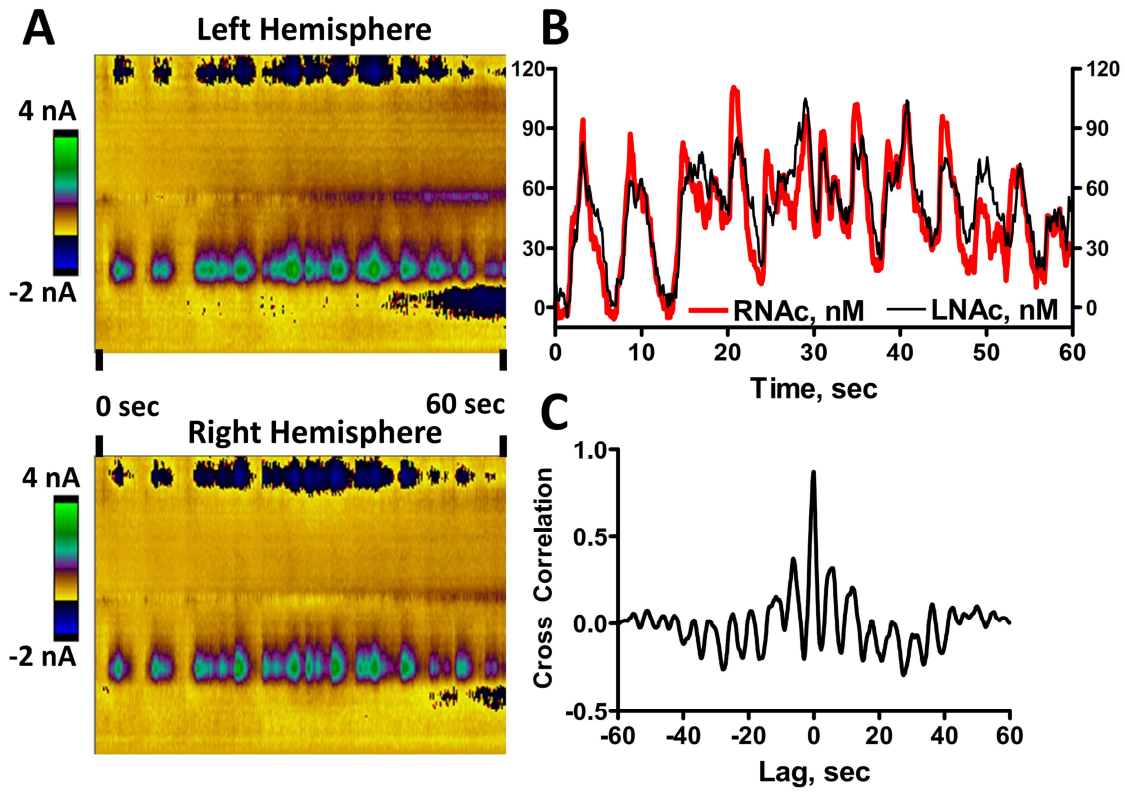


**Figure 1.4.** Measurement of dopamine transients in nucleus accumbens of both hemispheres in anesthetized rat after pharmacological alteration with raclopride and cocaine.

Color plots [59] of voltammetric data for spontaneous dopamine transients in nucleus accumbens of left and right hemispheres after application of raclopride with cocaine (A). Concentration traces for spontaneous dopamine transients (B). Cross correlation of signals from left and right hemispheres (C).

## DISSERTATION OUTLINE

The dissertation consists of six chapters. Chapter 1, “Advancements in Probing Neurochemistry with Fast-Scan Cyclic Voltammetry”, introduces FSCV and provides description of the technique with the advancements that were made in recent years. Additionally, challenges that were addressed in this work are outlined there. Chapter 2, “Carbon Microelectrodes with a Renewable Surface” describes effects of waveforms with different anodic potentials on carbon surface and its relation to sensitivity of carbon-fiber microelectrodes. Chapter 3, “Characterization of Local pH Changes in Brain Using Fast-Scan Cyclic Voltammetry with Carbon Microelectrodes” focuses on origin of peaks in cyclic voltammograms for pH changes observed in brain in vivo. The mechanism of interference for detection of pH with FSCV is shown and the pH signal in vivo is verified with hypercapnia (increase in concentration of carbon dioxide in breathing mixture). Chapter 4, “Carbon Microelectrode Arrays Compatible with Fast-Scan Cyclic Voltammetry” describes evolution of designs for MEAs and also evaluation of their performance in flow cell and for detection of dopamine in brain in vivo. Chapter 5, “Instrumentation for Fast-Scan Cyclic Voltammetry Combined with Electrophysiology for Behavioral Experiments in Freely Moving Animals” has detailed description of instrumentation that was developed in the group for FSCV experiments. Chapter 6, “Evidence of Contralateral Synchronization of Transient Dopamine Release in Nucleus Accumbens In Vivo” describes endogenous dopamine transients in both hemispheres and provides evidence of their synchronization with and without pharmacological manipulation.

## REFERENCES


1. Lorenz, K., *Behind the mirror: a search for a natural history of human knowledge*. Harcourt Brace Jovanovich: 1978.

2. *Brain facts: a primer on the brain and nervous system*. Society for Neuroscience: 2008.

3. Kandel, E. R., *In search of memory: the emergence of a new science of mind*. W.W. Norton & Co.: 2007.

4. Hodgkin, A., *Chance and design: reminiscences of science in peace and war*. Cambridge University Press: 1994.

5. Iversen, L. L.; Iversen, S.; Dunnett, S.; Bjorklund, A., *Dopamine Handbook*. Oxford University Press: 2009.

6. Kandel, E. R.; Schwartz, J. H.; Jessell, T. M., *Principles of neural science*. McGraw-Hill, Health Professions Division: 2000.

7. Humphrey, D. R.; Schmidt, E. M., *Extracellular single-unit recording methods*. Humana Press: Clifton, N.J., 1991; Vol. 15.

8. Nicolelis, M. A. L., *Methods for neural ensemble recordings*. 2nd ed.; CRC Press: Boca Raton, 2008.

9. Kaila, K.; Ransom, B. R., *pH and brain function*. Wiley-Liss: New York, 1998; p xiii, 688 p.

10. Carter, M.; Shieh, J. C., *Guide to Research Techniques in Neuroscience*. Academic Press: 2009.

11. Watson, C. J.; Venton, B. J.; Kennedy, R. T., In Vivo Measurements of Neurotransmitters by Microdialysis Sampling. *Analytical Chemistry* 2006, 78, (5), 1391-1399.

12. Robinson, D. L.; Hermans, A.; Seipel, A. T.; Wightman, R. M., Monitoring Rapid Chemical Communication in the Brain. *Chemical Reviews* 2008, 108, (7), 2554-2584.

13. Hermans, A.; Keithley, R. B.; Kita, J. M.; Sombers, L. A.; Wightman, R. M., Dopamine detection with fast-scan cyclic voltammetry used with analog background subtraction. *Analytical Chemistry* 2008, 80, (11), 4040-4048.

14. Michael, A. C.; Borland, L. M., *Electrochemical methods for neuroscience*. CRC Press/Taylor & Francis: 2007.

15. Garris, P. A.; Ensman, R.; Poehlman, J.; Alexander, A.; Langley, P. E.; Sandberg, S. G.; Greco, P. G.; Wightman, R. M.; Rebec, G. V., Wireless

transmission of fast-scan cyclic voltammetry at a carbon-fiber microelectrode: proof of principle. *Journal of Neuroscience Methods* 2004, 140, (1-2), 103-115.

16. Takmakov, P.; McKinney, C. J.; Carelli, R. M.; Wightman, R. M., Instrumentation for Fast-Scan Cyclic Voltammetry Combined with Electrophysiology for Behavioral Experiments in Freely Moving Animals. *Review of Scientific Instruments* 2011, submitted.

17. Jaquins-Gerstl, A.; Michael, A. C., Comparison of the brain penetration injury associated with microdialysis and voltammetry. *Journal of Neuroscience Methods* 2009, 183, (2), 127-135.

18. Clark, J. J.; Sandberg, S. G.; Wanat, M. J.; Gan, J. O.; Horne, E. A.; Hart, A. S.; Akers, C. A.; Parker, J. G.; Willuhn, I.; Martinez, V.; Evans, S. B.; Stella, N.; Phillips, P. E. M., Chronic microsensors for longitudinal, subsecond dopamine detection in behaving animals. *Nat Meth* 2009, 7, (2), 126-129.

19. Keithley, R. B. T., P; Bucher, E S; Belle, A M, Owesson-White C A; Park, J; Wightman, R M, Improving In Vivo Dopamine Sensitivity with Faster-Scan Cyclic Voltammetry. *Analytical Chemistry* 2011, submitted.

20. Park, J.; Kile, B. M.; Wightman, R. M., In vivo voltammetric monitoring of norepinephrine release in the rat ventral bed nucleus of the stria terminalis and anteroventral thalamic nucleus. *European Journal of Neuroscience* 2009, 30, (11), 2121-2133.

21. Hashemi, P.; Dankoski, E. C.; Petrovic, J.; Keithley, R. B.; Wightman, R. M., Voltammetric Detection of 5-Hydroxytryptamine Release in the Rat Brain. *Analytical Chemistry* 2009, 81, (22), 9462-9471.

22. Venton, B. J.; Michael, D. J.; Wightman, R. M., Correlation of local changes in extracellular oxygen and pH that accompany dopaminergic terminal activity in the rat caudate-putamen. *Journal of Neurochemistry* 2003, 84, (2), 373-381.

23. Takmakov, P.; Zachek, M. K.; Keithley, R. B.; Bucher, E. S.; McCarty, G. S.; Wightman, R. M., Characterization of Local pH Changes in Brain Using Fast-Scan Cyclic Voltammetry with Carbon Microelectrodes. *Analytical Chemistry* 2010, 82, (23), 9892-9900.

24. Swamy, B. E. K.; Venton, B. J., Subsecond detection of physiological adenosine concentrations using fast-scan cyclic voltammetry. *Analytical Chemistry* 2007, 79, (2), 744-750.

25. Sanford, A. L.; Morton, S. W.; Whitehouse, K. L.; Oara, H. M.; Lugo-Morales, L. Z.; Roberts, J. G.; Sombers, L. A., Voltammetric Detection of Hydrogen Peroxide at Carbon Fiber Microelectrodes. *Analytical Chemistry* 2010, 82, (12), 5205-5210.

26. Phillips, P. E. M.; Wightman, R. M., Critical guidelines for validation of the selectivity of in-vivo chemical microsensors. *Trac-Trends in Analytical Chemistry* 2003, 22, (9), 509-514.

27. Baur, J. E.; Kristensen, E. W.; May, L. J.; Wiedemann, D. J.; Wightman, R. M., Fast-Scan Voltammetry of Biogenic-Amines. *Analytical Chemistry* 1988, 60, (13), 1268-1272.

28. Bath, B. D.; Michael, D. J.; Trafton, B. J.; Joseph, J. D.; Runnels, P. L.; Wightman, R. M., Subsecond adsorption and desorption of dopamine at carbon-fiber microelectrodes. *Analytical Chemistry* 2000, 72, (24), 5994-6002.

29. Zachek, M. K.; Hermans, A.; Wightman, R. M.; McCarty, G. S., Electrochemical dopamine detection: Comparing gold and carbon fiber microelectrodes using background subtracted fast scan cyclic voltammetry. *Journal of Electroanalytical Chemistry* 2008, 614, (1-2), 113-120.

30. McCreery, R. L., *Carbon electrodes: structural effects on electron transfer kinetics*. Marcel-Dekker: New York, 1991; Vol. 17, p 221-373.

31. McCreery, R. L., Advanced carbon electrode materials for molecular electrochemistry. *Chemical Reviews* 2008, 108, (7), 2646-2687.

32. Hafizi, S.; Kruk, Z. L.; Stamford, J. A., Fast Cyclic Voltammetry - Improved Sensitivity to Dopamine with Extended Oxidation Scan Limits. *Journal of Neuroscience Methods* 1990, 33, (1), 41-49.

33. Heien, M. L. A. V.; Phillips, P. E. M.; Stuber, G. D.; Seipel, A. T.; Wightman, R. M., Overoxidation of carbon-fiber microelectrodes enhances dopamine adsorption and increases sensitivity. *Analyst* 2003, 128, (12), 1413-1419.

34. Zachek, M. K.; Takmakov, P.; Moody, B.; Wightman, R. M.; McCarty, G. S., Simultaneous Decoupled Detection of Dopamine and Oxygen Using Pyrolyzed Carbon Microarrays and Fast-Scan Cyclic Voltammetry. *Analytical Chemistry* 2009, 81, (15), 6258-6265.

35. de Castro, C. M.; Vieira, S. N.; Goncalves, R. A.; Brito-Madurro, A. G.; Madurro, J. M., Electrochemical and morphologic studies of nickel incorporation on graphite electrodes modified with polytyramine. *Journal of Materials Science* 2008, 43, (2), 475-482.

36. Takmakov, P.; Zachek, M. K.; Keithley, R. B.; Walsh, P. L.; Donley, C.; McCarty, G. S.; Wightman, R. M., Carbon Microelectrodes with a Renewable Surface. *Analytical Chemistry* 2010, 82, (5), 2020-2028.

37. Bard, A. J.; Faulkner, L. R., *Electrochemical Methods*. Wiley New York: 2001.

38. Garris, P. A.; Collins, L. B.; Jones, S. R.; Wightman, R. M., Evoked Extracellular Dopamine in-Vivo in the Medial Prefrontal Cortex. *Journal of Neurochemistry* 1993, 61, (2), 637-647.

39. Knable, M. B.; Weinberger, D. R., Dopamine, the prefrontal cortex and schizophrenia. *Journal of Psychopharmacology* 1997, 11, (2), 123-131.

40. Kawagoe, K. T.; Garris, P. A.; Wightman, R. M., pH-Dependent Processes at Nafion(R)-Coated Carbon-Fiber Microelectrodes. *Journal of Electroanalytical Chemistry* 1993, 359, (1-2), 193-207.

41. Runnels, P. L.; Joseph, J. D.; Logman, M. J.; Wightman, R. M., Effect of pH and surface functionalities on the cyclic voltammetric responses of carbon-fiber microelectrodes. *Analytical Chemistry* 1999, 71, (14), 2782-2789.

42. Chen, B. T.; Rice, M. E., Calibration factors for cationic and anionic neurochemicals at carbon-fiber microelectrodes are oppositely affected by the presence of Ca2+ and Mg2+. *Electroanalysis* 1999, 11, (5), 344-348.

43. Shou, M. S.; Ferrario, C. R.; Schultz, K. N.; Robinson, T. E.; Kennedy, R. T., Monitoring dopamine in vivo by microdialysis sampling and on-line CE-laser-induced fluorescence. *Analytical Chemistry* 2006, 78, (19), 6717-6725.

44. Roitman, M. F.; Stuber, G. D.; Phillips, P. E. M.; Wightman, R. M.; Carelli, R. M., Dopamine operates as a subsecond modulator of food seeking. *Journal of Neuroscience* 2004, 24, (6), 1265-1271.

45. Venton, B. J.; Zhang, H.; Garris, P. A.; Phillips, P. E. M.; Sulzer, D.; Wightman, R. M., Real-time decoding of dopamine concentration changes in the caudate-putamen during tonic and phasic firing. *Journal of Neurochemistry* 2003, 87, (5), 1284-1295.

46. Doucet, G.; Descarries, L.; Garcia, S., Quantification of the Dopamine Innervation in Adult-Rat Neostriatum. *Neuroscience* 1986, 19, (2), 427-&.

47. German, D. C.; Manaye, K. F., Midbrain Dopaminergic-Neurons (Nuclei A8, A9, and A10) - 3-Dimensional Reconstruction in the Rat. *Journal of Comparative Neurology* 1993, 331, (3), 297-309.

48. Anden, N. E.; Fuxe, K.; Hamberge.B; Hokfelt, T., A Quantitative Study on Nigro-Neostriatal Dopamine Neuron System in Rat. *Acta Physiologica Scandinavica* 1966, 67, (3-4), 306-&.

49. Hanna, G. R.; Johnson, R. N., A Rapid and Simple Method for Fabrication of Arrays of Recording Electrodes. *Electroencephalography and Clinical Neurophysiology* 1968, 25, (3), 284-&.

50. Wightman, R. M., Microvoltammetric Electrodes. *Analytical Chemistry* 1981, 53, (9), 1125-&.

51. Compton, R. G.; Banks, C. E., *Understanding voltammetry*. World scientific publishing: Singapore, 2007; p 371 p.

52. Kim, J.; Song, X.; Kinoshita, K.; Madou, M.; White, B., Electrochemical studies of carbon films from pyrolyzed photoresist. *Journal of the Electrochemical Society* 1998, 145, (7), 2314-2319.

53. Zachek, M. K.; Park, J.; Takmakov, P.; Wightman, R. M.; McCarty, G. S., Microfabricated FSCV-compatible microelectrode array for real-time monitoring of heterogeneous dopamine release. *Analyst* 2010, 135, (7), 1556-1563.

54. Zachek, M. K.; Takmakov, P.; Park, J.; Wightman, R. M.; McCarty, G. S., Simultaneous monitoring of dopamine concentration at spatially different brain locations in vivo. *Biosensors & Bioelectronics* 2010, 25, (5), 1179-1185.

55. Venton, B. J.; Wightman, R. M., Pharmacologically induced, subsecond dopamine transients in the caudate–putamen of the anesthetized rat. *Synapse* 2007, 61, (1), 37-39.

56. Park, J.; Aragona, B. J.; Kile, B. M.; Carelli, R. M.; Wightman, R. M., In Vivo Voltammetric Monitoring of Catecholamine Release in Subterritories of the Nucleus Accumbens Shell. *Neuroscience* 2010, 169, (1), 132-142.

57. Pritzel, M.; Sarter, M.; Morgan, S.; Huston, J. P., Interhemispheric nigrostriatal projections in the rat: Bifurcating nigral projections and loci of crossing in the diencephalon. *Brain Research Bulletin* 1983, 10, (3), 385-390.

58. Shi, W.-X., Slow Oscillatory Firing: A Major Firing Pattern of Dopamine Neurons in the Ventral Tegmental Area. *Journal of Neurophysiology* 2005, 94, (5), 3516-3522.

59. Michael, D. J.; Joseph, J. D.; Kilpatrick, M. R.; Travis, E. R.; Wightman, R. M., Improving data acquisition for fast scan cyclic voltammetry. *Analytical Chemistry* 1999, 71, (18), 3941-3947.

# Chapter 2

## Carbon Microelectrodes with a Renewable Surface.

### INTRODUCTION

Carbon electrodes have several beneficial properties including a wide positive potential window, simplicity of surface modifications, and low cost. [1, 2] These benefits have allowed applications of carbon electrodes in energy sources [3] and electroanalytical detection. [4] Recent progress in the development of nanostructured carbon for electrochemical sensors [5] and introduction of carbon based electronics [6] additionally highlight the important role of this material for a variety of future applications in both fundamental research and industrial processes.

Carbon microelectrodes are widely used in bioanalytical chemistry for the detection of neurotransmitters, signaling molecules, and their metabolites. [4] Due to their small size, microelectrodes can be used to probe chemical environments with high spatial resolution. [7, 8] When coupled with fast scan cyclic voltammetry (FSCV), carbon-fiber microelectrodes are capable of detecting and resolving analytes in real time. This technique has proven to be a valuable tool for providing a relationship between neurotransmitter release in the brain and animal behavior, which helps to establish functionality of several neurocircuits, particularly the dopaminergic system responsible for reward seeking behavior and learning. [9, 10] Carbon electrodes have been shown to be much superior to other electrodes for this type of in vivo measurement. [11]

Different treatments have been employed to increase adsorption and electron-transfer kinetics at carbon electrodes because these factors influence sensitivity, selectivity and response time. Physical treatments include traditional electrode polishing (glassy carbon), [2] vacuum heat treatment (glassy carbon), [12] laser activation of electrode surfaces (glassy carbon) [13] and flame etching (carbon fibers). [14] All produce changes in the structure of carbon surfaces that lead to the desired electrochemical response. Despite the success of these physical pretreatments for achieving particular electrode properties, these approaches have several disadvantages. First, it is difficult to predict electrode performance when comparing different pretreatment methodologies on different forms of carbon. McCreery and coworkers have developed a relationship between carbon electrode surface structure and electron-transfer kinetics, [15] however this paradigm does not consider adsorption that plays an important role for the many electroactive analytes including catechols. [16, 17] A second limitation is that these surfaces cannot be renewed once implanted within a biological system. This is particularly important for in vivo voltammetry since it is difficult to repeat the sensitivity enhancing treatment step during the biological experiment. Thus, the reported procedures have limited applicability for in vivo work particularly for experiments with freely moving animals.

Another pretreatment approach that has proven to be useful is electrochemical oxidation of carbon. Oxidation of carbon fibers with a DC potential of 2.5 V leads to an electrode with a greatly increased capacitance due to fracturing of the fiber. [18] This treatment is reported to increase the amount of oxides on the fiber surface. [19] Oxidation of carbon fibers with a triangular waveform extended to 3 V (repeated at 70 Hz) irreversibly alters their electrochemical response. [20, 21] Electron-transfer kinetics are accelerated for many species and adsorption is greatly enhanced. [22] Repetitive FSCV at

carbon-fiber microelectrodes with a potential limit of 1.4 V vs Ag/AgCl has been shown to increase adsorption when compared to the use of potential limit of 1.0 V while maintaining current stability both in vitro and in vivo. [23, 24] Increased adsorption enhances sensitivity but, at the same time, the background amplitude is also increased. This treatment differs from others in that the waveform is continually applied during the analytical measurement. However, the mechanisms behind this enhancement with extended voltage scans are unknown.

The small size of carbon-fiber microelectrodes limits the surface analysis techniques that can be used to investigate chemical changes on the carbon surface. In this work we have used pyrolyzed photoresist film (PPF) carbon electrodes to investigate the underlying changes that arise with increased positive limits during repetitive scans. PPF films have similar electrochemical properties as carbon-fiber microelectrodes but can be patterned into a variety of shapes using microfabrication techniques. [25-28] These carbon surfaces were probed with X-ray photoelectron spectroscopy (XPS) and atomic force microscopy (AFM). Our findings indicate that the surface of these electrodes is constantly renewed by using periodic application of waveforms with an extended anodic potential.

## MATERIALS AND METHODS

### Chemicals.

All chemicals were obtained from Sigma-Aldrich (St. Louis, MO, USA) unless otherwise noted and used as received. Solutions were prepared using doubly distilled water. Electrochemical experiments were done in PBS buffer (140 mM NaCl, 3 mM KCl, 10 mM $NaH_2PO_4$, pH = 7.4). Stock solutions of catechols were prepared in 0.1 N $HClO_4$ and diluted to the desired concentration immediately before use.

**Fabrication of Carbon Fiber Microelectrodes.**

Cylindrical microelectrodes were constructed using a T-650 carbon fiber (Thornel, Amoco Corp., Greenville, SC, USA) as previously described. [29] Briefly, individual carbon fibers were aspirated into glass capillaries (A-M Systems, Carlsborg, WA, USA) using vacuum. Afterwards, the capillaries were pulled and sealed with a micropipette puller (Narishige, Tokyo, Japan). The quality of the pulled capillaries was examined with an optical microscope. The carbon fibers were cut to an exposed length of 100 μm. Before electrochemical experiments, electrodes were soaked in isopropanol purified with Norit A activated carbon (ICN, Costa Mesa, CA, USA) for at least 20 min to remove surface impurities. [17] Electrical connection to the carbon fiber was made with electrolyte (4 M $CH_3COOK$ and 0.15 M KCl), and a stainless steel wire.

**Fabrication of PPF Electrodes.**

Two types of PPF microelectrodes that differed in their insulation were fabricated. SU-8 insulated PPF electrodes were used for studies of background current change with electrochemical treatment and silicon nitride insulated PPF electrodes were used for XPS and AFM studies. The PPF microelectrodes were fabricated as described previously. [28] Briefly, photoresist (AZ1518, AZ Electric Materials, Branchburg, NJ, USA) was spun on a 3" fused silica wafer and patterned using standard photolithographic techniques. The patterned wafer was subsequently pyrolyzed at 1000 ℃ under a forming gas atmosphere (5% $H_2$, 95% $N_2$). A microprocessor controlled tube furnace (Sentro Tech, Inc., Berea, OH, USA) was used to ramp the temperature at 5 ℃/min and it was held at 1000 ℃ for one hour. Samples were allowed to cool to room temperature under the forming gas atmosphere prior to exposure to air.

To obtain contrast for XPS mapping studies a non-carbon dielectric was required. For this application, a $Si_3N_4$ layer deposited by plasma-enhanced chemical vapor

deposition (PECVD) was used to insulate the PPF microelectrodes. The $Si_3N_4$ films were deposited using an Advanced Vacuum Vision 310 PECVD System (Lomma, Sweden). Monosilane (2% $SiH_4/N_2$) and ammonia ($NH_3$) gases were used at electronically mass controlled flow rates. The films were deposited at a rate of 7.5 nm/min to a final thickness of 500 nm. The exposed microelectrode area was photolithographically defined, and subsequently etched using reactive ion etching (Semi Group Inc, USA) under a fluoroform ($CHF_3$) and oxygen atmosphere. The pyrolyzed carbon served as a sufficient etch stop for this process. All deposition and etch rates were determined using a Tencor, P-6 profilometer (KLA-Tencor Inc, Milpitas, CA, USA). To obtain non-roughened and non-fluorinated samples, PPF microelectrodes were insulated with SU-8 3010, as previously reported. [28] External connections to the PPF were made using silver epoxy (MG Chemicals, Burlington, Ontario, Canada) and stainless steel wires. The device was cut with a dicing saw into its final form that had four PPF electrodes, each of which was 75 μm by 100 μm. Electrodes with such areas are compatible with small spot XPS measurements with a 27 μm diameter.

**Electrochemical Experiments.**

Cyclic voltammograms were acquired with an EI-400 potentiostat used in two electrode mode and TH-1 software (ESA Inc, Chemsfold, MA, USA) written in LabVIEW (National Instruments, Austin, TX, USA). The waveform was generated and the voltammetric signal was acquired with an ADC/DAC card PCI-6251 (National Instruments). A PCI-6711 DAC board (National Instruments) was used to synchronize waveform application, data acquisition and TTL pulses for the flow injection valve. The output waveform was filtered with a low pass 2 kHz filter to eliminate digitization steps.

For electrochemical measurements, three triangular waveforms were used. The first waveform (referred to as the 1.0 V waveform) was a ramp from - 0.4 V to 1.0 V and

back to - 0.4 V at a scan rate of 300 $Vs^{-1}$ repeated at 10 Hz with a rest potential of - 0.4 V between scans. A second waveform (referred to as the 1.3 V waveform) was a ramp from - 0.4 V to 1.3 V and back to - 0.4 V at scan rate of 400 $Vs^{-1}$ repeated at 60 Hz, also with a rest potential of - 0.4 V between scans. The third waveform (referred to as the 1.4 V waveform) was a ramp from - 0.6 to 1.4 V and back to -0.6 V at scan rate of 400 $Vs^{-1}$ repeated at 60 Hz with a rest potential of - 0.6 V between scans. The latter two extended waveforms were applied at a frequency of 60 Hz to intensify any oxidative etching effects and to reduce the duration of the electrochemical experiments. In each experiment background current was allowed to stabilize for 15 minutes. [24]

Evaluation of the adsorption of catechols employed the same waveforms but with a repetition frequency of 1 Hz. The charge was obtained by integrating the oxidation peak of the cyclic voltammogram as previously described. [17] The area of the electrode was calculated from microelectrode dimensions measured with an optical microscope. To account for contributions from diffusion, cyclic voltammograms were simulated with DigiSim software (Bioanalytical Systems Inc, West Lafayette, IN, USA) using kinetic parameters and diffusion coefficients reported before. [30, 31] The amount of adsorbed analyte was obtained by subtracting the computed diffusional component from the measured charge and converting it to the number of moles using Faraday's law.

For tyramine fouling experiments, the carbon fiber microelectrode was cycled for 15 minutes in buffer with the 1.3 V waveform at 60 Hz. The response to 500 nM dopamine in a flow injection system was monitored for 10 consecutive injections 3 minutes apart using the 1.0 V waveform for detection (10 Hz application frequency). Then, the electrode was purposely fouled by applying the 1.0 V waveform at 10 Hz in 15 mM solution of tyramine in PBS buffer for 15 minutes. Afterwards, the response to 500 nM dopamine was again evaluated with the 1.0 V waveform for 10 consecutive injections

3 minutes apart (10 Hz application frequency). The recovery of electrode sensitivity was evaluated by cycling the electrode with the 1.3 V waveform in PBS buffer for 15 minutes at 60 Hz followed by testing with 500 nM dopamine in the flow-injection system with the 1.0 waveform for 10 consecutive injections 3 minutes apart (10 Hz application frequency). The responses for the 10 consecutive injections for each condition were averaged and normalized to the pre-tyramine injections.

All potentials are reported versus a Ag/AgCl reference electrode. Electrochemical measurements were performed in a grounded Faraday cage.

**Flow Injection Apparatus.**

The flow injection analysis system consisted of a syringe pump (Harvard Apparatus, Holliston, MA) that directed buffer solution through a Teflon tube to a 6-port injection valve (Rheodyne, Rohnert Park, CA, USA) at rate of 0.5 mL per minute. The injection valve was controlled by a 12 V DC solenoid and was used to introduce analyte from an injection loop (volume of 0.7 mL) into an electrochemical cell. The carbon-fiber microelectrode was placed inside the opening of the Teflon tube to eliminate the diffusion broadening and a reference electrode was placed within ~ 20 mm of the working electrode. [32]

**Electrochemical Modification of PPF Electrodes.**

Electrochemical experiments involving PPF microelectrodes were accomplished using a drop of buffer placed on top of the microelectrodes and a reference electrode was lowered into the buffer. The three different waveforms were applied to separate electrodes for 30 minutes. Electrodes were rinsed with water, dried in air and the surface was analyzed with XPS and AFM.

**XPS Analysis.**

Drops of saturated $NiI_2$ solution were deposited onto the four corners surrounding each of the electrodes using a pressure ejection to help locate the PPF microelectrode during XPS analysis. Glass capillaries with a 0.68 mm inner diameter (AM Systems, Sequim, WA, USA) were pulled on a Sachs-Flaming Micropipette Puller Model PC-84 (Sutter Instruments, Novato, CA, USA) and bumped to a final inner diameter of 10-15 µm at the tip. Approximately 20 – 30 µm diameter droplets were then deposited onto the substrate under an inverted microscope Nikon Eclipse TE 300 (Nikon, Lewisville, TX, USA) at 5-10 psi for 10-100 ms using a Picospritzer (Parker Instruments, Pine Brook, NJ, USA). The solution was then allowed to evaporate for approximately 15 minutes in a 100 ºC oven.

To investigate the chemical composition of the native PPF surface, a separate sample was prepared. A cooled wafer with a carbon film was transferred from the furnace to the XPS instrument in a desiccator under $N_2$ to minimize oxidation by atmospheric oxygen and to record the XPS spectra of a freshly prepared PPF surface. No subsequent insulation steps were done for this sample.

XPS analysis was performed with a Kratos Axis Ultra DLD X-ray Photoelectron Spectrometer (Kratos Analytical Inc, Chestnut Ridge, NY, USA) using a monochromatic Al $K_\alpha$ x-ray source. The surface was mapped for the Si 2p and Ni $2p_{3/2}$ lines to spatially locate the electrode. Spectra were taken from the center of the electrode with a sampling area with diameter of 27 µm.

**AFM Imaging.**

AFM images were obtained with a MFP3D Atomic Force Microscope (Asylum Research, Santa Barbara, CA, USA) in tapping mode. After the various electrochemical modifications of PPF electrodes, the surface was examined in 5 µm by 5 µm areas. The

sampling spots were randomly chosen from different locations of the PPF electrode to ensure representative sampling and averaging. The roughness for each sample was calculated for several 1 μm by 1 μm spots in Igor Pro 6.1 (WaveMetrics Inc, Lake Oswego, OR, USA). AFM data were plotted using ARgyle Light software (Asylum Research, Santa Barbara, CA, USA).

**Scanning Electron Microscopy.**

Carbon-fiber microelectrodes were imaged before and after electrochemical treatment with an FEI Quanta 200 FEG environmental scanning electron microscope (FEI Company, Hillsboro, OR, USA).

**Optical Microscopy.**

Etched PPF microelectrodes were imaged with Nikon Eclipse TE 300 inverted microscope (Nikon, Lewisville, TX, USA). Pictures were taken with Nikon digital camera. Etched carbon-fiber microelectrodes were photographed with an IR-1000 infrared CCD monochrome video camera (DAGE-MTI, Michigan City, IN) fixed to a Nikon FN-S2N upright microscope and collected with Video Advantage ® ADX PCI card and software (Turtle Beach, Elmsford, NY). Images were processed using Adobe Photoshop (Adobe Systems, Inc, San Jose, CA, USA).

**Data Analysis.**

For adsorption studies, cyclic voltammograms for catechols were background subtracted, digitally filtered and averaged using TH-1 software (ESA Inc, Chemsfold, MA, USA) using previously reported methodology. [17] XPS data for loss of fluorine was analyzed with a one-way ANOVA with Dunnett's post test using GraphPad Prism (GraphPad Software, San Diego, CA, USA). SEM images were processed using ImageJ (Rasband, W.S., ImageJ, National Institutes of Health, Bethesda, MD, USA).

Statistical analysis of the data and generation of the plots were done using MS Excel and GraphPad Prism. All numbers are reported as averages ± standard deviation.

## RESULTS AND DISCUSSION

### Effect of Applied Potential on Background Current of Carbon Microelectrodes.

Due to its small size and geometry, the surface chemistry of the carbon-fiber microelectrode is difficult to study with modern surface-analysis techniques. To circumvent this problem, we used PPF electrodes that are more amenable to AFM and XPS analysis. PPF has been shown to be structurally similar to glassy carbon. [26] Like carbon-fiber microelectrodes, PPF was previously reported to have similar increases in sensitivity towards dopamine when extended waveforms were used with FSCV. [28] The area of the PPF electrodes in this work was 7500 $\mu m^2$ which is 7-8 times larger than the area of a 100 µm long cylindrical carbon-fiber microelectrode (~ 1000 $\mu m^2$). This area was selected as a compromise so that iR drop was only slightly greater than that of carbon-fiber microelectrodes but so that there was sufficient area for surface analysis.

The high scan rates used in FSCV induce large background currents at carbon electrodes that originate from charging of the electrode double layer [33] and oxidation and reduction of electrochemically active surface groups. [34, 35] The background current is linearly proportional to the scan rate and electrode area. Application of the extended waveforms led to increases in background currents on carbon-fiber microelectrodes (**Figure 2.1 A** - **C**). Similarly, cycling of PPF electrodes over 15 minutes with the 1.3 V waveform (**Figure 2.1 E** and **H**) and with the 1.4 V waveform (**Figure 2.1 F** and **I**) increased the background current but cycling with 1.0 V waveform did not lead to any change (**Figure 2.1 D** and **G**). The increase in the background current for the extended waveforms compared with the 1.0 V waveform was more pronounced for PPF

electrodes. The possible reason for this observation is the fact that initially PPF is mostly hydrogen terminated with only a small amount of surface oxygen groups. [27, 36] We hypothesize that this renders the microelectrode surface hydrophobic and unwettable. In turn, this unwettable surface repels the electrolyte solution and reduces the capacitance of the double layer which leads to a decreased background current.

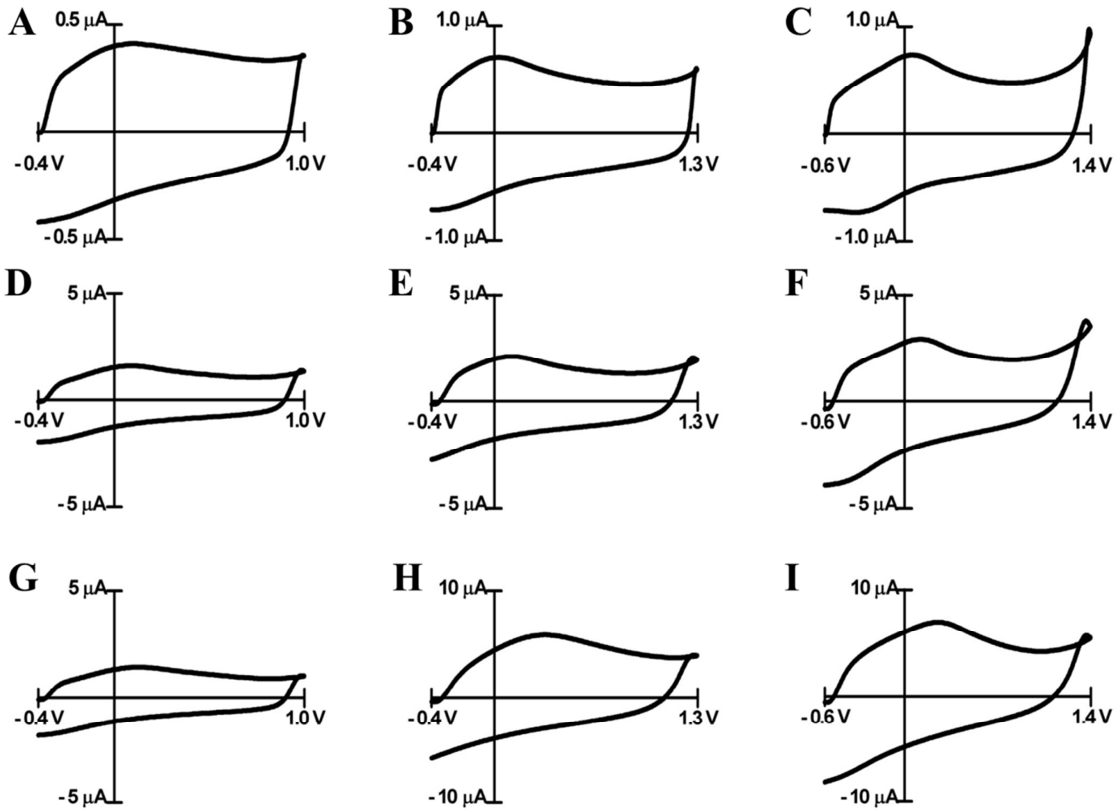


**Figure 2.1.** Cyclic voltammograms in PBS buffer recorded at carbon fiber electrodes (A-C) and PPF electrodes (D - I).

Carbon fiber microelectrodes were cycled at 60 Hz to the potential limits shown for 30 min prior to the recording of these voltammograms. Background currents for PPF electrodes are shown prior to cycling (D - F) and at the end (30 min) (G - I) of cycling. The anodic potential limits are 1.0 V for A, D and G (300 V/s), 1.3 V for B, E and H (400 V/s), and 1.4 V for C, F and I (400 V/s).

As the potential limit is made more positive, the current at the most positive potential shows a slight increase at both PPF and carbon-fiber electrodes. This feature has been previously assumed to arise from oxidation of carbon at these positive potentials. [24] Such a process could increase the amount of oxides on the carbon surface and could cause a loss of electrode mass as is found when passing current through bundles of carbon fibers to generate carbon dioxide. [37] Indeed, overoxidation of highly ordered pyrolyzed graphite (HOPG) induces the formation of blisters on the surface of HOPG presumably due to evolution of carbon dioxide. [38] Besides formation of $CO_2$, oxidation of carbon surfaces has been shown to cause exfoliation of carbon either as graphite oxide as was suggested to occur during the blistering of HOPG [38] or as carbon particles or nanocrystals. [39-41] These observations imply that scanning to the higher potentials might change the surface of carbon electrode. Surface analysis techniques were used to establish the occurrence of these processes on the carbon surface with the electrochemical treatment.

**Characterization of Surface Effects of Potential Cycling on PPF Electrodes.**

XPS was used to sample the elemental composition of PPF electrode surfaces. For a sample prepared without insulation and stored in a desiccator to prevent oxidation by atmospheric oxygen, XPS showed approximately 5% surface oxygen (**Figure 2.2A**), a value similar to that previously reported. [26, 27] Subsequent deposition of the $Si_3N_4$ insulation followed by etching with a fluoroform/oxygen plasma introduced a fluorine marker on the surface (F/C atomic ratio of 0.15 ± 0.09, **Figure 2.2B**). The deposition of fluorine on the surface after treatment with fluoroform/oxygen plasma has been previously reported. [42] Cycling the electrodes with either the 1.3 V (F/C ratio of 0.008 ± 0.008, **Figure 2.2C**) or the 1.4 V (**Figure 2.2D**, fluorine was not detected) waveforms for 30 minutes removed fluorine from the surface in a manner that depends on the

maximum applied potential (summarized in **Figure 2.2E**). In contrast, potential scans to 1.0 V do not result in the removal of the fluorine marker (data not shown). These results indicate that the fluorine introduced on the surface during the $Si_3N_4$ etching is removed by cycling the electrode to the more positive potentials of 1.3 or 1.4 V. The surface oxygen content also increased to 21 ± 8% after treatment with both 1.3 V and 1.4 V waveforms.

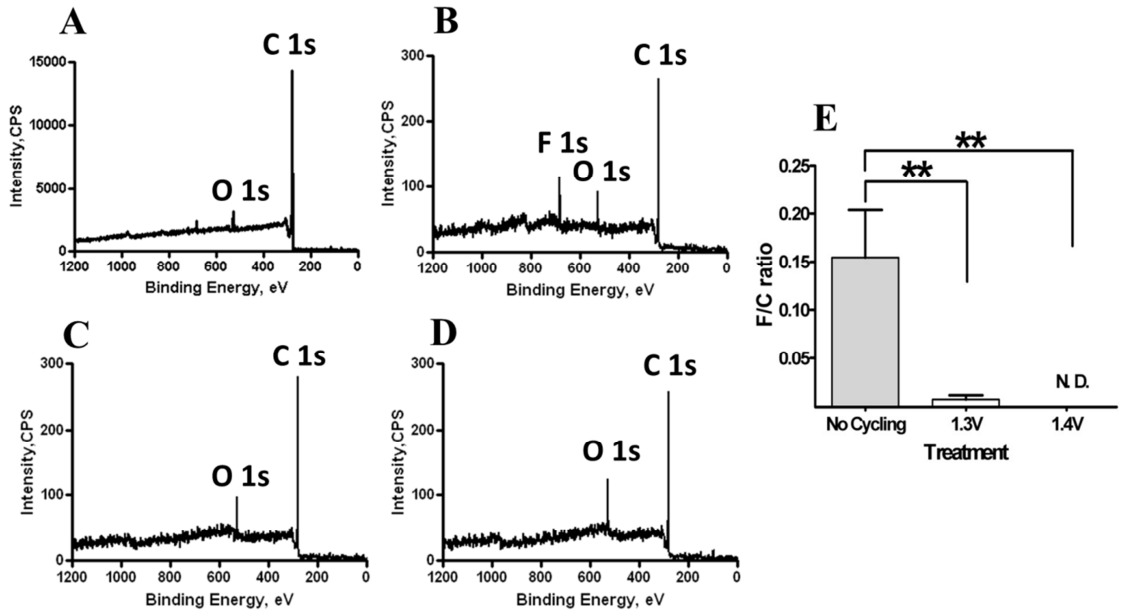


**Figure 2.2.** XPS spectra of PPF electrode surfaces.

F 1s, O 1s and C 1s indicate characteristic peaks for fluorine, oxygen and carbon, respectively. (A) PPF electrode before any treatment. (B) PPF electrode after coating with silicon nitride, removal of insulation by etching with $CHF_3/O_2$ and subsequent immersion in buffer solution. (C, D) PPF electrode after 30 minute treatment with the 1.3 V waveform and the 1.4 V waveform, respectively. Each waveform was repeated at 60 Hz. (E) Summary of F/C atomic ratios for PPF electrodes before treatment and after 1.3 V, and 1.4 V treatments. N. D. – no fluorine was detected; double asterisk represents $p < 0.01$ for one way variance ANOVA statistical test ($n = 4$ for each condition).

**Physical Changes Caused by Electrochemical Potential Limits.**

The roughness of the PPF electrodes used in this work was established with AFM. The roughness of a freshly prepared PPF surface was comparable to the roughness of the fused silica substrate (**Figure 2.3A**) with a RMS roughness of 0.45 ± 0.03 nm vs 0.94 ± 0.06 nm for the fused silica substrate (data not shown). However, when the PPF was coated with silicon nitride, and the insulator was subsequently etched and removed with a fluoroform/oxygen plasma, the resulting PPF surface showed a considerable increase in roughness (RMS 18 ± 5 nm, **Figure 2.3B**). The formation of rough features on the carbon surface was caused by the fluoroform/oxygen plasma used for $Si_3N_4$ removal that has been reported to slowly etch carbon. [42]

Surface roughness was also evaluated after electrochemical scanning. Application of the 1.3 V waveform at 60 Hz for 30 min caused a decrease in the surface roughness (RMS 9 ± 5 nm, **Figure 2.3C**) compared to the surface after etching. Smoothing of the carbon surface was even more pronounced with the 1.4 V waveform (RMS 5 ± 3 nm, **Figure 2.3D**). The difference in etching rates between the two extended waveforms is consistent with the XPS data for fluorine tracking where the larger overpotential caused more substantial removal of fluorine. **Figure 2.3E** graphically illustrates the change in surface roughness for different treatments. Repetitive scanning to 1.0 V did not alter the surface roughness (data not shown).

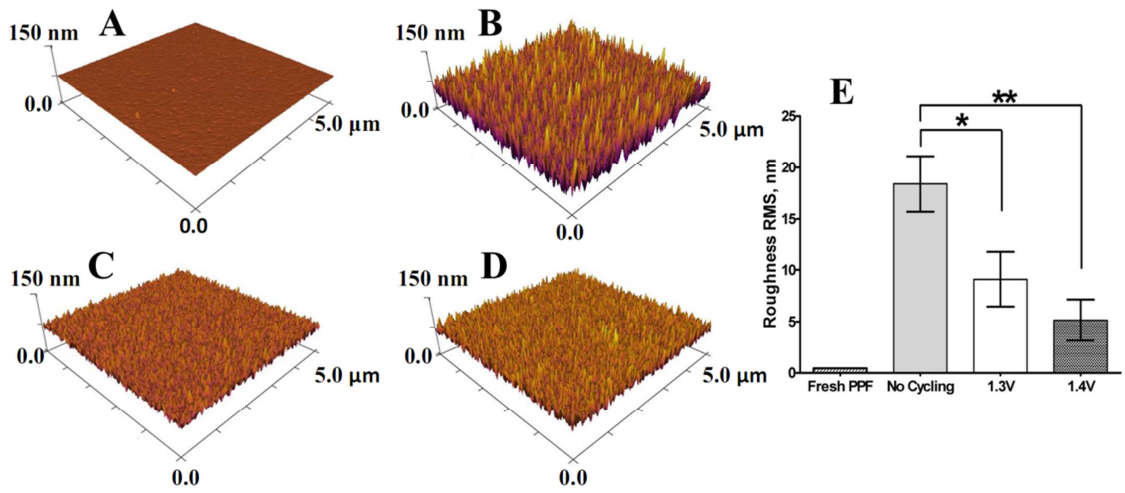


**Figure 2.3.** AFM images of the PPF electrode surface morphology after different treatment conditions.

(A) PPF electrode before any treatment. (B) PPF electrode after coating with silicon nitride, removal of insulation by etching with $CHF_3$ and subsequent immersion in buffer solution. (C, D) PPF electrodes prepared as for (B) but following 30 minute treatment with the 1.3 V waveform and the 1.4 V waveform, respectively. Each waveform was repeated at 60 Hz. (E) Summary of surface roughness for PPF electrodes before treatment and after 1.3 V, and 1.4 V treatments. Single and double asterisks represent $p < 0.05$ and $p < 0.01$, respectively, for one way variance ANOVA statistical test ($n = 3$ for each condition).

The AFM data revealed that the topography of fluoroform/oxygen plasma treated PPF electrodes before electrochemical treatment have peak-to-valley roughness values on the scale of 80 nm per 5 μm of lateral length. Application of the extended waveforms for 30 minutes led to the formation of a surface with 10 – 20 nm peak-to-valley change in height per 5 μm of lateral length. These results suggest that complete etching of a PPF electrode with a thickness of 400 nm could be accomplished within hours with these electrochemical treatments.

This hypothesis was verified by examining the electrode after multiple scans. During scanning the background current was monitored using both the 1.3 V and 1.4 V waveforms. The use of the PPF electrodes with the 1.3 V waveform applied at 60 Hz led to a decrease in the background within 10 hours and a similar disappearance of the background with the 1.4 V waveform after 1.5 hours. After the disappearance of the background, optical microscopy was used to examine the PPF microelectrodes. In both cases, the PPF electrodes had disappeared (**Figure 2.4C**, **D**). The electrodes did not disappear if they were immersed in the buffer solution (**Figure 2.4B**) for a similar time period without potential control or when they were scanned repetitively to 1.0 V. From the thickness of the PPF layer (400 nm), an estimate of the time for electrode disintegration can be established from the decrease in the background current. Etching rates were estimated to be 0.7 nm/min for the 1.3 V waveform and 4.4 nm/min for the 1.4 V waveform, both repeated at 60 Hz. The roughness of these electrodes is not directly responsible for the etching because complete electrode dissolution within similar time frames was also observed for SU-8 insulated PPF electrodes (data not shown).

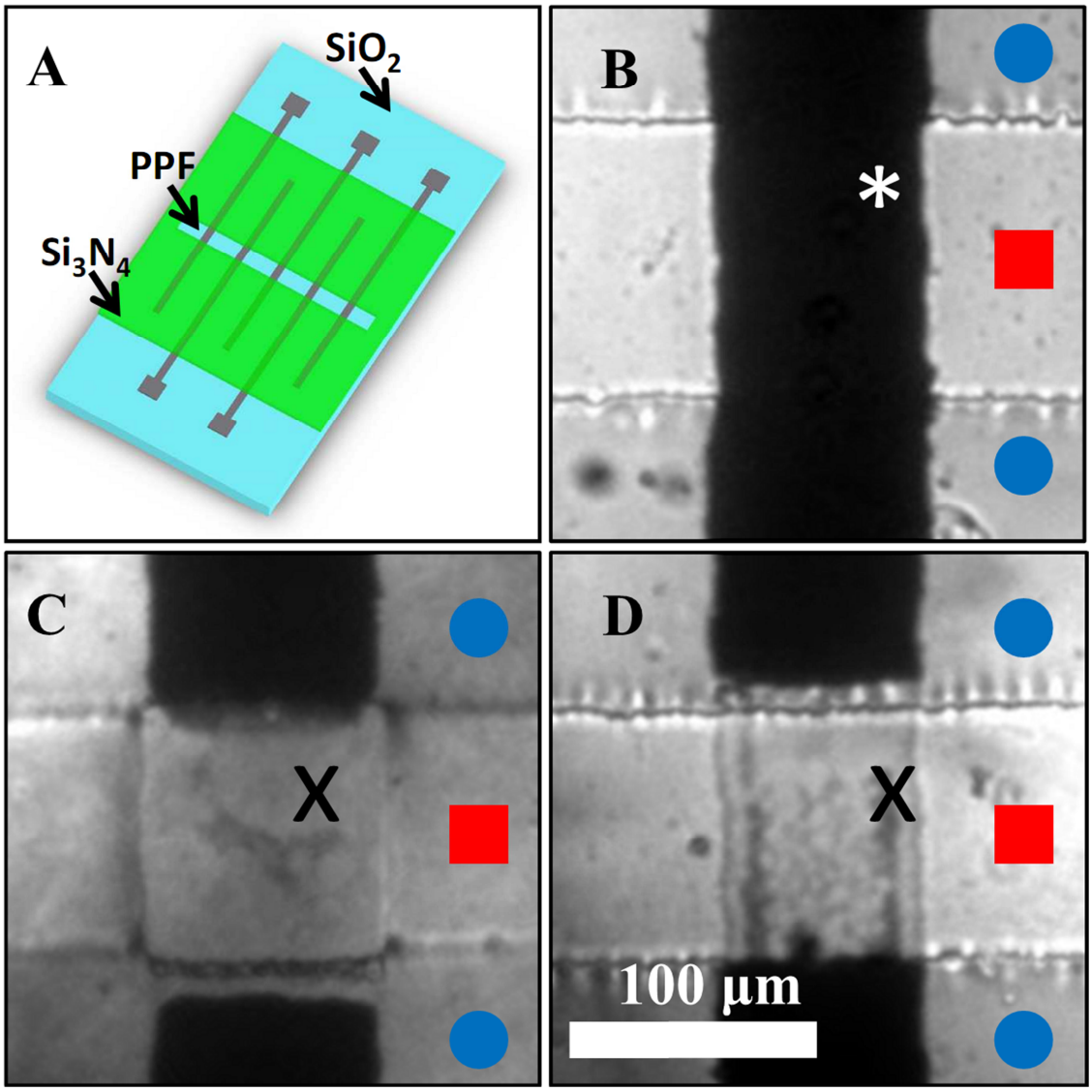


**Figure 2.4.** Images of PPF electrodes after prolonged treatment with the extended waveforms.

Optical microscopy images of PPF electrodes for different electrochemical treatment conditions. (A) schematic of microfabricated chip in which a $SiO_2$ wafer served as a substrate on which PPF electrodes were deposited followed by $Si_3N_4$ insulation. (B) PPF electrode immersed in the buffer before any electrochemical treatment. (C and D) PPF after 10 hour treatment with the 1.3 V waveform and after 1.5 hour treatment with the 1.4 V waveform, respectively. Blue circles mark silicon nitride insulation. Red squares mark areas exposed from insulation. A white asterisk marks the carbon electrode and black Xs mark etched electrodes.

Do the waveforms with extended anodic potentials cause etching of only PPF electrodes, or do they affect other forms of carbon as well? PAN-type carbon fibers were used as a comparison. Carbon-fiber microelectrodes are routinely used for voltammetric detection of catecholamines both *in vitro* and *in vivo*. The diameter of the most popular carbon fibers (T-650) used in these types of experiments is 5 μm. If etching takes place on a carbon-fiber microelectrode, then it should be possible to observe the change in carbon-fiber diameter with optical or electron microscopy. As a control experiment, the 1.0 V waveform was applied at 60 Hz for 65 hours; it showed no significant change in carbon fiber diameter (compare **Figure 2.5 A** and **B**). However, prolonged application of the 1.3 V waveform at 60 Hz led to complete etching of the carbon-fiber microelectrode within 65 hours (**Figure 2.5C**). Application of the 1.4 V waveform led to a much faster etch rate causing the complete dissolution of the carbon fiber within just 6 hours (**Figure 2.5D**). For complete etching of the carbon fiber within 6 hours as seen with the 1.4 V waveform, the etching rate would be 7.5 nm/min, in the same range as observed at PPF electrodes.

Electron microscopy revealed in greater detail the oxidative etching-induced changes of the carbon fiber (**Figure 2.5E** and **Figure 2.5F**). The average decrease in diameter of the carbon fibers was 0.9 ± 0.4 μm (n = 4) after 30 hour treatment with the 1.3 V waveform. Thus, application of the 1.3 V waveform to the carbon-fiber microelectrode produced a linear etch rate of 0.24 ± 0.11 nm/min, which is smaller than the etch rate observed for PPF electrodes.

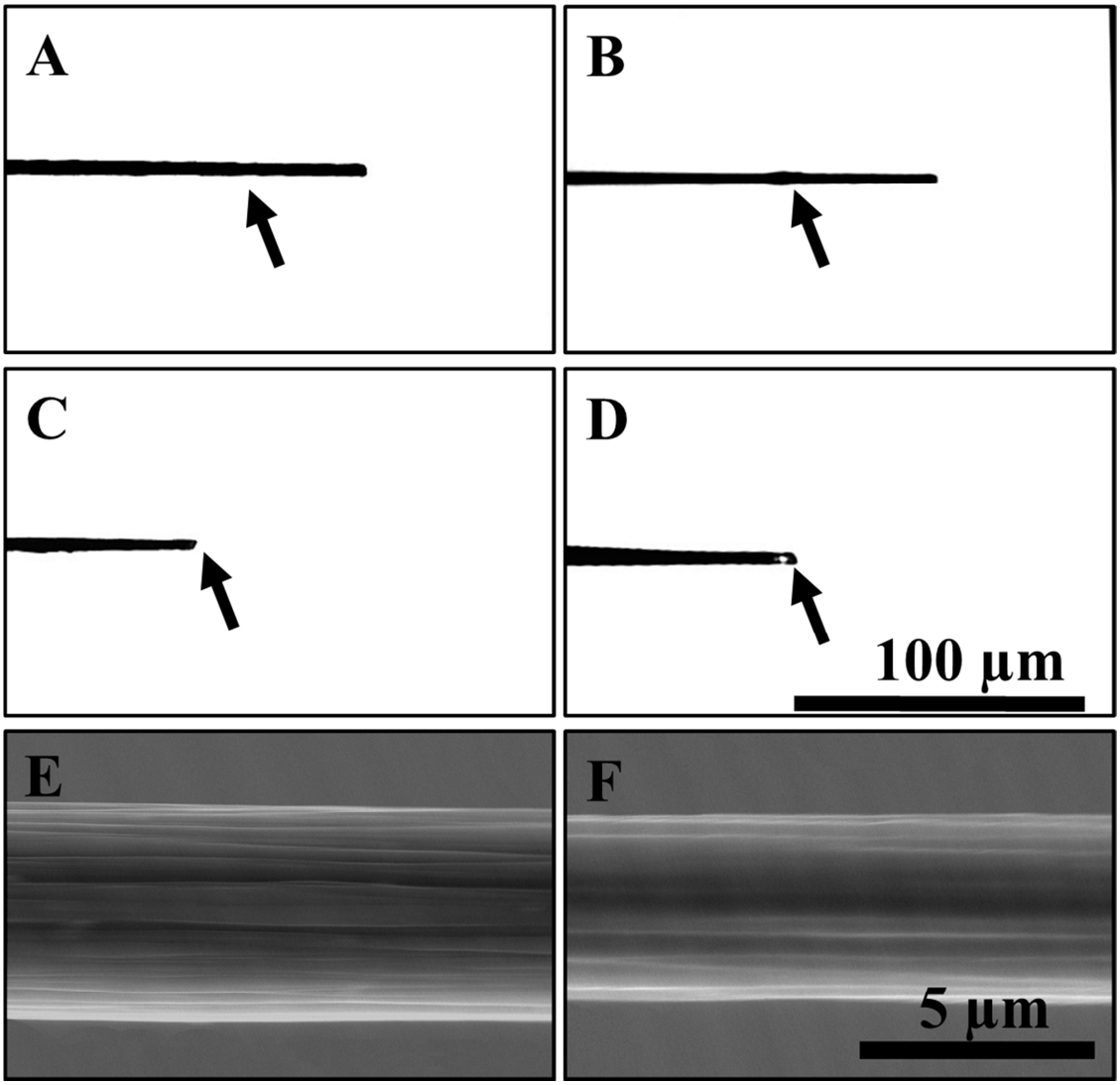


**Figure 2.5.** Images of carbon fiber microelectrodes after prolonged treatment with the extended waveforms.

Optical microscopy (A-D) and SEM (E and F) images display the disappearance of the carbon fiber tip after electrochemical etching. The black arrow indicates the location of the end of the glass seal. A carbon fiber microelectrode before treatment (A) and after 65 hours (B) of treatment with the 1.0 V waveform at 60 Hz. Treatment with the 1.3 V waveform for 65 hours at 60 Hz (C) and for 6 hours at 60 Hz with the 1.4 V waveform (D) led to the disappearance of the carbon fiber. SEM imaging of T-650 carbon fiber cylinder microelectrodes showed a 0.9 ± 0.4 µm (n = 4) reduction in diameter of the carbon fiber after 30 hours of treatment with the 1.3 V waveform. The same carbon fiber before (E) and after (F) such treatment.

The etching of the carbon fibers also takes place with the extended waveforms applied at lower frequencies. Complete etching of carbon fibers was observed after 36 hours of application of the 1.4 V waveform at 10 Hz. This was achieved after 1.3·x $10^6$ potential cycles with the 1.4 V waveform and after 1.4 x $10^7$ potential cycles with the 1.3 V waveform. Thus, the oxidative etching rate is linearly proportional to the frequency of the applied waveform.

**Increased Adsorption of Catecholamines Resulting from Oxidative Etching of Carbon-Fiber Microelectrodes.**

Regeneration of a fresh electrode in real time is advantageous during many electrochemical experiments. The chief benefit of this electrochemical surface treatment is the consistency in the electrochemical properties of carbon electrodes from experiment to experiment since the surface is renewed repeatedly. However, it is important to establish electrochemical performance of this surface towards redox active molecules. The kinetics and thermodynamics of electrochemical oxidation for catechols on carbon have been well documented, [30] and the biological importance of these molecules as neurotransmitters and metabolites makes them the analyte of choice. [7] As previously established, catecholamines strongly adsorb to the carbon surface. [16, 17] Many researchers utilize the extended waveforms because it has previously been reported to increase the adsorption of dopamine onto the electrode surface. [24] Catechols with different functional groups were used in this work to probe the nature of adsorption sites on the carbon at extended potential limits.

The use of the 1.3 V and 1.4 V waveforms significantly increased adsorption of positively charged dopamine (**Figure 2.6A**) with the 1.4 V waveform having the most pronounced effect. A lesser effect was observed for a neutral molecule, 4-methylcatechol (4MC) (**Figure 2.6B**). Again, the 1.4 V waveform demonstrated the

greatest increase in adsorption. Adsorption of negatively charged 3,4-dihydroxyphenylacetic acid (DOPAC) was also promoted by the extended waveform (**Figure 2.6C**). Curiously, the surface coverage for both 4MC and DOPAC was almost identical for the 1.0 V waveform which suggests that the catechol moiety is responsible for the affinity of these molecules towards carbon. This effect was previously explained through a π- π stacking mechanism between the catechol benzene ring and the aromatic π- π system of the carbon electrode. [43] A similar increase in surface coverage was observed for 4MC and DOPAC with the use of the 1.3 V waveform. Adsorption of DOPAC for the 1.4 V waveform was almost identical to the 1.3 V waveform. The 1.4 V waveform has a more negative holding potential (- 0.6 V) so electrostatic repulsion may be greater, hindering the adsorption of DOPAC as compared to the neutral 4MC. Overall, these data indicate that the use of extended waveforms generates a highly adsorptive surface for catechols that facilitates their detection. We hypothesize that this property can be attributed to constant regeneration of adsorption sites.

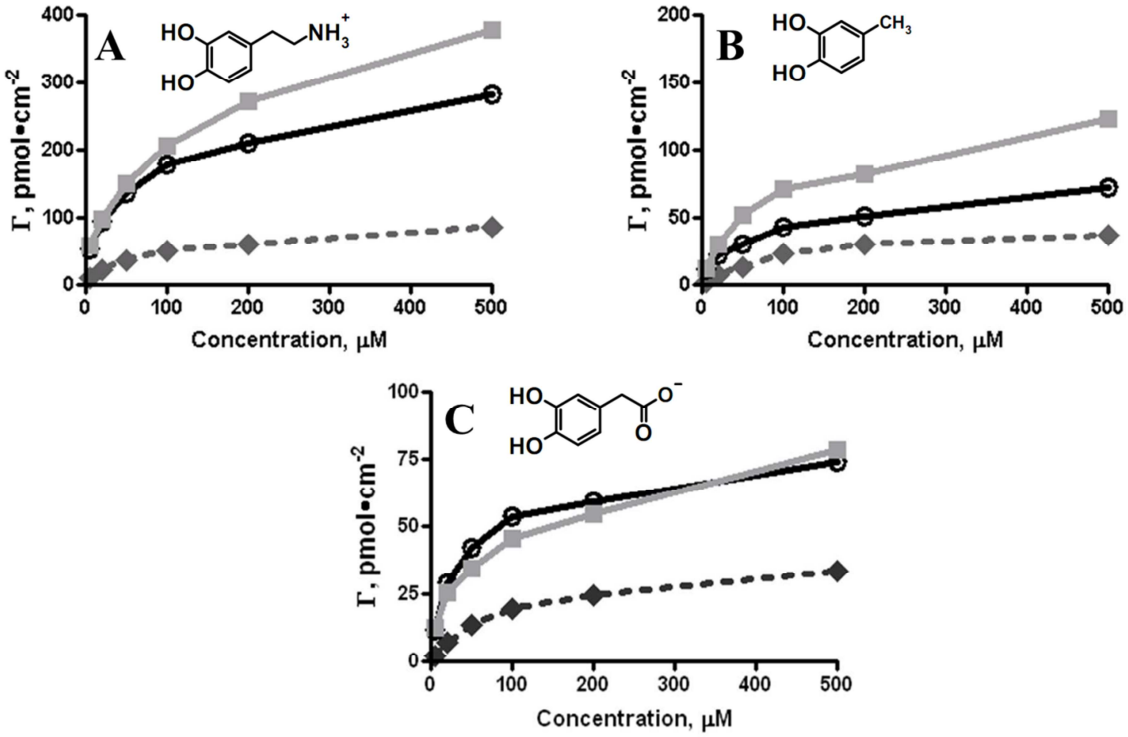


**Figure 2.6.** Application of the extended waveforms facilitates adsorption of catechols with different functional groups.

Adsorption isotherms for the 1.0 V waveform (filled dark grey diamonds), for the 1.3 V waveform (open black circles) and for the 1.4 V waveform (filled grey squares) were obtained by FSCV measurements in a flow injection system. Dopamine (A), 4MC (B) and DOPAC (C) experience increased adsorption for the extended waveforms.

Previously, this increase in catecholamine adsorption was attributed to the formation of high affinity adsorption sites composed from surface oxides. [24] The oxides are thought to be introduced by the oxidation of carbon at higher anodic potentials, and this is supported by our observation of high O/C atomic ratios by XPS after scanning to 1.3 V or 1.4 V. In previous reports the passing of a substantial amount of charge through bundles of carbon fibers has been shown also to result in a decrease in the mass of the electrode indicating that the oxidation of carbon-fiber surfaces leads to either evolution of carbon dioxide and its further dissolution in the liquid phase [37] or generation of graphite oxide [38] and carbon particles or nanocrystals. [39-41] Also electrochemical etching of carbon etching was reported before for bundles of carbon fibers, [44] glassy carbon, [45] and PPF, [44] however in all these cases high DC potentials and high current densities were used in highly basic or acidic solutions that makes it difficult to use these methods for in vivo experiments.

Interestingly, the XPS study of oxidized carbon fiber bundles indicated formation of carboxylic and ester surface bond groups on the carbon after electrooxidation. [37] The carboxylic groups could act as high affinity binding sites for dopamine due to electrostatic interactions. The possibility of similar electrostatic interaction as the origin of increased adsorption was confirmed by previous work by Hermans et al. [46] In that case, the increase in adsorption of dopamine was observed after immobilization of negatively charged sulfonate groups on the carbon surface.

We hypothesize that the carbon overoxidation proceeds through the formation of carboxylic groups on the carbon surface with further oxidation through Kolbe-like electrolysis. [47, 48] In this hypothesized reaction the oxidation of surface-confined carboxylic groups leads to the formation of carbon dioxide. The process can function in cyclical manner constantly generating carboxylic groups as well as consuming them by

formation of $CO_2$. Our hypothesis implies that cyclic regeneration prevents fouling of active sites by the irreversible adsorption of impurities and products of oxidation of analytes.

**Recovery of Fouled Carbon Microelectrodes by Overoxidative Surface Renewal.**

To test the hypothesis that the continuous etching of the carbon electrode with the use of extended waveforms regularly regenerates a fresh carbon surface, we purposefully fouled the carbon-fiber microelectrodes by electropolymerization of tyramine. The electrooxidation products of tyramine are known to polymerize and form an impermeable film on the electrode surface which deteriorates electrode sensitivity. [49-51] Carbon-fiber microelectrodes were first treated with the 1.3 V waveform (60 Hz) for 15 minutes to generate a fresh and active surface. Subsequently, the response to 500 nM dopamine in a flow injection system with the 1.0 V waveform (10 Hz) was measured. This waveform was shown not to alter the carbon fiber surface (**Figure 2.7A** and **D**, data for 3 microelectrodes pooled together). The sensitivity of the electrodes was 19 ± 4 nA for 500 nM dopamine. The microelectrodes were then passivated by immersing them in a 15 mM solution of tyramine, and the 1.0 V waveform (10 Hz) was applied to the electrode for 15 minutes. The electrodes were then tested for their sensitivity to dopamine and it was found that tyramine treatment decreased the sensitivity of the electrode to dopamine to 0.6 ± 0.4 nA or 3 % of its initial value.

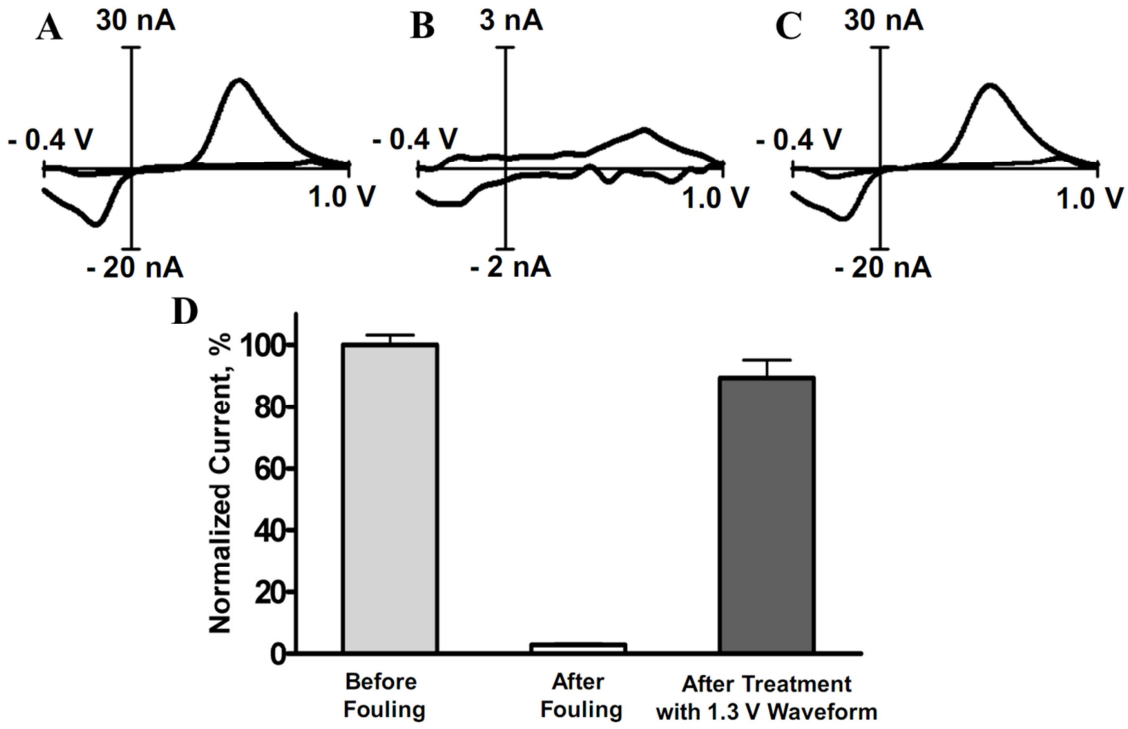


**Figure 2.7.** Sensitivity of a carbon fiber towards 500 nM dopamine fouled by polymerization of tyramine is recovered by brief application of the extended waveform.

The sensitivity was monitored with flow injection analysis of 500 nM dopamine. (A) A representative background subtracted cyclic voltammogram for dopamine before fouling. (B) Electrode fouling by cycling in 15 mM tyramine for 15 minutes almost completely abolishes sensitivity to dopamine. (C) The sensitivity of the electrode is completely recovered by cycling for 15 minutes with the 1.3 V waveform. (D) Averaged change (n=3) in sensitivity towards dopamine at aforementioned treatment conditions shown as a percent change in cyclic voltammogram peak currents.

The cyclic voltammograms of dopamine were substantially distorted in shape (**Figure 2.7B** and **D**). However, 15 minutes of cycling with the 1.3 V waveform almost completely restored sensitivity towards dopamine (**Figure 2.7C** and **D**). These data demonstrate that the application of the extended waveform regenerates the electrode surface and creates new active sites for catecholamine adsorption. The surface cleaning induced by the extended waveform also confirms previously suggested activation of carbon surface if scanned to 1.4 V that facilitates oxidation of histamine on carbon-fiber microelectrode. [52]

**CONCLUSIONS.**

This work demonstrates that the use of the waveforms with extended anodic potentials for FSCV (up to 1.3 V and 1.4 V vs Ag/AgCl) at carbon electrodes causes oxidative etching of the surface, a process that is not detectable with similar scans to 1.0 V. PPF microelectrodes were used to establish the effect with the aid of surface analysis techniques (XPS and AFM). Both XPS and AFM tracking of surface integrity showed etching of the carbon electrode following the application of these waveforms. Exposure of PPF microelectrodes to the extended waveforms for long periods of time (up to 10 hours) led to complete etching of the electrodes, confirmed with optical microscopy. Oxidative etching was shown to occur on carbon-fiber microelectrodes with complete removal observed after 65 hours (for the 1.3 V waveform) or 6 hours (for the 1.4 V waveform). We postulate that the etching occurs as a consequence of evolution of carbon dioxide or exfoliation of graphite oxide and/or carbon particles take place. Oxidative etching of the carbon electrodes with the extended waveforms provides a number of benefits in electroanalytical detection.

The important result of oxidative etching is the continuous regeneration of a fresh carbon surface. The ability to renew electrode surfaces helps to prevent electrode fouling. The demonstrated effect maybe the reason why carbon-fiber microelectrodes remain active in vivo which makes a carbon microelectrode a useful analytical tool for the in vivo detection of catecholamines since the state of the surface can be restored by a simple electrochemical procedure. In addition, microelectrodes with a renewable surface open new horizons for the use of waveforms with extended anodic potential limits for the electrochemical detection in chemically complex environments since this continual surface regeneration prevents electrode fouling and maintenance of electrode sensitivity.

## REFERENCES


1. McCreery, R. L., *Carbon electrodes: structural effects on electron transfer kinetics*. Marcel-Dekker: New York, 1991; Vol. 17, p 221-373.

2. Kissinger, P. T.; Heineman, W. R., *Laboratory Techniques in Electroanalytical Chemistry*. Marcel Dekker Inc: 1996.

3. Pandolfo, A. G.; Hollenkamp, A. F., Carbon properties and their role in supercapacitors. *Journal of Power Sources* 2006, 157, (1), 11-27.

4. McCreery, R. L., Advanced carbon electrode materials for molecular electrochemistry. *Chemical Reviews* 2008, 108, (7), 2646-2687.

5. Balasubramanian, K.; Burghard, M., Biosensors based on carbon nanotubes. *Analytical and Bioanalytical Chemistry* 2006, 385, (3), 452-468.

6. Avouris, P.; Chen, Z. H.; Perebeinos, V., Carbon-based electronics. *Nature Nanotechnology* 2007, 2, (10), 605-615.

7. Robinson, D. L.; Hermans, A.; Seipel, A. T.; Wightman, R. M., Monitoring rapid chemical communication in the brain. *Chemical Reviews* 2008, 108, (7), 2554-2584.

8. Kita, J. M.; Wightman, R. M., Microelectrodes for studying neurobiology. *Current Opinion in Chemical Biology* 2008, 12, (5), 491-496.

9. Owesson-White, C. A.; Cheer, J. F.; Beyene, M.; Carelli, R. M.; Wightman, R. M., Dynamic changes in accumbens dopamine correlate with learning during intracranial self-stimulation. *Proceedings of the National Academy of Sciences of the United States of America* 2008, 105, (33), 11957-11962.

10. Roitman, M. F.; Wheeler, R. A.; Wightman, R. M.; Carelli, R. M., Real-time chemical responses in the nucleus accumbens differentiate rewarding and aversive stimuli. *Nature Neuroscience* 2008, 11, (12), 1376-1377.

11. Zachek, M. K.; Hermans, A.; Wightman, R. M.; McCarty, G. S., Electrochemical dopamine detection: Comparing gold and carbon fiber microelectrodes using background subtracted fast scan cyclic voltammetry. *Journal of Electroanalytical Chemistry* 2008, 614, (1-2), 113-120.

12. Fagan, D. T.; Hu, I. F.; Kuwana, T., Vacuum Heat-Treatment for Activation of Glassy-Carbon Electrodes. *Analytical Chemistry* 1985, 57, (14), 2759-2763.

13. Poon, M.; Mccreery, R. L., Insitu Laser Activation of Glassy-Carbon Electrodes. *Analytical Chemistry* 1986, 58, (13), 2745-2750.

14. Strand, A. M.; Venton, B. J., Flame etching enhances the sensitivity of carbon-fiber microelectrodes. *Analytical Chemistry* 2008, 80, (10), 3708-3715.

15. Chen, P. H.; McCreery, R. L., Control of electron transfer kinetics at glassy carbon electrodes by specific surface modification. *Analytical Chemistry* 1996, 68, (22), 3958-3965.

16. Baur, J. E.; Kristensen, E. W.; May, L. J.; Wiedemann, D. J.; Wightman, R. M., Fast-Scan Voltammetry of Biogenic Amines. *Analytical Chemistry* 1988, 60, (13), 1268-1272.

17. Bath, B. D.; Michael, D. J.; Trafton, B. J.; Joseph, J. D.; Runnels, P. L.; Wightman, R. M., Subsecond adsorption and desorption of dopamine at carbon-fiber microelectrodes. *Analytical Chemistry* 2000, 72, (24), 5994-6002.

18. Gotch, A. J.; Kelly, R. S.; Kuwana, T., Characterization and modeling of the nonfaradaic response of ultrahigh surface area carbon fibers by electrochemical flow injection analysis. *Journal of Physical Chemistry B* 2003, 107, (4), 935-941.

19. Xie, Y. M.; Sherwood, P. M. A., X-Ray Photoelectron Spectroscopic Studies of Carbon-Fiber Surfaces .11. Differences in the Surface-Chemistry and Bulk Structure of Different Carbon-Fibers Based on Poly(Acrylonitrile) and Pitch and Comparison with Various Graphite Samples. *Chemistry of Materials* 1990, 2, (3), 293-299.

20. Gonon, F.; Buda, M.; Cespuglio, R.; Jouvet, M.; Pujol, J. F., Invivo Electrochemical Detection of Catechols in the Neostriatum of Anesthetized Rats - Dopamine or Dopac. *Nature* 1980, 286, (5776), 902-904.

21. Gonon, F. G.; Fombarlet, C. M.; Buda, M. J.; Pujol, J. F., Electrochemical Treatment of Pyrolytic Carbon-Fiber Electrodes. *Analytical Chemistry* 1981, 53, (9), 1386-1389.

22. Kovach, P. M.; Ewing, A. G.; Wilson, R. L.; Wightman, R. M., Invitro Comparison of the Selectivity of Electrodes for Invivo Electrochemistry. *Journal of Neuroscience Methods* 1984, 10, (3), 215-227.

23. Hafizi, S.; Kruk, Z. L.; Stamford, J. A., Fast Cyclic Voltammetry - Improved Sensitivity to Dopamine with Extended Oxidation Scan Limits. *Journal of Neuroscience Methods* 1990, 33, (1), 41-49.

24. Heien, M. L. A. V.; Phillips, P. E. M.; Stuber, G. D.; Seipel, A. T.; Wightman, R. M., Overoxidation of carbon-fiber microelectrodes enhances dopamine adsorption and increases sensitivity. *Analyst* 2003, 128, (12), 1413-1419.

25. Kim, J.; Song, X.; Kinoshita, K.; Madou, M.; White, B., Electrochemical studies of carbon films from pyrolyzed photoresist. *Journal of the Electrochemical Society* 1998, 145, (7), 2314-2319.

26. Ranganathan, S.; McCreery, R.; Majji, S. M.; Madou, M., Photoresist-derived carbon for microelectromechanical systems and electrochemical applications. *Journal of the Electrochemical Society* 2000, 147, (1), 277-282.

27. Ranganathan, S.; McCreery, R. L., Electroanalytical performance of carbon films with near-atomic flatness. *Analytical Chemistry* 2001, 73, (5), 893-900.

28. Zachek, M. K.; Takmakov, P.; Moody, B.; Wightman, R. M.; McCarty, G. S., Simultaneous Decoupled Detection of Dopamine and Oxygen Using Pyrolyzed Carbon Microarrays and Fast-Scan Cyclic Voltammetry. *Analytical Chemistry* 2009, 81, (15), 6258-6265.

29. Cahill, P. S.; Walker, Q. D.; Finnegan, J. M.; Mickelson, G. E.; Travis, E. R.; Wightman, R. M., Microelectrodes for the measurement of catecholamines in biological systems. *Analytical Chemistry* 1996, 68, (18), 3180-3186.

30. Deakin, M. R.; Wightman, R. M., The Kinetics of Some Substituted Catechol/Ortho-Quinone Couples at a Carbon Paste Electrode. *Journal of Electroanalytical Chemistry* 1986, 206, (1-2), 167-177.

31. Gerhardt, G.; Adams, R. N., Determination of Diffusion-Coefficients by Flow-Injection Analysis. *Analytical Chemistry* 1982, 54, (14), 2618-2620.

32. Kristensen, E. W.; Wilson, R. L.; Wightman, R. M., Dispersion in Flow-Injection Analysis Measured with Microvoltammetric Electrodes. *Analytical Chemistry* 1986, 58, (4), 986-988.

33. Bard, A. J.; Faulkner, L. R., *Electrochemical Methods*. Wiley New York: 2001.

34. Kawagoe, K. T.; Garris, P. A.; Wightman, R. M., Ph-Dependent Processes at Nafion(R)-Coated Carbon-Fiber Microelectrodes. *Journal of Electroanalytical Chemistry* 1993, 359, (1-2), 193-207.

35. Runnels, P. L.; Joseph, J. D.; Logman, M. J.; Wightman, R. M., Effect of pH and surface functionalities on the cyclic voltammetric responses of carbon-fiber microelectrodes. *Analytical Chemistry* 1999, 71, (14), 2782-2789.

36. Hermans, A. Fabrication and applications of dopamine-sensitive electrodes. Ph. D. Thesis, University of North Carolina at Chapel Hill, 2007.

37. Yue, Z. R.; Jiang, W.; Wang, L.; Gardner, S. D.; Pittman, C. U., Surface characterization of electrochemically oxidized carbon fibers. *Carbon* 1999, 37, (11), 1785-1796.

38. Goss, C. A.; Brumfield, J. C.; Irene, E. A.; Murray, R. W., Imaging the Incipient Electrochemical Oxidation of Highly Oriented Pyrolytic-Graphite. *Analytical Chemistry* 1993, 65, (10), 1378-1389.

39. Zhou, J. G.; Booker, C.; Li, R. Y.; Zhou, X. T.; Sham, T. K.; Sun, X. L.; Ding, Z. F., An electrochemical avenue to blue luminescent nanocrystals from multiwalled carbon nanotubes (MWCNTs). *Journal of the American Chemical Society* 2007, 129, (4), 744-745.

40. Lu, J.; Yang, J. X.; Wang, J. Z.; Lim, A. L.; Wang, S.; Loh, K. P., One-Pot Synthesis of Fluorescent Carbon Nanoribbons, Nanoparticles, and Graphene by the Exfoliation of Graphite in Ionic Liquids. *ACS Nano* 2009, 3, (8), 2367-2375.

41. Zheng, L. Y.; Chi, Y. W.; Dong, Y. Q.; Lin, J. P.; Wang, B. B., Electrochemiluminescence of Water-Soluble Carbon Nanocrystals Released Electrochemically from Graphite. *Journal of the American Chemical Society* 2009, 131, (13), 4564-+.

42. Lee, C. M.; Pai, Y. H.; Shieu, F. S., Ultrahydrophobic and Microporous Electrodes Fabricated by Fluorocarbon Plasma Etching of Carbon Fiber. *Journal of the Electrochemical Society* 2009, 156, (8), B923-B926.

43. Soriaga, M. P.; Hubbard, A. T., Determination of the Orientation of Adsorbed Molecules at Solid-Liquid Interfaces by Thin-Layer Electrochemistry - Aromatic-Compounds at Platinum-Electrodes. *Journal of the American Chemical Society* 1982, 104, (10), 2735-2742.

44. Ssenyange, S.; Du, R.; Mcdermott, M. T., Fabrication of arrays of carbon micro- and nanostructures via electrochemical etching. *Micro & Nano Letters* 2009, 4, (1), 22-26.

45. Kiema, G. K.; Aktay, M.; McDermott, M. T., Preparation of reproducible glassy carbon electrodes by removal of polishing impurities. *Journal of Electroanalytical Chemistry* 2003, 540, 7-15.

46. Hermans, A.; Seipel, A. T.; Miller, C. E.; Wightman, R. M., Carbon-fiber microelectrodes modified with 4-sulfobenzene have increased sensitivity and selectivity for catecholamines. *Langmuir* 2006, 22, (5), 1964-1969.

47. Kolbe, H., Zersetzung der Valeriansäure durch den elektrischen Strom. *Annalen der Chemie und Pharmacie* 1849, 64 (3), 339–341.

48. Lund, H.; Hammerich, O., *Organic Electrochemistry*. 4th ed.; M. Dekker: New York, 2001; p vii, 1393 p.

49. Tenreiro, A. M.; Nabais, C.; Correia, J. P.; Fernandes, F. M. S. S.; Romero, J. R.; Abrantes, L. M., Progress in the understanding of tyramine electropolymerisation mechanism. *Journal of Solid State Electrochemistry* 2007, 11, (8), 1059-1069.

50. de Castro, C. M.; Vieira, S. N.; Goncalves, R. A.; Brito-Madurro, A. G.; Madurro, J. M., Electrochemical and morphologic studies of nickel incorporation on graphite electrodes modified with polytyramine. *Journal of Materials Science* 2008, 43, (2), 475-482.

51. Cooper, S. E.; Venton, B. J., Fast-scan cyclic voltammetry for the detection of tyramine and octopamine. *Analytical and Bioanalytical Chemistry* 2009, 394, (1), 329-336.

52. Pihel, K.; Hsieh, S.; Jorgenson, J. W.; Wightman, R. M., Electrochemical Detection of Histamine and 5-Hydroxytryptamine at Isolated Mast-Cells. *Analytical Chemistry* 1995, 67, (24), 4514-4521.

# Chapter 3

# Characterization of Local pH Changes in Brain Using Fast-Scan Cyclic Voltammetry with Carbon Microelectrodes.

## INTRODUCTION

Tight regulation of tissue pH is essential for living organisms. [1] The homeostatic value of pH represents a compromise between a multitude of processes that either generate, or consume both acidic and basic species. The most important factors in pH control are the processes of energy conversion and respiration. In higher-order mammals the brain consumes the most energy of any organ, accounting for up to 25% of the total metabolic energy expenditure. [2] This large energy demand can be accomplished only through the fast delivery of nutrients and soluble gasses, such as oxygen. Besides sizable energy requirements, the brain also requires approximately 20% of the cardiovascular output. [2] Neural activity is heterogeneous throughout the brain, and localized activation of certain brain regions will increase the local rate of metabolism, and subsequently local cerebral blood flow. [2] This link between region specific neural activity and the increase in regional consumption of nutrients (glucose) and oxygen is the basis for numerous brain imaging techniques such as blood oxygenation level dependent functional magnetic resonance imaging (BOLD fMRI) and positron emission tomography (PET). [2] Monitoring pH in an intact brain, therefore, could provide important information regarding the mechanisms of metabolism and blood flow.

There are two major counteracting processes that control pH in the brain. Generally, metabolism involves the utilization of glucose either aerobically, with

production of carbon dioxide, or anaerobically with production of lactic acid and carbon dioxide. The production of these species results in an acidic pH shift. [2-4] In concert with metabolism, a spike in neural activity causes an increase in local blood flow that facilitates the clearance of carbon dioxide, which is expired through the respiratory system, [5] leading to local alkaline pH shifts. The rapid dynamics of metabolism and carbon dioxide clearance suggests that local changes in pH can be used as a measurement of regional neural activity, which could help understand biological bases of behavior. [6, 7] This opportunity provides the motivation for the development of a technique for accurate and spatially precise measurements of pH in the brain of freely moving animals.

There are several types of existing analytical methods for in vivo pH measurements. [8] The first group of techniques consists of spectroscopic methods based on pH-induced changes in absorbance or fluorescence of pH sensitive dyes, or on the chemical shifts in nuclear magnetic resonance (NMR) signal for phosphorus in phosphate groups. [2] Methods based on spectroscopy in the visible spectrum are widely used for in vitro studies, but they are less convenient to use for in vivo pH measurements. NMR based imaging has the advantage of being non-invasive, however, in animal experiments NMR does not allow for behavioral paradigms that require unrestricted animal movement.

The second group of methods is based on potentiometric measurements, implementing pH-sensitive microelectrodes. These ion-selective sensors are in the form of either glass microelectrodes [9] or solid state microelectrodes based on metal oxides with iridium oxide being the most popular. [10] These methods are advantageous for in vitro tissue preparations where the chemical composition of the solution can be controlled. However, the transfer of these techniques for pH measurements in freely

moving animals is problematic. Glass microelectrodes are fragile and can easily break during implantation or during the experiment. Metal oxide microelectrodes are robust but they are prone to interference from redox species, [11] such as 3,4-dihydroxyacetic acid (DOPAC) and ascorbic acid that are present in the extracellular fluid. [12] Also, obtaining subsecond temporal resolution is difficult with these probes. [13] Other limitations of potentiometric measurements in general are their substantial drift, and their susceptibility to electronic noise. Indeed, environmental factors that alter the electrode potential can be mistakenly identified as a pH shifts. [14]

Fast-scan cyclic voltammetry (FSCV) with carbon-fiber microelectrodes was previously described as a method to measure pH in the brain in vivo. [5, 15, 16] The advantages of this approach to measuring local pH changes include the small probe size that leads to minimal tissue damage [17], excellent spatial resolution, subsecond temporal resolution and the ability to use the sensor chronically. [18] Another distinguishing feature of FSCV detection of pH is the presence of a characteristic cyclic voltammogram (CV) for pH changes. The CV can be used as an electrochemical fingerprint for the qualitative identification of a pH signal, which can help to avoid any ambiguity associated with experimental artifacts that can be present using potentiometric measurements.

In addition to pH measurement, carbon-fiber microelectrodes coupled with FSCV are used for detection of catecholamines in vitro and in vivo. [19, 20] In previous studies in vivo shifts in pH were considered to be an interference for dopamine detection, and attempts were made to lessen the amplitude of this interference. [21] Since then, advancements in the field of in vivo voltammetry such as an increase in sensitivity towards dopamine, [22] the use of principal component regression for analysis of in vivo data [23] and the establishment of the physiological relevance of in vivo pH shifts after

electrical stimulation [5] led to the realization that pH signals obtained with FSCV are valuable indicators of brain activity rather than an undesired artifact. [6, 15]

Cyclic voltammetry provides the opportunity to qualitatively identify an analyte through its electrochemical signature (i.e. cyclic voltammogram). [24, 25] The identification of peaks can be difficult, however, when multiple physical processes take place simultaneously. Understanding the electrochemical processes responsible for the shape of the background-subtracted cyclic voltammogram relating to pH changes is crucial for appropriate interpretation of in vivo electrochemical data because of the opportunities for chemical interference in the brain.

The fast scan rates used with in vivo cyclic voltammetry result in a substantial background current due to charging of the electrode double layer and redox reactions of electrochemically active surface groups. [21] The background current remains constant for time periods less than 90 sec, so it can be digitally subtracted from the cyclic voltammogram when recorded in the presence of the electrochemically active species.

Peaks in the background subtracted cyclic voltammogram in response to a pH change are caused by a shift in the background of carbon electrode. The shape and magnitude of the background shift are defined by the electrochemically active surface groups present on the electrode surface. Surface oxide groups such as phenols, ortho- and para-quinones, carbonyls, lactones and carboxylic acids are reported to be found on carbon surface. [26] All of these groups are either susceptible to protonation-deprotonation or electrochemical oxidation/reduction reactions involving protons. The first comprehensive analytical method for quantifying of these groups on carbon electrode surface were developed in the 1960s in the form of a Boehm titration, [27] and were subsequently improved by modern instrumental physical methods for

characterization of carbon surface. [28] However, neither of these methods can be used in situ to establish a connection between specific types of active surface groups with peaks observed in the cyclic voltammogram during an electrochemical experiment.

Despite the aforementioned advantages of in vivo pH detection using FSCV, the electrochemistry behind the origins of its CV generation is poorly characterized. Furthermore, the shape of the CV recorded in vivo often differs from those recorded in vitro. This shortcoming casts doubt on the identity of electrochemical signal observed in the brain. In this work we characterized FSCV pH signal in vitro to establish possible inferences and to make sure that FSCV measurement of pH satisfies the criteria for in vivo biosensors previously suggested. [29]

## MATERIALS AND METHODS

### Chemicals.

All chemicals were obtained from Sigma-Aldrich (St. Louis, MO, USA) unless otherwise noted and used as received. Solutions were prepared using doubly distilled deionized water. Electrochemical experiments were done in PBS buffer (140 mM NaCl, 3 mM KCl, 10 mM $NaH_2PO_4$, pH 7.4). A stock solution of 10 mM DOPAC was prepared in 0.1 N $HClO_4$ and diluted to the desired concentration immediately before use with the working buffer.

### Fabrication of Carbon Fiber Microelectrodes.

Cylindrical microelectrodes were constructed using a T-650 carbon fiber (Thornel, Amoco Corp., Greenville, SC, USA) as previously described. [30] Briefly, individual carbon fibers were aspirated into glass capillaries (A-M Systems, Carlsborg, WA, USA). Afterwards, the capillaries were pulled with a micropipette puller (Narishige, Tokyo, Japan). The carbon fibers extruding from the pulled tip were cut to length of ~

100 μm under an optical microscope. Before electrochemical experiments, electrodes were soaked in isopropanol purified with Norit A activated carbon (ICN, Costa Mesa, CA, USA) for at least 20 min to remove surface impurities. [31] Electrical connection to the carbon fiber was made with an electrolytic solution (4 M $CH_3COOK$ and 0.15 M KCl), and a stainless steel wire.

**Electrochemical Experiments.**

Cyclic voltammograms were acquired with either an EI-400 potentiostat used in two electrode mode (for flow injection experiments) or UEI (UNC Department of Chemistry Electronic Shop) potentiostat (for in vivo experiments) and TH-1 software (ESA Inc, Chemsfold, MA, USA) written in LabVIEW (National Instruments, Austin, TX, USA). The waveform was generated and the voltammetric signal was acquired with a PCI-6251 ADC/DAC card (National Instruments). A PCI-6711 DAC board (National Instruments) was used to synchronize waveform application, data acquisition and TTL pulses for the flow injection valve. The output waveform was filtered with a low pass 2 kHz filter to eliminate digitization steps as previously described. [32] Some data are presented in form of color plots. [33]

A triangular waveform with potential limits ranging from - 0.4 V to 1.3 V was used at a scan rate of 400 $Vs^{-1}$ for all voltammetric measurements. This waveform was applied at 10 Hz with a rest potential of - 0.4 V between scans. Prior to measurements, carbon-fiber microelectrodes were electrochemically pretreated with this waveform at frequency of 60 Hz for 15 minutes. [22] Potentials are reported versus an Ag/AgCl reference electrode. Electrochemical measurements were performed in a grounded Faraday cage.

All data was analyzed and plotted using TH-1 software, MS Excel (Microsoft Corporation, Redmond, WA) or GraphPad Prism (GraphPad Software, San Diego, CA, USA). All values are given as averages with sample standard deviation unless the otherwise stated.

**Flow Injection Apparatus.**

The flow-injection analysis system consisted of a syringe pump (Harvard Apparatus, Holliston, MA) that directed buffer solution through a Teflon tube to a 6-port injection valve (Rheodyne, Rohnert Park, CA, USA) at rate of 0.5 mL per minute as previously described. [34] The injection valve was controlled by a 12 V DC solenoid and was used to introduce analyte from an injection loop (volume of 0.7 mL) into an electrochemical cell. The carbon-fiber microelectrode was placed inside the opening of the Teflon tube to eliminate diffusional broadening and the reference electrode was placed within ~ 20 mm of the working electrode. [34]

**Animal Experimentation.**

In vivo experiments were conducted in male Sprague-Dawley rats (250-400 g), (Charles River Laboratories, Wilmington, MA). Rats were anesthetized with urethane (50% w/w saline solution, 3 ml/kg, i.p.) and mounted in a stereotaxic frame (Kopf instruments, Tujunga, CA) which included a mounted gas anesthesia mask (Parkland Scientific, Inc, Coral Springs, FL). The animal was provided with compressed air (60 mbar) for breathing under normal conditions. Holes for electrodes were drilled in skull precisely in the regions of interest using stereotaxic coordinates (caudate-putamen: + 1.2 mm anterior-posterior and + 2.1 mm medial-lateral to bregma for hypercapnia experiments and nucleus accumbens: + 2.2 mm anterior-posterior and +1 .5 mm medial-lateral to study the effect of DOPAC on pH change cyclic voltammograms). [35] The reference electrode (Ag/AgCl) was placed contralaterally to the working electrode. The

bipolar stimulating electrode (Plastics One, Roanoke, VA, USA) was placed in the substantia nigra/ventral tegmental area (SN/VTA) (- 5.6 mm anterior-posterior and + 1.0 mm medial-lateral to bregma). TH-1 software was used to generate biphasic stimulation pulses (60 pulses, 60 Hz, 300 µA, 2 ms per phase) which were sent to optically insulated, constant current stimulators (NeuroLog System, Hertfordshire, UK) and synchronized to occur between voltammetric scans.

The position of the working electrode (- 4.5 mm dorsal-ventral from the skull surface) and the stimulating electrode (- 7.5 mm dorsal-ventral from the skull surface) were optimized to maximize electrically evoked basic pH change. [5] Once the basic pH change after electrical stimulation was observed, hypercapnic states were induced by switching the breathing gas from compressed air to compressed carbon dioxide (also at 60 mbar) for brief period of time (5-10 seconds) and then switched back to air.

All animal protocols and care were approved by the Institutional Animal Care and Use Committee of the University of North Carolina at Chapel Hill.

## RESULTS AND DISCUSSION

### Characterization of the Peaks in Cyclic Voltammogram for pH change.

Previous work using carbon microelectrodes has suggested that two of the peaks in the background subtracted cyclic voltammogram for a pH change are due to the background shift associated with the pH-dependent electrochemical oxidation of a hydroquinone moiety on the carbon surface [21, 36-38]:

$$QH_{2s} = Q_s + 2e^- + 2H^+ \quad (3.1)$$

where $QH_{2s}$ and $Q_s$ denote the reduced and oxidized form of a surface bond hydroquinone-like moiety whose structure is unknown. There are two peaks (**Figure 3.1A**) in the background subtracted cyclic voltammogram for acidic pH shift that correspond to this electrochemical reaction. Here, these peaks are denoted as a QH-peak (for the hydroquinone to quinone transition occurring at approximately 0.3 V on the positive sweep at a pH of 7.4) and a Q-peak (for the quinone to hydroquinone transition occurring at approximately - 0.3 V on the negative sweep at a pH of 7.4). There are several pieces of evidence in support of this hypothesis. Recently, it was demonstrated that hydroxide groups exist on carbon-fiber microelectrodes when used in similar FSCV experiments. [39] Also, carbon electrodes that were purposefully modified with hydroquinone moiety show the same hydroquinone oxidation-reduction peaks on cyclic voltammograms as peaks in the background of electrochemically oxidized carbon-fiber microelectrodes. [16, 40] Furthermore, the QH-peak in the background current is located at the same potential (~ 0.09V, **Figure 3.2C**) as oxidation peak of surface immobilized hydroquinone moiety. [16] Moreover, the QH-peak shifts with pH in a similar way as it was previously reported. [21]

In addition to these two hydroquinone peaks, there is a third peak at potential of -0.2 V on the anodic sweep that denoted here as the C-peak (**Figure 3.1A** and **B**). A background subtracted cyclic voltammogram for basic pH shift (**Figure 3.1B**) implies that increase in pH decreases capacitance (C-peak) and also causes a shift of QH- and Q-peaks of the background current. The nature of the C-peak was investigated further in this work.

The advantage of using FSCV on carbon-fiber microelectrodes for the detection of pH changes is the signature voltammogram (**Figure 3.1A** and **B**) that enables qualitative identification of pH shifts. Since fast-scan cyclic voltammetry is differential technique, typically only background subtracted cyclic voltammograms are used for data representation. In a background subtracted cyclic voltammogram each peak has two possible origins. Oxidation of analyte at certain potential produces a peak after subtraction in the same fashion as it is in traditional cyclic voltammogram. Besides this, shift in position of the peaks in background produces peaks in background subtracted cyclic voltammograms. In case of pH changes both of these events might take place. Because of this, the amplitude of current for characteristic peaks in background subtracted cyclic voltammogram is used for calibration and not the peak potential as it was suggested elsewhere. [16]

The magnitude of the current for each of the peaks varies linearly with pH shifts within physiological pH range from 7.2 to 7.6. The slopes for the calibration curves are – 52 ± 2 nA/pH for the C-peak, - 42 ± 1 nA/pH for the QH-peak and 110 ± 2 nA/pH for the Q-peak (n = 3). $R^2$ values of the linear fit are 0.95, 0.97 and 0.99 for C-peak, QH-peak and Q-peak respectively.

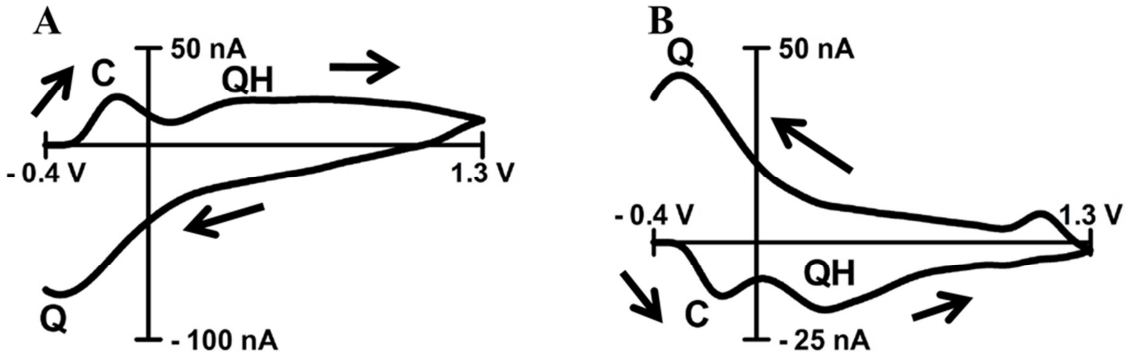


**Figure 3.1.** Background subtracted cyclic voltammograms of pH shifts.

Identification of peaks in background-subtracted cyclic voltammograms for acidic (- 0.25 pH units, A) and basic (+ 0.25 pH units, B) pH changes, taken relative to an absolute pH of 7.4. The direction of the scans is indicated by black arrows. C-, QH- and Q-peaks are labeled. For basic pH shift (B), C-peak and QH-peak are located at - 0.13 V and 0.27 V on anodic scan, respectively. Q-peak is located at - 0.3 V on cathodic scan.

**Capacitive Contributions to the Cyclic Voltammogram for pH change.**

The potentials where oxidation and reduction occur for an electrochemical reaction are a function of the propensity of a species to give and receive electrons, electron-transfer kinetics and analyte mass-transport. For these reasons electrochemical peaks in cyclic voltammograms related to a specific faradaic redox processes are generally located at well-defined positions. In contrast, the nonfaradaic process of the charging of the double layer produces peaks which are potential independent, and are instead defined by the time constant (RC) of the electrode given that the capacitance of the double layer does not change appreciably in a certain potential window. [24] The potential dependency of peaks, therefore, can be used to distinguish between faradaic and nonfaradaic processes.

To distinguish whether the observed peaks were faradaic or nonfaradaic processes, the initial potential was applied at three different values (- 0.4 V to - 0.5 and - 0.6 V). The position of the QH- and Q-peaks remained consistent for both acidic (**Figure 3.2A**) and basic (**Figure 3.2B**) pH shifts with all three initial potentials, confirming that these peaks have faradaic origin. On the contrary, the C-peak in a pH cyclic voltammogram shifted 0.1 V and 0.2 V relative to that with an initial potential of - 0.4 V for the - 0.5 and - 0.6 V potential limits respectively. This potential dependence indicates that the C-peak results from a change in a nonfaradaic process related to charging of the double layer. In the background cyclic voltammogram from which the pH changes were extracted, the potential of the C-peak coincides with a current deflection that occurs around - 0.2 V (**Figure 3.2C**) with initial potential of - 0.4V. This deflection was also shifted 0.1 V and 0.2 V for the - 0.5 and - 0.6 V potential expansions, respectively (**Figure 3.2C**). This current deflection has been previously attributed to double layer charging [22] and our current work clearly illustrates the validity of this assignment. This

result establishes a link between a change in pH and its effect on the double layer capacitance. Specifically a change in pH leads to a shift of the background current, which leads to the appearance of this peak upon background subtraction. As this peak arises from non-faradaic processes and not a chemical reaction, it will be referred as the C-peak throughout the rest of this manuscript.

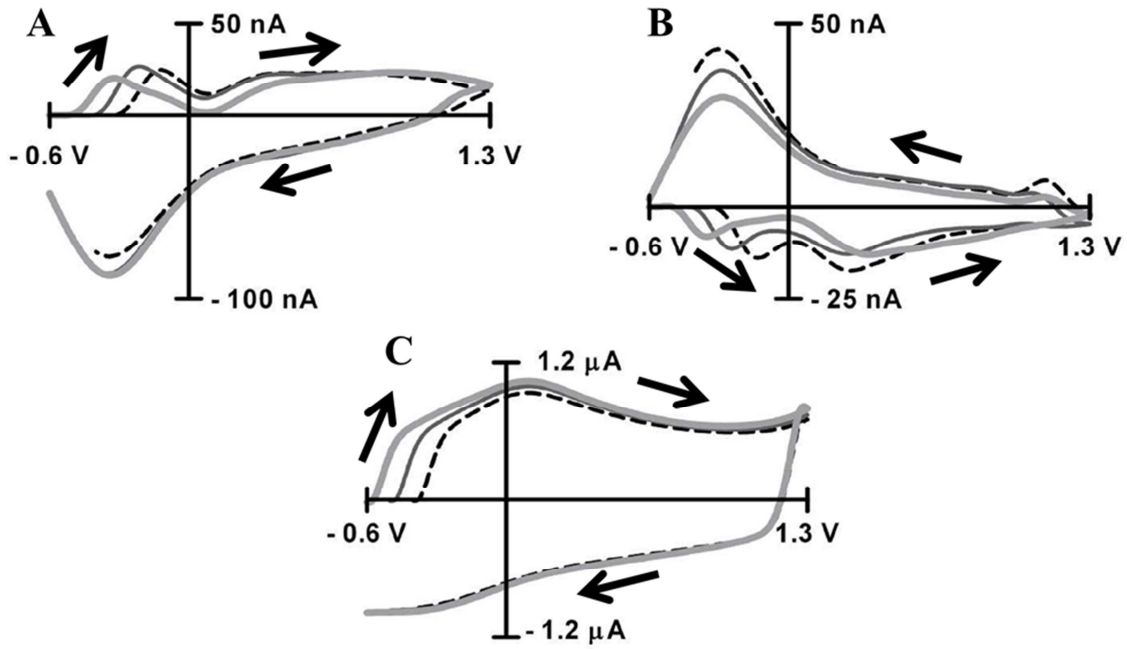


**Figure 3.2.** Capacitive peak identification relating to pH changes.

Background-subtracted cyclic voltammograms for acidic (- 0.25 pH units, A) and basic (+ 0.25 pH units, B) pH changes. Potential windows range from - 0.6 V (light gray line), - 0.5 V (dark gray line) and - 0.4 V (dotted black line) to 1.3V. Cyclic voltammograms of background current for potential windows starting from - 0.6 V (light gray line), - 0.5 V (dark gray line) and - 0.4V (dotted black line) to 1.3V (C). Cyclic voltammograms were recorded at scan rate of 400V $s^{-1}$ in PBS buffer at pH 7.4.

**Background-subtracted Cyclic Voltammograms due to the Adsorption of Electrochemically Inert Species.**

Background-subtracted FSCV at carbon-fiber microelectrodes was developed as a technique for detection of electrochemically active biogenic amines, [19] primarily dopamine. The electrochemical conditions used for FSCV were optimized to increase sensitivity towards catecholamines. The adsorption of catecholamines to the carbon-fiber surface is mainly responsible for the low limits of detection (tens of nM) reached by FSCV. [22] At physiological concentrations of dopamine, adsorbed molecules account for up to 95% of the electrochemical current while only 5% results from molecules that diffuse towards the microelectrode during the potential sweep. [31, 41] Catecholamine adsorption is generally achieved by holding the microelectrode for 100 milliseconds (for 10 Hz frequency) at a negative potential (- 0.4 V) between voltammetric sweeps. This leads to amplification of catecholamine adsorption due to electrostatic interaction [22] between positively charged dopamine molecules and the carbon surface. However, holding at a negative potential additionally promotes the adsorption of other species, especially those that are positively charged and those containing aromatic moieties. The contribution of adsorption to the FSCV procedure was demonstrated previously [31]; however the effect of the adsorption with respect to pH measurements was not studied.

The adsorption of organic molecules to the electrode surface will affect the charging of the double layer by changing the double-layer capacitance. Therefore, the adsorption of these species will produce background-subtracted cyclic voltammograms that can be thought of as additive to any faradaic electrochemistry that occurs. [24, 25, 31] Generally, adsorption of neutral species on the uncharged surface causes a decrease in double layer capacitance since it displaces ions in the double layer further away from the electrode. If the adsorbing species is charged, the surface has charged groups, or

electrode is held at some non-zero potential then the prediction of direction of the change in double-layer capacitance becomes more complex. Detailed quantitative description of the change in interfacial capacitance of a carbon electrode associated with adsorption is difficult because the nature and amount of active groups is unknown. Furthermore, as suggested in our previous work, [42] the composition of the carbon surface is not static but dynamically changes and depends on parameters of the electrochemical experiment (i.e. anodic potential limit). Previously, we suggested the existence of carboxylic groups on the surface of carbon-fiber microelectrode when higher anodic potential limits are used. [42] Here we investigate the adsorption of various species onto the carbon surface to test this hypothesis.

β-phenylethylamine (PEA) at pH 7.4 is an electrochemically inert, positively charged, aromatic amine and has high affinity to carbon microelectrodes held at negative potentials. [31] When exposed to the carbon-fiber surface, it adsorbs, decreasing the double layer capacitance in a potential dependent fashion. This process results in a background-subtracted cyclic voltammogram with noticeable peaks (**Figure 3.3A**). If the decrease in double layer capacitance is potential independent then it should lead to a square-like cyclic voltammogram resulting due to altering the RC constant of the electrochemical cell. However, the background subtracted cyclic voltammograms related to PEA adsorption have a well pronounced negative peak. This shape indicates desorption of PEA induced by electrostatic repulsion when the potential of the electrode goes into the positive region.

Higher concentrations of PEA led to an increase in the amount of adsorbed molecules causing a measureable change in the background current. An adsorption isotherm that relates negative charge from the cyclic voltammogram to PEA concentration can be constructed (**Figure 3.3D**). The charge, which is proportional to

surface coverage, does not reach saturation in the concentration range evaluated. This lack of saturation indicates that the adsorption mechanism is not Langmuiric, but can be described rather by a Freundlich isotherm:

$$Q = \alpha C^{\gamma} \tag{3.2}$$

where Q is charge, C is concentration and α and γ are empirical parameters. The Freundlich isotherm generally describes an adsorption process at a surface with heterogeneous adsorption sites. [43] Such is the case for carbon surfaces, as it was reported in earlier studies of electrosorption of organic molecules on carbon fibers. [44]

The tendency of electrochemically inert organic molecules to adsorb to carbon-fiber microelectrodes was previously reported for several drugs including nomifensine and GBR-12909 (dopamine transporter blockers). [45] Both of these molecules are hydrophobic, positively charged, aromatic amines at physiological pH and apparently these properties strengthen their affinity for carbon surfaces. The fact that the presence of these molecules reduces FSCV sensitivity towards dopamine suggests that they compete for the same adsorption sites as catecholamines on carbon surfaces or, which is also possible, adsorption of these molecules renders the carbon surface hydrophobic and, hence, less wettable which in turn reduces dopamine adsorption

Interestingly, adsorption of phenylacetic acid (PAA) leads to an increase in background current which is observed as a positive peak after the background subtraction (**Figure 3.3C**). At pH 7.4 PAA is a negatively charged aromatic species that is electrochemically inert. The increase in the background current can be explained by the fact that adsorption of PAA brings additional negative charge to the electrode surface which in turn shifts the electrode potential further from the potential of zero charge and

attracts more positively charged counter ions. This potential shift, therefore, leads to an increase in double layer capacitance.

However, organic aromatic molecules are not the only species that have affinity to the carbon electrode surface. Positively charged calcium ions also can adsorb to a carbon surface. This again results in a change of the background current and a cyclic voltammogram with negative peak (**Figure 3.3B**). Adsorption isotherms of $Ca^{2+}$ constructed for a range of concentrations from 5 to 500 µM also implies a Freundlich adsorption mechanism (**Figure 3.3E**). The endogenous concentration of $Ca^{2+}$ in the extracellular fluid is 1-2 mM and it is tightly regulated. [46] This concentration corresponds to the relatively flat part of the isotherm which means that moderate changes in calcium concentration should not affect the microelectrode sensitivity towards pH shifts or catecholamine detection.

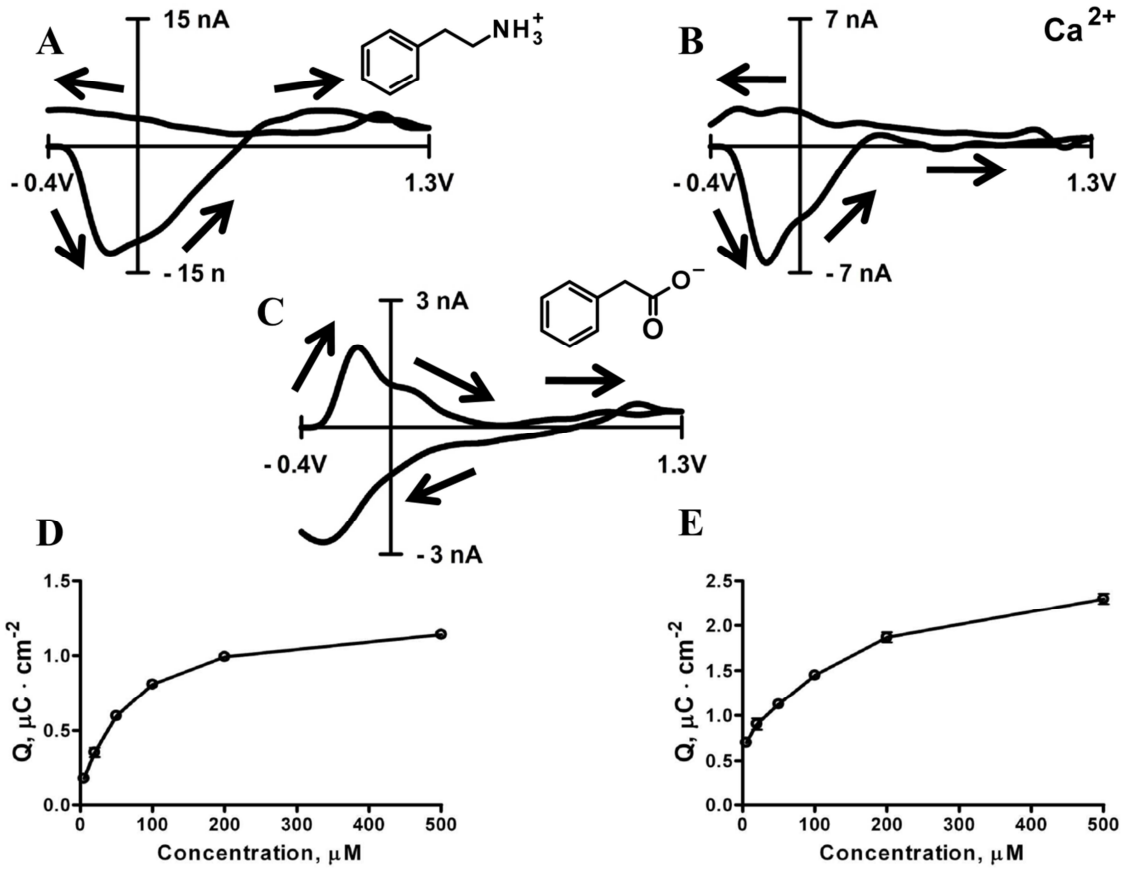


**Figure 3.3.** Adsorption of electrochemically inert species at carbon-fiber microelectrodes.

Background subtracted cyclic voltammogram for 20 μM of β-phenylethylamine (A), 20 μM $Ca^{2+}$ (B) and 20 μM phenylacetic acid (C). The dependence of adsorption-induced changes in background charge from β-phenylethylamine (D) and $Ca^{2+}$ (E). All cyclic voltammograms are the average of 5 voltammograms recorded for a 5 second bolus injection. Cyclic voltammograms were recorded at scan rate of 400 V $s^{-1}$ in PBS buffer at pH 7.4.

Previously, it was shown that both $Ca^{2+}$ and $Mg^{2+}$ ions reduce FSCV sensitivity to dopamine; [47, 48] this again suggests that these ions adsorb to the same adsorption sites as dopamine. The surface-bound carboxylic groups might be of critical importance to this adsorption process. [42] Alkali-earth metals have a strong tendency to form complexes with ligands that have carboxylic groups such as EDTA. [49] We hypothesize that the formation of such complexes with carboxylic groups on carbon surface is also possible. In fact, barium ions binding to surface bound carboxylic and hydroxylic groups on carbon was used as a labeling technique to quantify the amount of these groups with X-ray photoelectron spectroscopy (XPS); [50] therefore, the formation of these complexes with calcium is a viable possibility. Also, it was shown that calcium ions can strongly adsorb to surface immobilized carboxylic groups and completely eliminate the voltammetric peak related to protonation-deprotonation of these carboxylic groups. [51] Indirect confirmation of the carboxylic-group hypothesis may be given if the presence of calcium leads to the suppression of the C-peak in the background charging current.

**Distortion of Cyclic Voltammograms for pH Change due to Adsorption of Electrochemically Inert Species.**

The experimental data presented here implies that alteration of the double layer induced by protonation/deprotonation of the electrode surface causes the C-peak in the pH change cyclic voltammogram. Since other chemical species are present that can perturb the electrode double layer, it is logical to propose that the presence of these species in solution may alter the shape of the pH change cyclic voltammogram. This interference does not abolish the sensitivity to the pH changes, but distorts the shape of the cyclic voltammogram which can make it difficult to identify the signal for pH change.

The distortion of the pH change cyclic voltammogram in the presence of adsorbing species was investigated to provide a qualitative relationship between in vivo

and in vitro data. PEA at a concentration of 500 µM decreases the amplitude of the C-, QH- and Q-peaks (**Figure 3.4A**). Also, it changes the relative height of C-peak compared to the QH-peak. Normally, the amplitude of the C-peak is larger than QH-peak, but the addition of PEA decreased the amplitude of the C-peak to greater extent than the QH-peak, making the amplitudes of both peaks approximately equal. Calcium at a concentration of 500 µM has a similar effect on the cyclic voltammogram in addition to a more pronounced effect on the amplitude of the Q-peak (**Figure 3.4B**).

The addition of tris(hydroxymethyl)aminomethane (TRIS) at 15 mM also decreased the amplitude of all three peaks with the dramatic suppression in C-peak (**Figure 3.4C**). Traditionally, TRIS based buffer has been used for post in vivo calibration of carbon-fiber microelectrodes, but inconsistencies existed between the cyclic voltammograms obtained for pH shifts measured in vitro using TRIS buffer and those obtained through in vivo experiments. The use of TRIS buffer is therefore not advised for pH calibration since it distorts both the shape and amplitude of the response to pH changes.

The data suggest adsorptive species might interfere with detection of pH changes using FSCV with carbon-fiber microelectrodes. Brain extracellular fluid contains small organic molecules including amino acids and proteins which can adsorb to the carbon surface. [52] Nevertheless, successful use of FSCV for detection of pH shifts in dopaminergic brain regions for several years proves that this interference is minimal. [5, 6, 15] Furthermore, the recent discovery the carbon electrode surface regeneration occurs when the potential is scanned to 1.3V [42] assures that long term deterioration of the carbon electrode surface is minimized.

We recommend the use of QH-peak for pH detection. The amplitude of the C-peak is sensitive to adsorption. The Q-peak is unsatisfactory because it can be pushed to more negative potentials so it is not completely within the potential window of the cyclic voltammogram.

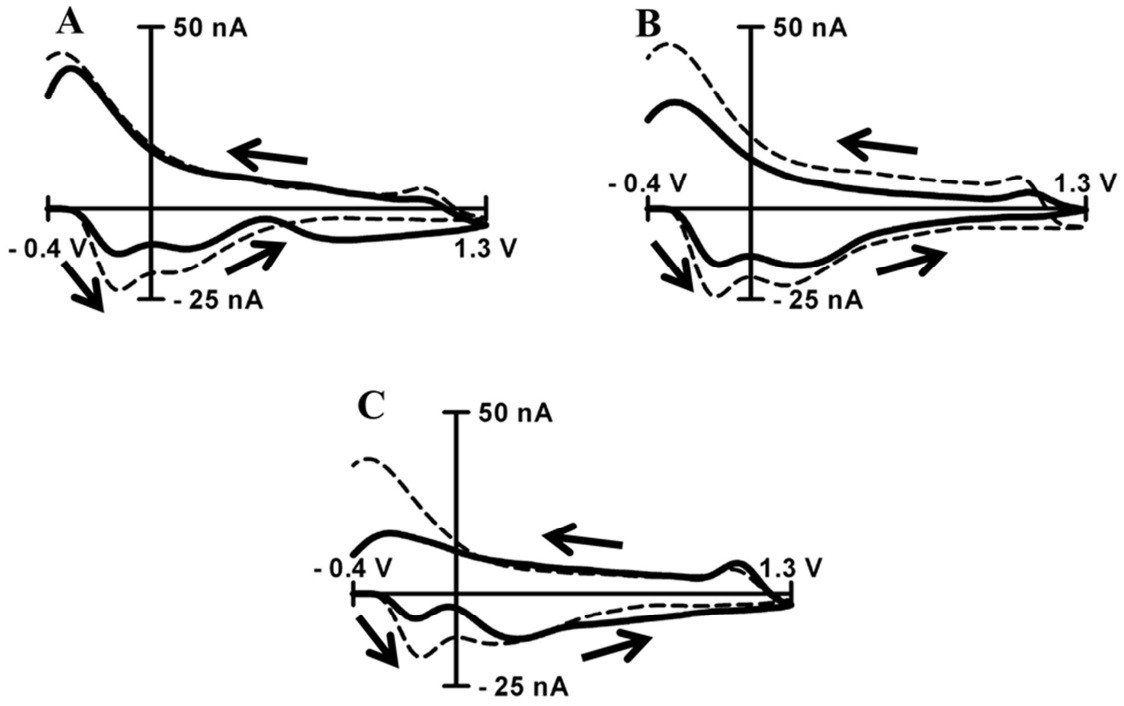


**Figure 3.4.** Interference from adsorptive species to background subtracted cyclic voltammograms for pH.

Background subtracted cyclic voltammograms for basic pH shift (+ 0.25) in PBS (dashed thin trace) and in the presence of electrochemically inert species (solid thick trace). Species of interference are β-phenylethylamine at 500 μM (A), $Ca^{2+}$ at 500 μM (B), or TRIS at 15 mM (C). Cyclic voltammograms were recorded at scan rate of 400V $s^{-1}$ in PBS buffer at pH 7.4.

**Distortion of Cyclic Voltammogram for pH Change from DOPAC.**

Changes in pH should cause a shift in the electrochemical peaks that originate from all electrochemical reactions that involve either protons or hydroxides. [38] The shift in the redox peaks of surface bound hydroquinone moieties causes the appearance of QH- and Q-peaks in cyclic voltammogram for a pH change. Besides surface bound electroactive groups, there are many electrochemically active species in the extracellular fluid of the rat striatum which may participate in redox reactions involving protons. The most abundant are ascorbic acid, uric acid, homovanillic acid and DOPAC. [53] Any of these species can potentially interfere with pH detection since they have proton-dependent electrochemistry.

DOPAC is a major metabolite of dopamine that has similar electrochemical properties. In addition, DOPAC is the catechol that is present in the brain in highest concentration. The concentration of DOPAC in rat striatum is about 20-30 μM [12, 54] compared to about 20 nM for dopamine. [55] Also, FSCV is ten times more sensitive to dopamine than DOPAC; [56] it is not enough to account for the one thousand difference in concentration between DOPAC and dopamine. This makes DOPAC a likely cause of distortion for pH cyclic voltammogram.

Since DOPAC is a catechol, it follows the same oxidation reaction pathway as other catechols (Equation 1). Thus, an acidic pH shift should shift the cyclic voltammogram for DOPAC to more positive potentials. In the background subtracted voltammogram this will result in two additional peaks on the cyclic voltammogram for a pH shift. In vitro experiments confirm this hypothesis. **Figure 3.5** shows cyclic voltammograms of DOPAC in PBS buffer and shows the appearance of additional peaks at ~ 0.6 V on the anodic scan and ~ - 0.2 V on the cathodic scan for acidic pH shift (**Figure 3.5A**). Peaks at the same potentials are also present for a basic pH shift (**Figure**

**3.5B**). These extra peaks are visible in cyclic voltammograms for electrically evoked pH change in vivo. As expected, some in vivo cyclic voltammograms indeed have these peaks (**Figure 3.5C**). The anodic peak was well pronounced and located at the same potential as it was in vitro (compare to **Figure 3.5B**) while the cathodic peak is merged together with QH-peak.

Ascorbic acid can be an interferent, but it has slow electron transfer and irreversible electrochemistry at given conditions. [22] It is unlikely that ascorbic acid is responsible for distortion of in vivo cyclic voltammogram for pH change since that distortion it features two peaks. Also, uric acid can potentially interfere, but we suspect that its extracellular concentration in rat striatum is small since tissue damage is minimal with carbon-fiber microelectrode. [57] In turn, homovanillic acid has quasi-reversible electrochemistry and can produce two peaks. However, position of peak from interference at ~ 0.6 V in cyclic voltammogram recorded in vivo makes homovanillic acid improbable candidate because at given conditions it oxidizes at ~ 0.8V, [22] thus in case of interference the peak would be at ~ 0.8V as well.

This distortion induced by DOPAC was not previously reported, however it is critical for qualitative identification of pH signal in vivo. Although DOPAC is generally absent in the post-calibration buffer, its addition should be considered to better mimic the in vivo environment.

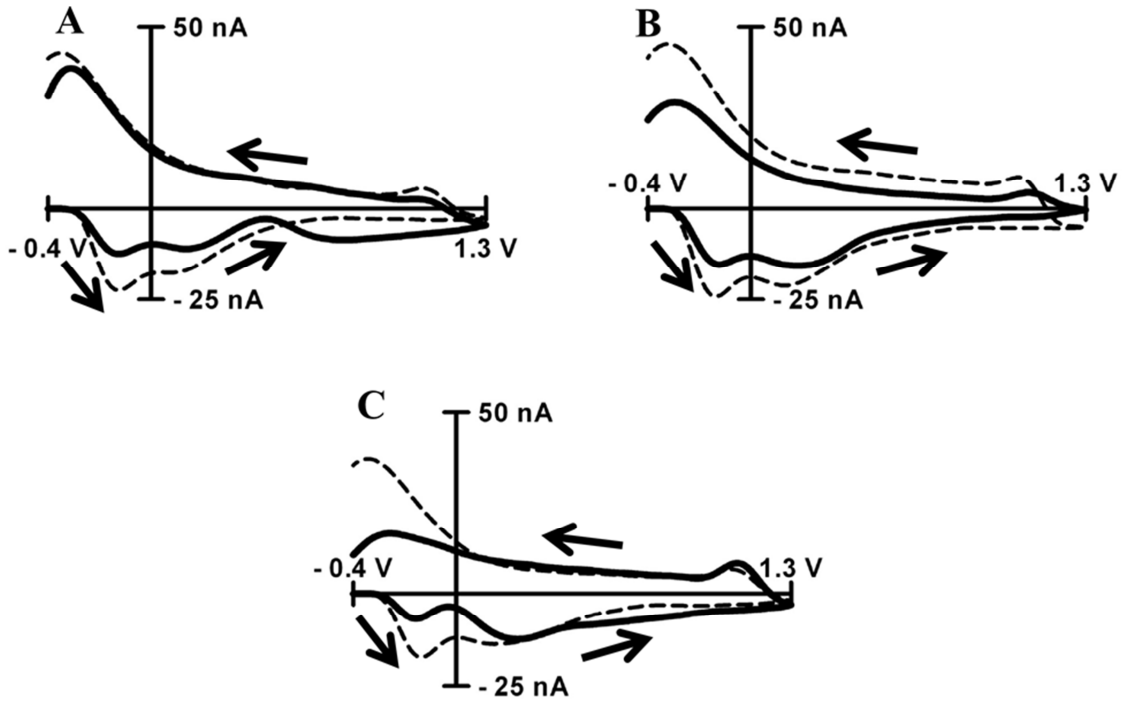


**Figure 3.5.** The effect of DOPAC adsorption on the background-subtracted pH change cyclic voltammogram.

The presence of DOPAC (20 μM) significantly distorts background-subtracted cyclic voltammograms for acidic (- 0.25 pH units, A) and basic pH change (+ 0.25 pH units, B). Cyclic voltammograms for pH shifts without DOPAC (dashed line) and with DOPAC (solid line). The cyclic voltammogram for basic pH shift in presence of DOPAC resembles certain cyclic voltammograms for pH shift recorded in brain in vivo (C). The extra peaks are marked with asterisks. Arrows show the direction of the scan. In vitro cyclic voltammograms were recorded at a scan rate of 400 V $s^{-1}$ in PBS buffer at pH 7.4. In vivo cyclic voltammograms were recorded in nucleus accumbens after electrical stimulation of dopaminergic neurons.

**Verification of FSCV pH Signal with Acidosis Induced by Hypercapnia.**

According to previously suggested criteria for the validation of signals from an in vivo biosensor, physiological relevance of the obtained data should be established. [29] In case of in vivo pH sensor, transiently induced pH shift in the brain is required. The shift should be well controlled and the physiological mechanism behind this pH change should be well understood. These requirements are necessary for establishing confidence that the pH is actual chemical species that are measured with the sensor.

Electrical stimulation of neurons is widely used in study of neuronal transmission. In our previous work we showed that electrical stimulation of dopaminergic neurons can be used to induce transient pH change. [5] However, before pH changes induced by electrical stimulation were detected with FSCV, it was not obvious that such stimulation of dopamine neurons should cause basic pH changes.

In this work the concentration of carbon dioxide in inhaled air was altered to produce hypercapnia and induce acidosis. Hypercapnia is a physiological effect caused by an increase in carbon dioxide in the blood and it is well known to produce transient pH changes in the brain. [3, 58-60] In hypercapnia experiment, the breathing mixture for the anesthetized animal was transiently changed from air to carbon dioxide for a 5 second interval. All of the data cyclic voltammograms recorded in the 30 seconds interval around carbon dioxide inhalation are shown in the form of a color plot where the ordinate is the applied potential and the abscissa is time with current encoded in false color [33] (**Figure 3.6A**). A representative cyclic voltammogram obtained during acidosis (20 sec after application of carbon dioxide) contains all of the characteristic peaks as an acidic pH cyclic voltammogram acquired in vitro (compare **Figure 3.6B** with **Figure 3.2B**). Besides C-, QH- and Q-peak it also has a DOPAC related peak at potential of ~ 0.7 V on anodic scan. Current traces at a potential of +0.15 V (QH-peak) shows monophasic

drop in pH calculated to be 0.05 pH units (**Figure 3.6C**). Previous studies of hypercapnia in similar conditions using glass pH microelectrode had much slower time resolution (5 minutes). The drop in pH of ~ 0.8 units was observed in first 5 minutes after application of carbon dioxide. [58] Since time resolution of FSCV is much better and only first 20 seconds of hypercapnia was investigated, it is reasonable to observe smaller drop in pH.

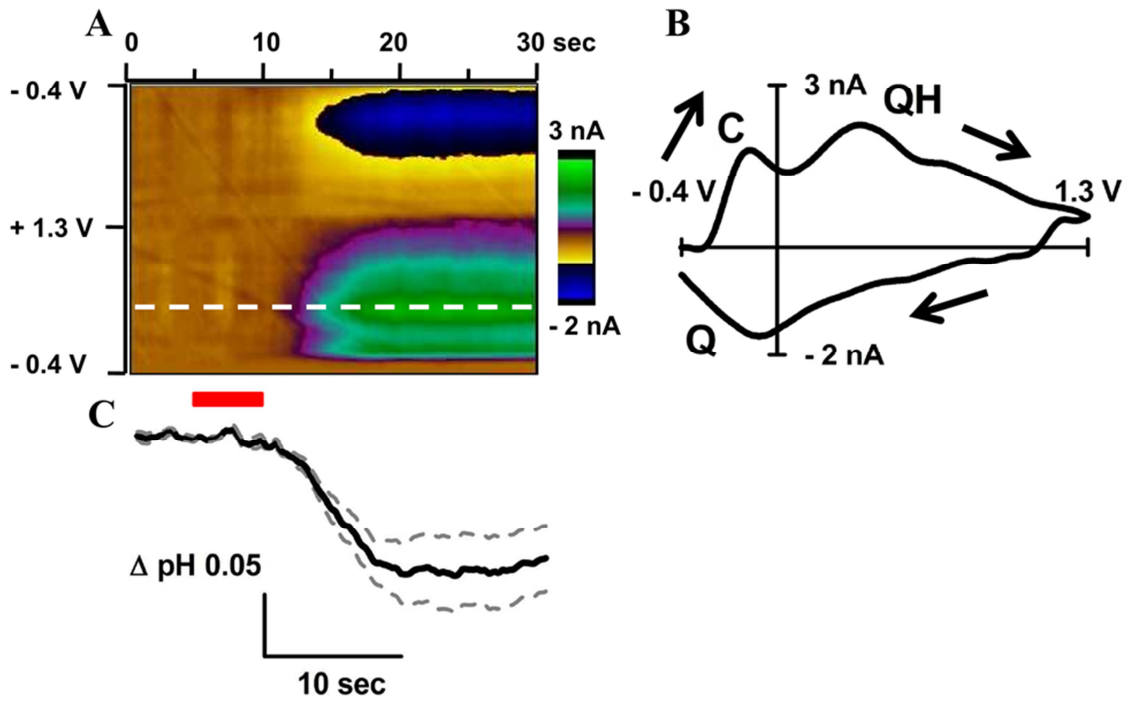


**Figure 3.6.** Monitoring of brain acidosis induced by hypercapnia in vivo with FSCV on carbon-fiber microelectrodes.

Color plot for an acidic pH change induced by the change of a breathing mixture from air to $CO_2$ (A). Red bar marks 5 sec of $CO_2$ application. Dotted white line shows potential at which current trace for QH-peak was taken. Cyclic voltammogram recorded after hypercapnia induced acidosis reached maximum and stabilized (from 20 to 30 sec). C-peak, QH-peak (on the forward scan) and Q-peak (on the backward scan) are labeled (B). Time course of pH change obtained for QH-peak (C). Thick black solid line represents the mean and thin gray dashed lines represent standard error.

## CONCLUSIONS.

Background subtracted fast-scan cyclic voltammetry with carbon-fiber microelectrodes can be used as a reliable method for the detection of transient pH changes in intact brain tissue in vivo. The presence of the signature cyclic voltammogram for pH is an excellent qualitative indicator that allows for the selective identification of proton concentration change over fluctuations associated with other chemical species. However, interference from electrochemically inert species, and from electrochemically active species with proton-dependent electrochemistry, can distort the shape of the cyclic voltammogram for pH shifts. This distortion should be taken in consideration both for in vivo experiments and in vitro calibration of carbon-fiber microelectrodes to maintain selectivity for pH measurements. Acidosis induced by hypercapnia was used as a convenient method to change in pH in the brain. Comparing the cyclic voltammograms recorded with this pH sensor in vitro with voltammograms obtained during transient physiological pH changes in vivo induced by hypercapnia was used as a verification that the signals obtained from the sensor is actually pH changes.

However, there are several limitations of FSCV with respect to pH measurements. FSCV is only good for differential measurements, so absolute value of pH cannot be established. Also, only measurements on short time scale of no more than 120 seconds are possible due to drift of the electrode background. In some cases this limitation can be fixed using analog background subtraction technique. [61] Furthermore, glass-encased carbon microelectrodes are fragile and, probably, less robust than microfabricated potentiometric IrOx probes. [10] However, the silica encased carbon fibers used chronically [18] and recently developed pyrolyzed photoresist carbon arrays for in vivo applications [62] are much more robust and hopefully replace the fragile glass microelectrodes in the future.

## REFERENCES


1. Heisler, N., *Acid-base regulation in animals*. Elsevier: Amsterdam ;New York; New York, NY, U.S.A., 1986.

2. Kaila, K.; Ransom, B. R., *pH and brain function*. Wiley-Liss: New York, 1998; p xiii, 688 p.

3. Siesjo, B. K., Regulation of Cerebrospinal-Fluid pH. *Kidney International* 1972, 1, (5), 360-374.

4. Chesler, M., Regulation and modulation of pH in the brain. *Physiological Reviews* 2003, 83, (4), 1183-1221.

5. Venton, B. J.; Michael, D. J.; Wightman, R. M., Correlation of local changes in extracellular oxygen and pH that accompany dopaminergic terminal activity in the rat caudate-putamen. *Journal of Neurochemistry* 2003, 84, (2), 373-381.

6. Roitman, M. F.; Wheeler, R. A.; Wightman, R. M.; Carelli, R. M., Real-time chemical responses in the nucleus accumbens differentiate rewarding and aversive stimuli. *Nature Neuroscience* 2008, 11, (12), 1376-1377.

7. Ziemann, A. E.; Allen, J. E.; Dahdaleh, N. S.; Drebot, I. I.; Coryell, M. W.; Wunsch, A. M.; Lynch, C. M.; Faraci, F. M.; Howard, M. A.; Welsh, M. J.; Wemmie, J. A., The Amygdala Is a Chemosensor that Detects Carbon Dioxide and Acidosis to Elicit Fear Behavior. *Cell* 2009, 139, (5), 1012-1021.

8. Korostynska, O.; Arshak, K.; Gill, E.; Arshak, A., Review paper: Materials and techniques for in vivo pH monitoring. *Ieee Sensors Journal* 2008, 8, (1-2), 20-28.

9. Fedirko, N.; Svichar, N.; Chesler, M., Fabrication and use of high-speed, concentric H+- and Ca2+-selective microelectrodes suitable for in vitro extracellular recording. *Journal of Neurophysiology* 2006, 96, (2), 919-924.

10. Johnson, M. D.; Kao, O. E.; Kipke, D. R., Spatiotemporal pH dynamics following insertion of neural microelectrode arrays. *Journal of Neuroscience Methods* 2007, 160, (2), 276-287.

11. Fog, A.; Buck, R. P., Electronic Semiconducting Oxides as pH Sensors. *Sensors and Actuators* 1984, 5, (2), 137-146.

12. Bassetomusk, A.; Rebec, G. V., Regional Distribution of Ascorbate and 3,4-Dihydroxyphenylacetic Acid (Dopac) in Rat Striatum. *Brain Research* 1991, 538, (1), 29-35.

13. Kinlen, P. J.; Heider, J. E.; Hubbard, D. E., A Solid-State pH Sensor-Based on a Nafion-Coated Iridium Oxide Indicator Electrode and a Polymer-Based Silver-Chloride Reference Electrode. *Sensors and Actuators B-Chemical* 1994, 22, (1), 13-25.

14. Galster, H., *pH measurement : fundamentals, methods, applications, instrumentation*. VCH: Weinheim, Federal Republic of Germany ; New York, NY, USA, 1991; p xvii, 356 p.

15. Cheer, J. F.; Wassum, K. M.; Wightman, R. M., Cannabinoid modulation of electrically evoked pH and oxygen transients in the nucleus accumbens of awake rats. *Journal of Neurochemistry* 2006, 97, (4), 1145-1154.

16. Makos, M. A.; Omiatek, D. M.; Ewing, A. G.; Heien, M. L., Development and Characterization of a Voltammetric Carbon-Fiber Microelectrode pH Sensor. *Langmuir* 2010, 26, (12), 10386-10391.

17. Jaquins-Gerstl, A.; Michael, A. C., Comparison of the brain penetration injury associated with microdialysis and voltammetry. *Journal of Neuroscience Methods* 2009, 183, (2), 127-135.

18. Clark, J. J.; Sandberg, S. G.; Wanat, M. J.; Gan, J. O.; Horne, E. A.; Hart, A. S.; Akers, C. A.; Parker, J. G.; Willuhn, I.; Martinez, V.; Evans, S. B.; Stella, N.; Phillips, P. E. M., Chronic microsensors for longitudinal, subsecond dopamine detection in behaving animals. *Nat Meth* 2009, 7, (2), 126-129.

19. Robinson, D. L.; Hermans, A.; Seipel, A. T.; Wightman, R. M., Monitoring rapid chemical communication in the brain. *Chemical Reviews* 2008, 108, (7), 2554-2584.

20. Kita, J. M.; Wightman, R. M., Microelectrodes for studying neurobiology. *Current Opinion in Chemical Biology* 2008, 12, (5), 491-496.

21. Runnels, P. L.; Joseph, J. D.; Logman, M. J.; Wightman, R. M., Effect of pH and surface functionalities on the cyclic voltammetric responses of carbon-fiber microelectrodes. *Analytical Chemistry* 1999, 71, (14), 2782-2789.

22. Heien, M. L. A. V.; Phillips, P. E. M.; Stuber, G. D.; Seipel, A. T.; Wightman, R. M., Overoxidation of carbon-fiber microelectrodes enhances dopamine adsorption and increases sensitivity. *Analyst* 2003, 128, (12), 1413-1419.

23. Heien, M. L. A. V.; Khan, A. S.; Ariansen, J. L.; Cheer, J. F.; Phillips, P. E. M.; Wassum, K. M.; Wightman, R. M., Real-time measurement of dopamine fluctuations after cocaine in the brain of behaving rats. *Proceedings of the National Academy of Sciences of the United States of America* 2005, 102, (29), 10023-10028.

24. Bard, A. J.; Faulkner, L. R., *Electrochemical Methods*. Wiley New York: 2001.

25. Kissinger, P. T.; Heineman, W. R., *Laboratory Techniques in Electroanalytical Chemistry*. Marcel Dekker Inc: 1996.

26. McCreery, R. L., Advanced carbon electrode materials for molecular electrochemistry. *Chemical Reviews* 2008, 108, (7), 2646-2687.

27. Boehm, H. P.; Heck, W.; Sappok, R.; Diehl, E., Surface Oxides of Carbon. *Angewandte Chemie-International Edition* 1964, 3, (10), 669-&.

28. Boehm, H. P., Surface oxides on carbon and their analysis: a critical assessment. *Carbon* 2002, 40, (2), 145-149.

29. Phillips, P. E. M.; Wightman, R. M., Critical guidelines for validation of the selectivity of in-vivo chemical microsensors. *Trac-Trends in Analytical Chemistry* 2003, 22, (9), 509-514.

30. Cahill, P. S.; Walker, Q. D.; Finnegan, J. M.; Mickelson, G. E.; Travis, E. R.; Wightman, R. M., Microelectrodes for the measurement of catecholamines in biological systems. *Analytical Chemistry* 1996, 68, (18), 3180-3186.

31. Bath, B. D.; Michael, D. J.; Trafton, B. J.; Joseph, J. D.; Runnels, P. L.; Wightman, R. M., Subsecond adsorption and desorption of dopamine at carbon-fiber microelectrodes. *Analytical Chemistry* 2000, 72, (24), 5994-6002.

32. Zachek, M. K.; Takmakov, P.; Moody, B.; Wightman, R. M.; McCarty, G. S., Simultaneous Decoupled Detection of Dopamine and Oxygen Using Pyrolyzed Carbon Microarrays and Fast-Scan Cyclic Voltammetry. *Analytical Chemistry* 2009, 81, (15), 6258-6265.

33. Michael, D. J.; Joseph, J. D.; Kilpatrick, M. R.; Travis, E. R.; Wightman, R. M., Improving data acquisition for fast scan cyclic voltammetry. *Analytical Chemistry* 1999, 71, (18), 3941-3947.

34. Kristensen, E. W.; Wilson, R. L.; Wightman, R. M., Dispersion in Flow-Injection Analysis Measured with Microvoltammetric Electrodes. *Analytical Chemistry* 1986, 58, (4), 986-988.

35. Paxinos, G.; Watson, C., *The rat brain in stereotaxic coordinates*. Academic Press/Elsevier: Amsterdam; Boston, 2007.

36. Elliott, C. M.; Murray, R. W., Chemically Modified Carbon Electrodes. *Analytical Chemistry* 1976, 48, (8), 1247-1254.

37. Evans, J. F.; Kuwana, T., Introduction of Functional-Groups onto Carbon Electrodes Via Treatment with Radio-Frequency Plasmas. *Analytical Chemistry* 1979, 51, (3), 358-365.

38. Kawagoe, K. T.; Garris, P. A.; Wightman, R. M., pH-Dependent Processes at Nafion(R)-Coated Carbon-Fiber Microelectrodes. *Journal of Electroanalytical Chemistry* 1993, 359, (1-2), 193-207.

39. Roberts, J. G.; Moody, B. P.; McCarty, G. S.; Sombers, L. A., Specific Oxygen-Containing Functional Groups on the Carbon Surface Underlie an Enhanced Sensitivity to Dopamine at Electrochemically Pretreated Carbon Fiber Microelectrodes. *Langmuir* 2010, 26, (11), 9116-9122.

40. Aklilu, M.; Tessema, M.; Redi-Abshiro, M., Indirect voltammetric determination of caffeine content in coffee using 1,4-benzoquinone modified carbon paste electrode. *Talanta* 2008, 76, (4), 742-746.

41. Baur, J. E.; Kristensen, E. W.; May, L. J.; Wiedemann, D. J.; Wightman, R. M., Fast-Scan Voltammetry of Biogenic Amines. *Analytical Chemistry* 1988, 60, (13), 1268-1272.

42. Takmakov, P.; Zachek, M. K.; Keithley, R. B.; Walsh, P. L.; Donley, C.; McCarty, G. S.; Wightman, R. M., Carbon Microelectrodes with a Renewable Surface. *Analytical Chemistry* 2010, 82, (5), 2020-2028.

43. Tóth, J., *Adsorption : theory, modeling, and analysis*. Marcel Dekker: New York, 2002; p viii, 878 p.

44. Woodard, F. E.; Mcmackins, D. E.; Jansson, R. E. W., Electrosorption of Organics on 3-Dimensional Carbon-Fiber Electrodes. *Journal of Electroanalytical Chemistry* 1986, 214, (1-2), 303-330.

45. Davidson, C.; Ellinwood, E. H.; Douglas, S. B.; Lee, T. H., Effect of cocaine, nomifensine, GBR 12909 and WIN 35428 on carbon fiber microelectrode sensitivity for voltammetric recording of dopamine. *Journal of Neuroscience Methods* 2000, 101, (1), 75-83.

46. Somjen, G. G., *Ions in the brain : normal function, seizures, and stroke*. Oxford University Press: Oxford ; New York, 2004; p xxix, 470 p.

47. Kume-Kick, J.; Rice, M. E., Dependence of dopamine calibration factors on media Ca2+ and Mg2+ at carbon-fiber microelectrodes used with fast-scan cyclic voltammetry. *Journal of Neuroscience Methods* 1998, 84, (1-2), 55-62.

48. Chen, B. T.; Rice, M. E., Calibration factors for cationic and anionic neurochemicals at carbon-fiber microelectrodes are oppositely affected by the presence of Ca2+ and Mg2+. *Electroanalysis* 1999, 11, (5), 344-348.

49. Bell, C. F., *Principles and applications of metal chelation*. Clarendon Press: Oxford, 1977.

50. Denison, P.; Jones, F. R.; Watts, J. F., X-Ray Photoelectron Spectroscopic Analysis of Barium-Labeled Carbon-Fiber Surfaces. *Journal of Materials Science* 1985, 20, (12), 4647-4656.

51. Rosendahl, S. M.; Burgess, I. J., Electrochemical and infrared spectroscopy studies of 4-mercaptobenzoic acid SAMS on gold surfaces. *Electrochimica Acta* 2008, 53, (23), 6759-6767.

52. Abe, I.; Hayashi, K.; Kitagawa, M., The Adsorption of Amino-Acids from Water on Activated Carbons. *Bulletin of the Chemical Society of Japan* 1982, 55, (3), 687-689.

53. Justice, J. B., *Voltammetry in the Neurosciences: Principles, Methods, and Applications*. Humana Press: Clifton, NJ, 1987.

54. Gonon, F.; Buda, M.; Cespuglio, R.; Jouvet, M.; Pujol, J. F., Voltammetry in the Striatum of Chronic Freely Moving Rats - Detection of Catechols and Ascorbic-Acid. *Brain Research* 1981, 223, (1), 69-80.

55. Shou, M. S.; Ferrario, C. R.; Schultz, K. N.; Robinson, T. E.; Kennedy, R. T., Monitoring dopamine in vivo by microdialysis sampling and on-line CE-laser-induced fluorescence. *Analytical Chemistry* 2006, 78, (19), 6717-6725.

56. Heien, M. L. A. V.; Johnson, M. A.; Wightman, R. M., Resolving neurotransmitters detected by fast-scan cyclic voltammetry. *Analytical Chemistry* 2004, 76, (19), 5697-5704.

57. Duff, A.; Oneill, R. D., Effect of Probe Size on the Concentration of Brain Extracellular Uric-Acid Monitored with Carbon-Paste Electrodes. *Journal of Neurochemistry* 1994, 62, (4), 1496-1502.

58. Katsura, K.; Kristian, T.; Nair, R.; Siesjo, B. K., Regulation of Intracellular and Extracellular pH in the Rat-Brain in Acute Hypercapnia - a Reappraisal. *Brain Research* 1994, 651, (1-2), 47-56.

59. Brian, J. E., Carbon dioxide and the cerebral circulation. *Anesthesiology* 1998, 88, (5), 1365-1386.

60. Kintner, D. B.; Anderson, M. E.; Sailor, K. A.; Dienel, G.; Fitzpatrick, J. H.; Gilboe, D. D., In vivo microdialysis of 2-deoxyglucose 6-phosphate into brain: A novel method for the measurement of interstitial pH using P-31-NMR. *Journal of Neurochemistry* 1999, 72, (1), 405-412.

61. Hermans, A.; Keithley, R. B.; Kita, J. M.; Sombers, L. A.; Wightman, R. M., Dopamine detection with fast-scan cyclic voltammetry used with analog background subtraction. *Analytical Chemistry* 2008, 80, (11), 4040-4048.

62. Zachek, M. K.; Park, J.; Takmakov, P.; Wightman, R. M.; McCarty, G. S., Microfabricated FSCV-compatible microelectrode array for real-time monitoring of heterogeneous dopamine release. *Analyst* 2010, 135, (7), 1556-1563.

# Chapter 4

# Carbon Microelectrode Arrays Compatible with Fast-Scan Cyclic Voltammetry.

## INTRODUCTION

Fast-scan cyclic voltammetry (FSCV) has been applied for detection of electroactive analytes in the brain of rats and mice in vitro and in vivo. [1, 2] FSCV is traditionally used with carbon-fiber microelectrodes. [3] Microelectrodes are beneficial for a number of reasons including efficient mass transport, low charging current and small tissue damage caused by electrode implantation. [4, 5] Carbon electrodes resist fouling [6] and have many adsorption sites on the surface which facilitates preconcentration of aromatic biogenic amines on the electrode. [7]

While carbon-fiber microelectrodes have been the most common tools for in vivo voltammetry for the past 30 years, there are several disadvantages associated with these electrodes. First, microelectrode fabrication requires skilled manual labor and there is substantial variability from electrode to electrode. Second, these microelectrodes are very fragile and can break when lowered into the brain during experiments in freely moving animals.

In past decades microfabrication technology based on lithography, controlled metal deposition and etching has become widely available. [8] These advancements were applied for fabrication of the microelectrode arrays (MEAs) of noble metal electrodes. [9, 10]

Gold and platinum are excellent materials for traditional electrodes in traditional electrochemical experiments; however they are less suitable than carbon for FSCV. [11]

A decade ago several groups reported on the development of a new carbon material, pyrolyzed photoresist film (PPF), which is fabricated by pyrolysis of AZ type positive photoresist. [12-14] PPF provided very convenient way for production of carbon microelectrodes which is fully compatible with microfabrication technology. Previously, PPF was used for manufacturing of carbon-coated tungsten microelectrodes [15] and interdigitated microelectrodes. [16] Thus, PPF provides a route for development of MEAs compatible with FSCV detection of electrochemically active neurotransmitters in brain in vivo.

There are several reports concerning the application of MEAs for electrochemical detection. MEAs are frequently used as a macroscopic single electrode without independent control of each microelectrode in the array. [17] There are recent reports on independently controlled microelectrodes that were used for monitoring neurotransmitters in the brain using amperometry [18] and by measuring release from a single cell. [19]

In this chapter PPF based microfabricated microelectrode arrays are described. We have focused on the key advantage of these MEAs which is independent control of microelectrodes in the array and ability to use custom build waveforms on each electrode. MEAs of the first generation have been characterized using a flow injection system. Their application for detection of dopamine in several setups is shown. First, MEAs were used for measurement of dopamine concentration in four distinct spatial locations in the brain which can be used in the future to study heterogeneity of dopamine release. This approach was later realized by using MEAs of generation 2.0. Second,

simultaneous use of FSCV and amperometry for dopamine detection combines advantages of both techniques which are selectivity and fast time resolution. Third, decoupled simultaneous detection of dopamine and oxygen on the separate microelectrodes in the array with increased sensitivity for both species is demonstrated. These experiments are first published examples of multiplexed electrochemical detection that become possible with FSCV compatible MEAs. [20, 21].

## MATERIALS AND METHODS

### Chemicals and Drugs.

All chemicals and drugs were obtained from Sigma-Aldrich (St Louis, MO) and were used as delivered. Raclopride hydrochloride and cocaine hydrochloride dissolved in saline were administered intraperitoneally (i.p.) at 3 mg/kg and 15 mg/kg respectively. Characterization of microelectrode arrays in vitro as well as post in vivo electrode calibrations were done in a flow injection system with a Tris buffer solution (pH 7.4) consisting of 15 mM Tris, 140 mM NaCl, 3.25 mM KCl, 1.2 mM $CaCl_2$, 1.25 mM $NaH_2PO_4$, and 2.0 mM $Na_2SO_4$. Stock solutions of dopamine were made using 0.1 N $HClO_4$ and were diluted immediately prior to calibration. Determination of the concentration of oxygen in solution was done as previously described. [22]

### Fabrication of PPF Microelectrode Arrays of MEA 1.0 Generation.

PPF microelectrode arrays were fabricated in the Biomedical Microsensor Laboratory (BMMSL) at North Carolina State University. Fabrication of PPF was done as previously reported [12, 13, 16] with some modifications that allow the arrays to be compartible with FSCV. After an application of an adhesion promoter HDMS (hexamethyldisilazane), a positive tone photoresist (AZ1518, AZ Electric Materials, Branchburg, NJ) was spun on a 200 µm thick fused silica substrate (University Wafer,

Inc., Boston, MA) at 3000 rpm for 45 s. This resulted in a 2 µm thick layer of photoresist. After exposure and development of the desired pattern for the electrode arrays, the photoresist was pyrolyzed by subjecting it to 1000 ℃ under a forming gas atmosphere (5% $H_2$, 95% $N_2$) in a quartz tube furnace (Sentro Tech, Inc., Berea, OH). The temperature was ramped at 5 ℃/min and held at 1000 ℃ for 60 min. After pyrolysis, the film was then allowed to cool to room temperature before it was exposed to air.

A negative photoresist, SU-8 3010, was then used (MicroChem Corp, Newton, MA) to insulate the microelectrodes. After a second application of HMDS, SU-8 3010 was spun onto the substrate at 1500 rpm, resulting in a 12 µm thick polymer layer which was patterned using photolithographic techniques. The subsequent exposure, development, and curing of this layer defined the final microelectrode sizes and provided sufficient insulation for use in physiological buffer (pH 7.4). The film and substrate were cut into their final form using a dicing saw. External connections to the microelectrodes were made using stainless steel wires and silver epoxy (Epoxy Technology, Billerica, MA).

**Fabrication of PPF Microelectrode Arrays of MEA 2.0 Generation.**

A detailed description for fabrication of MEA 2.0 generation is described in literature. [21] Briefly, the pyrolyzed photoresist arrays were manufactured using equipment in three separate clean rooms: the BMMSL (NCSU), the NNF (NCSU), and the CHANL facility (UNC-Chapel Hill). All fabrication was done on 3" diameter and 200 µm thick, [100], prime grade silicon wafers (Silicon Quest Inc., Santa Clara, CA). First, LPCVD (low pressure chemical vapor deposition) of 3000 Å silicon nitride dielectric layer were performed. AZ 1518 photoresist spin coated on the wafer and heated up to form PPF layer. [20] 5000 Å thick low-stress silicon nitride layer was deposited with PECVD (plasma enhanced chemical vapor deposition) for insulation and selective etch of silicon

nitride layer via capacitively coupled reactive ion etching (RIE) using photoresist as a mask. Then, remasking with photoresist and etch of the extraneous silicon nitride to the host silicon wafer was performed followed by anisotropical frontside etch in 40% KOH at 80 ℃. After this, full etch of silicon nitride in sulation layer with RIE to the final insulation thickness of 2500 Å was done and wafer was fixed with thermal release tape. Backside DRIE thinning of wafer was done and MEAs was released by heating it on the hot plate. At the end devices were packaged and interface for connection to the headstage was done.

**Data Acquisition.**

A customized version of TH-1 software (ESA, Chelmsford, MA) written in LabVIEW (National Instruments, Austin, TX) was used for waveform output and data acquisition. The software was modified to allow output of two decoupled, time-independent, waveforms with two DAC/ADC cards (NI 6251 M and NI 6051 E). The third card (NI 6711) was used for triggering the DACs and ADCs as well as for synchronization of the electrochemical experiment with flow injection of the analytes. Electrochemical experiments were done in a two-electrode setup using an EI-400 biopotentiostat (ESA, Chelmsford, MA).

Experiments with multiple working electrodes were also done in a two-electrode setup using a “Quad UEI” head stage amplifier (University of North Carolina Department of Chemistry Electronics Shop). In both cases, a 400 V/s scan rate waveform, ranging from - 0.4 to 1.3 V, was applied to the working electrode from the DAC in reference to Ag/AgCl (Bioanalytical Systems, West Lafayette, IN). The applied waveforms were low pass filtered at 2 kHz. To minimize external electrical noise, flow injection analysis was performed inside a grounded Faraday cage.

For FSCV experiments involving the detection of dopamine and oxygen, two separate waveforms were generated. As with the single-electrode experiments, the waveform for detecting dopamine was from - 0.4 to + 1.3 V and back at scan rate of 400 V/s. For the detection of oxygen, a waveform was simultaneously generated that scans from - 0.4 to - 1.4 V and back at scan rate of 200 V/s. The slower scan rate facilitates consistent observation of the faradic peak current of oxygen.

For constant-potential amperometry experiments, the working electrode was held at a constant potential of + 0.8 V. To plot the final amperometric traces, 1000 data points were acquired over a 100 ms time frame and averaged. The amperometric data points were simultaneously acquired with the FSCV data.

Filtering, smoothing, averaging, and background subtraction of acquired data were done either in TH-1 software or in MS Excel. Electrochemical data are shown in either current-potential or current-time traces, plotted in GraphPad Prism 4.0 (GraphPad Software, San Diego, CA).

**Flow Injection Apparatus.**

As previously described [23], a flow injection system was constructed using a six-port injection valve (Upchurch Scientific, Oak Harbor, WA) positioned atop a two-position pneumatic actuator (Rheodyne, Rohnert Park, CA).

The pneumatic actuator was used in conjunction with a 12 V solenoid valve kit (Rheodyne) at 50 psi. A variable-resistance infusion pump (Harvard Apparatus, Holliston, MA) was used to introduce the buffer and analytes to the electrodes, which were situated in an electrochemical cell, at a constant rate of 2 mL/min. For studies involving oxygen, glass syringes were used and the flow injection system was fitted with PEEK tubing to limit unwanted entry or loss of oxygen.

**Experiments in Animals.**

In vivo anesthetized preparations were done using male Sprague-Dawley rats (300–370 g, Charles River Laboratories, Wilmington, MA) anesthetized using urethane (1.5 g/kg). Temperature was maintained at 37 ℃ using a heating pad (Harvard Apparatus, Holliston, MA, USA). MEAs were placed in the caudate putamen using a stereotaxic frame with respective anteroposterior (AP), mediolateral (ML) and dorsoventral (DV) coordinates (AP + 1.2 mm, ML + 2.4 mm, DV 4.5 to 6.5 mm) [24] measured from bregma. An Ag/AgCl reference electrode was placed in the contralateral cortex and it was employed for all in vivo experiments.

Dopamine release was electrically elicited in the brain areas of interest using a bipolar electrode situated in the ventral tegmental area (VTA, location of the dopaminergic cell bodies) as previously reported. [25] A bipolar stimulating electrode and voltage-to-current converter (NeuroLog System, Hertfordshire, UK) were used to apply stimulation pulses between voltammetric scans using the TH-1 software. Unless otherwise noted 60 pulses, 60 Hz biphasic stimulations were used (±300 μA, 2 ms per phase).

For all experiments, after obtaining a stable stimulated release baseline, which was collected every 4 min over a 30 min timeframe, raclopride and cocaine were administered subsequently via intraperitoneal injection (i.p.). Following raclopride injection, steady-state evoked release was observed after approximately 20 min, 5 files were then collected every 4 min over a 20 min window. Subsequent administration of cocaine followed, and files were collected in a similar manner.

## RESULTS AND DISCUSSION

**Design of Microfabricated Microelectrode Arrays for FSCV Detection.**

The purpose of this work was to design arrays of decoupled microelectrodes that could be individually addressed and provide independent information about concentration and identity of the species detected. Electrical insulation of the electrodes from each other was the first issue addressed. Electronic cross-talk is possible between electrodes in the array through direct connection by conductive parts. First, this issue was addressed during the development of microelectrodes of MEA 1.0 generation (**Figure 4.1A** and **B**). Electrical coupling through the substrate did not exist for MEA 1.0 since these arrays were fabricated using silicon oxide wafers. For microelectrodes of MEA 2.0 generation cross-talk through substrate was prevented by deposition of 3000 Å thick silicon nitride layer on top of silicon wafer.

However, electrical cross-talk was observed, for some of the arrays due to thin layer of AZ 1518 photoresist that was not removed during the development step and that was turned into a conducting carbon film after pyrolysis. The problem was solved by removing this thin PPF layer by exposing the wafer to air plasma for 1 min after the pyrolysis step. Also, since in FSCV alternating current is measured, capacitive and inductive coupling between microelectrodes is possible. For the chosen geometry (**Figure 4.1**) this was not an issue, however, it should be taken into account for closer spaced microelectrodes or connection pads and if faster changes in potential than that in FSCV are used.

Besides electrical cross-talk, diffusional cross-talk between microelectrodes in the array is possible. If microelectrodes are placed too close to each other so that their diffusion layers overlap, then they will act together as a macroscopic electrode with a planar diffusion profile. [26] For this geometry all benefits of multiple microelectrodes in the array are lost and it is difficult to establish longitudinal heterogeneity of analyte

concentration. The dimensions of the diffusion layer is defined by the time that the analyte has to diffuse to and from microelectrode and can be estimated as:

$$L = \sqrt{2Dt} \qquad (4.1)$$

In case of traditional FSCV detection of dopamine with 10 Hz of waveform application frequency, the time for dopamine to diffuse (t) is about 100 milliseconds and diffusion coefficient of dopamine is $6.0 \times 10^{-6}$ $cm^2/s$ [27]. It gives diffusion layer length, L, of ~ 11 µm. With this in mind, microelectrodes should be spaced at least 22 µm apart to prevent diffusional cross-talk. In the MEA 1.0 design the microelectrodes were four bands, 50 µm by 10 µm, placed in parallel 100 µm apart (**Figure 4.1A** and **B**). In MEA 2.0 design the microelectrodes were four bands 100 µm by 10 µm placed in along the same vertical axe 100 µm apart (**Figure 4.1C**). In both cases there should not be any diffusional cross-talk.

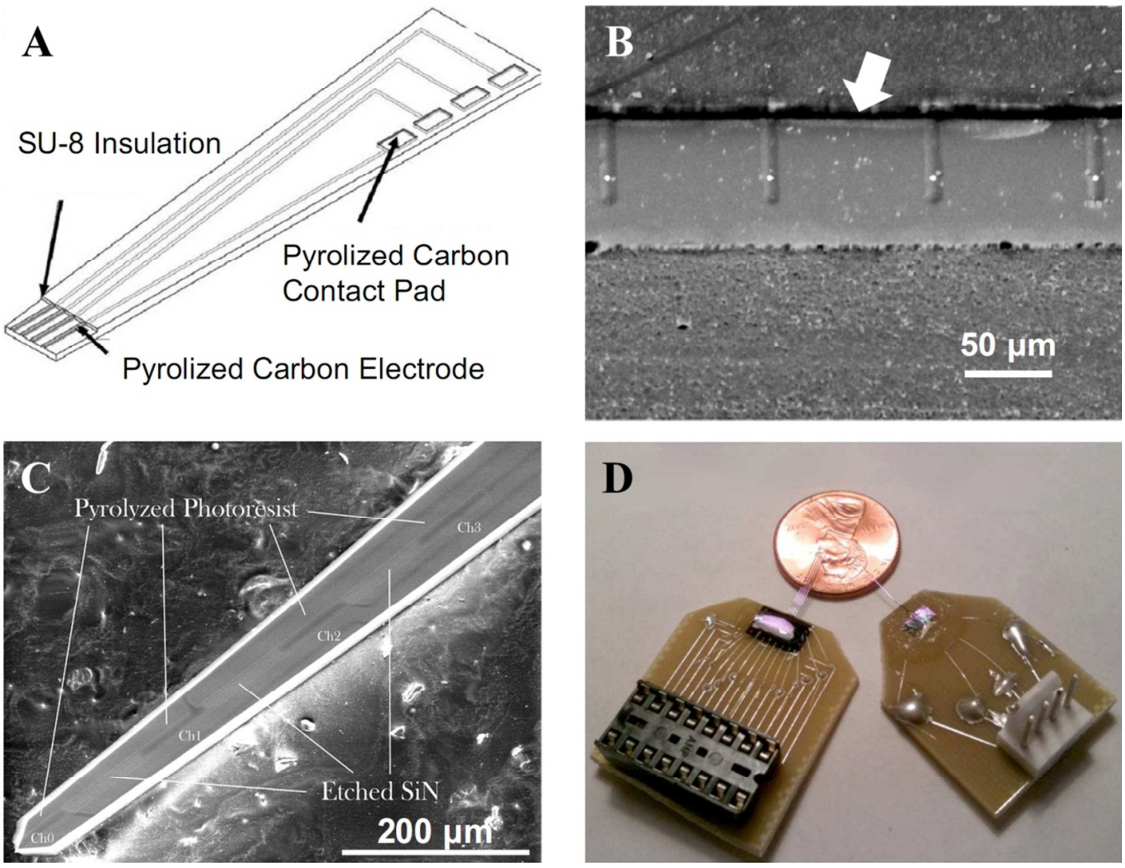


**Figure 4.1.** Microfabricated arrays of different generations.

(A) Drawing of the PPF microelectrode array device (not to scale) of the MEA 1.0 generation. (B) SEM image is taken of the PPF microelectrode array after dicing. Each of the four electrodes is 10 µm wide and 50 µm long. The white dots indicate the four electrodes, while the arrow indicates the insulation layer. (C) SEM image of an array of the MEA 2.0 generation. The channels indicated here are used throughout the chapter. Exposed pyrolyzed carbon is indicated as is the etched silicon nitride layer between the electrodes. Microelectrodes are 10 X 100 µm with 100 µm spacing between electrode sites. (D) Optical image of both a 16 channel and 4 channel MEA 2.0.

PPF was developed as a promising electrode material a decade ago. [12, 16, 28]. However, there are no reports on application of PPF as an electrode material for FSCV detection of catecholamines. Similarity between PPF and glassy carbon, as well as the susceptibility of PPF to electrochemical etching with extended voltammetric waveforms, [6] suggest that PPF microelectrodes are suitable for detection of dopamine using standard FSCV procedures. In flow cell electrochemical experiment, characteristic background subtracted cyclic voltammograms for dopamine are observed (**Figure 4.2 A**) on four separate microelectrodes in the array.

The key advantage of microfabrication is reproducibility and scalability. Four microelectrodes in MEA 1.0 have the same area and the same electrode material so cyclic voltammograms for homogeneous concentration of dopamine (**Figure 4.2A**) are indistinguishable from each other.

Sensitivity of MEA 1.0 to dopamine within linear range of concentrations (up to 5 μM) is 3.7 ± 0.2 nA/ μM (**Figure 4.2B**). The sensitivity of MEA 1.0 is comparable to the sensitivity of a carbon-fiber microelectrode since area of PPF microelectrodes is 500 $\mu m^2$ while area of 75 μm long carbon-fiber microelectrodes is ~ 1200 $\mu m^2$ with a typical sensitivity of 10-12 nA/μM. [29]

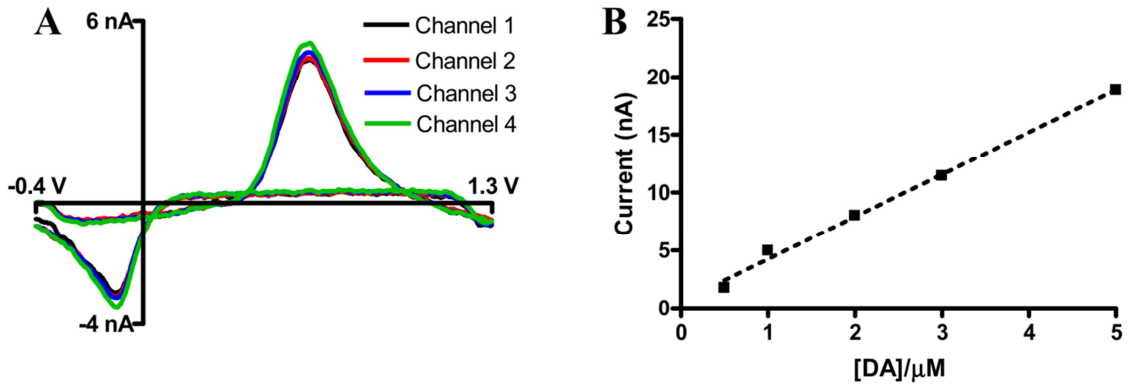


**Figure 4.2.** Detection of dopamine in flow cell with MEA 1.0.

(A) Cyclic voltammograms for 1 µM dopamine simultaneously recorded on 4 separate microelectrodes in the array. (B) Voltammetric peak current as a function of the dopamine concentration (within concentrations for linear range). The error bars are the standard deviation (n = 24, three measurements from eight electrodes). Measurements were done at 400 V/s and 10 Hz in Tris buffer, pH 7.4.

**Multiplexed Detection with Individually Addressable Microelectrode Arrays.**

Independent control of each microelectrode in the array enables different electrochemical techniques to be used simultaneously on the same probe and obtain more information about the chemical composition of the sample. Concurrent use of FSCV and amperometry for detection of dopamine on the adjacent microelectrodes enables the combined benefits of both techniques.

The advantages of FSCV are selectivity and sensitivity. Dopamine can be selectively detected in presence of its metabolites such as DOPAC and homovanillic acid and also in the presence of shifts in pH of the extracellular fluid with limits of detection down to 20-50 nM. [29, 30] However, the sensitivity of FSCV comes at the expense of time resolution. Cyclic voltammograms are collected at frequency of 10 Hz with the ~ 100 millisecond between scans allocated for dopamine adsorption and preconcentration on the electrode surface. [7] While this time resolution is suitable for monitoring dopamine release in the brain and establishing its correlation with behavior, FSCV might be not fast enough to investigate the time course of the release itself. The time of exocytosis of single catecholamine vesicle is less than 20 milliseconds. [31]

In constant potential amperometry, catecholamine molecules are oxidized on the electrode surface without any delay for adsorption and preconcentration. Amperometry is widely used for detection of catecholamine exocytosis. [31-33] However, it is impossible to distinguish between analytes with amperometry because amperometry does not yield characteristic voltammogram. Combination of FSCV with amperometry permits both identification of analytes and excellent time resolution. Simultaneous use of FSCV and constant potential amperometry with MEA 1.0 (**Figure 4.3**) demonstrates increased time resolution of amperometry over FSCV. The rise and fall time for amperometry was 0.8

and 0.7 seconds versus 1.9 and 2.1 seconds for FSCV, respectively (**Figure 4.3B** and **C**). Sensitivity was 12 pA/µM for amperometry and 5 nA/µM for FSCV.

Besides applications that require very fast time resolution, amperometry is frequently used for detection of products of enzymatic reactions, such as hydrogen peroxide. [34] Thus, combination of FSCV and amperometry on the same sensor might be beneficial for multiplexed monitoring of electrochemically active and electrochemically inert analytes that produce electrochemically active products through reaction with enzymes immobilized on the electrode surface.

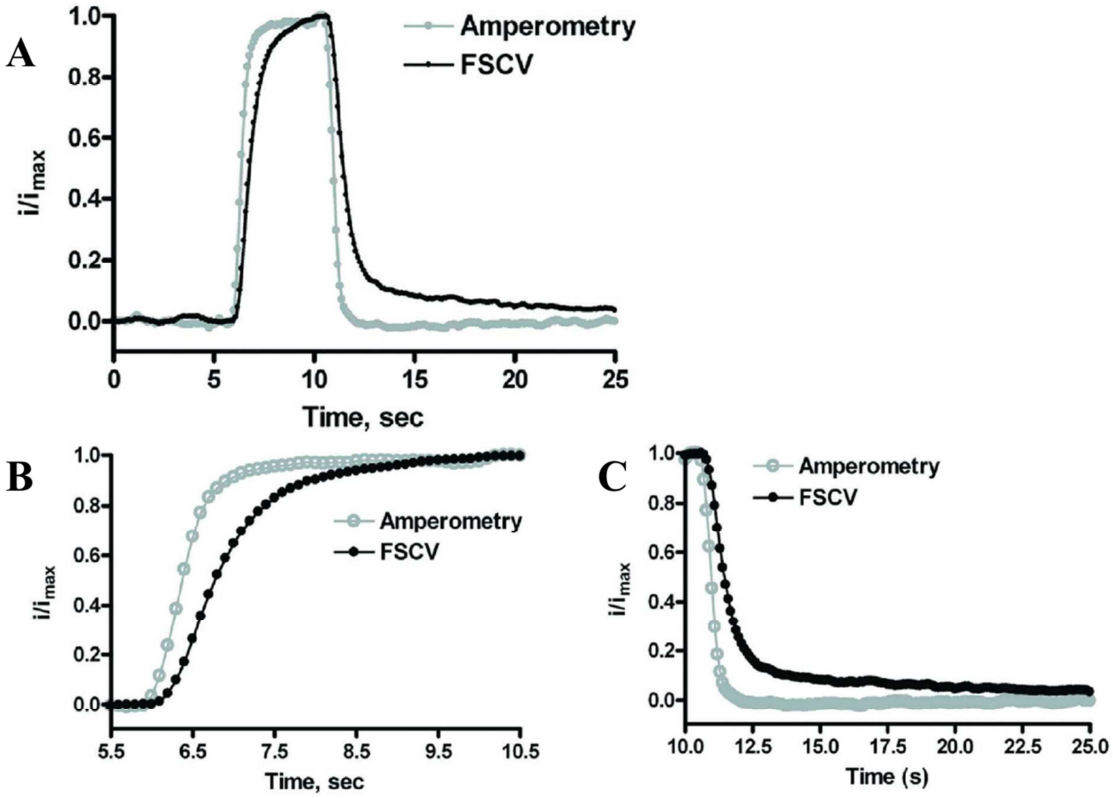


**Figure 4.3.** Simultaneous detection of dopamine using FSCV and amperometry.

FSCV was performed at 400 V/s at 10 Hz. The FSCV response shown is the peak current at the potential for dopamine oxidation recorded in successive voltammograms. The amperometric trace was collected at 15 kHz with $E_{app}$ = + 0.8 V (average of five traces). Both normalized signals are in response to a 5 s, 1 µM injection of dopamine in Tris buffer, pH 7.4.

The most efficient detection of a particular electrochemically active analyte can be done by designing a waveform that fits unique electrochemical properties of the analyte. Application of analyte-tailored waveforms to different microelectrodes in the array makes it possible to detect different analytes in the most efficient manner simultaneously.

Electrochemical monitoring of dopamine and oxygen in brain can be used to investigate the connection between neuronal activity and metabolism. [35] Both species are detected using FSCV on the same carbon-fiber microelectrode with the waveform that was tailored to be sensitive for both species with potential ramp from 0 V to + 0.8 V then to - 1.4 V and back to 0 V at 400 V/sec. However, the waveform was not optimal for detection of either dopamine or oxygen. Thus, optimized detection of these species on separate electrodes is beneficial.

Decoupled simultaneous detection of dopamine and oxygen is done by using specifically tailored waveforms on each of the microelectrodes (**Figure 4.4A**). Dopamine is detected with traditional waveform which is triangular ramp from - 0.4 V to 1.3 V and back at 400 V/sec. Oxygen is detected with reductive waveform which is triangular ramp from - 0.4 V to - 1.4 V and back at 200 V/sec. This choice of the waveforms is optimized for the mixture of both analytes such as there is no interference from each other (**Figure 4.4B** and **C**).

Decoupled detection helped to improve sensitivity for each of the species compare to what it was when both dopamine and oxygen were detected on the same microelectrode. The sensitivity for dopamine was $3.6 \times 10^{-4}$ nA/(µM × µm$^2$) and for oxygen it was $7.2 \times 10^{-5}$ nA/(µM × µm$^2$) with the old waveform. [22] Decoupled detection

lead to 30 and 3 fold improvement in sensitivity to $9 \times 10^{-3}$ and $2.1 \times 10^{-4}$ nA/(µM x µm$^2$) for dopamine and oxygen, respectively.

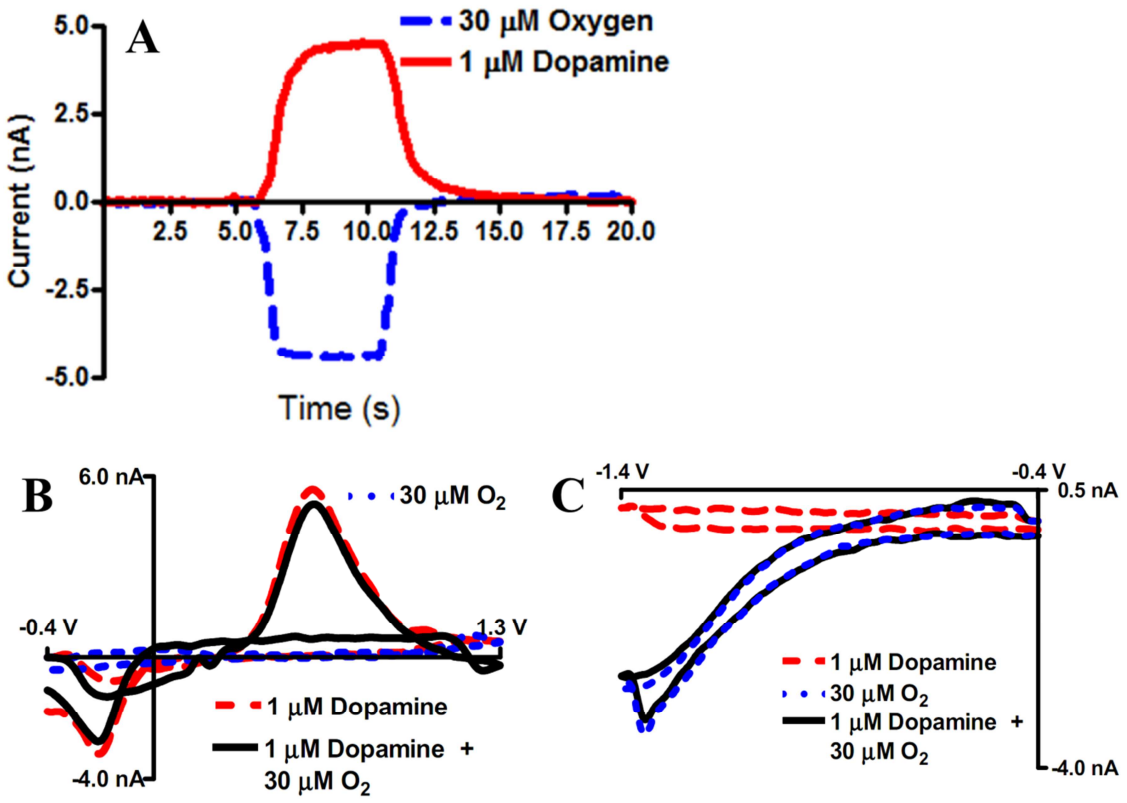


**Figure 4.4.** Simultaneous detection of dopamine and oxygen.

(A) Average of five peak current vs time traces depicting the simultaneous detection of physiologically relevant concentrations of dopamine and oxygen (5 s injection of both 1 µM dopamine and 30 µM oxygen). (B, C) Cyclic voltammograms recorded simultaneously using dopamine and oxygen waveforms: (dashed red line) 1 µM dopamine, (dotted blue line) 30 µM oxygen, (solid black line) 1 µM dopamine and 30 µM oxygen. Data collected at 400 V/s for dopamine and 200 V/s for oxygen at 10 Hz. Experiment performed in Tris buffer (pH 7.4).

**Microelectrode Arrays for Multisite Recording of Dopamine Release in Anesthetized Animals.**

MEAs of generation 1.0 were thoroughly characterized in flow cell. Unfortunately, MEA 1.0 electrodes were too big to be used in the brain. It was shown that implantation of the probes with diameter of 200 μm caused substantial tissue damage and no dopamine release can be observed near the probe of this size due to destruction of dopaminergic terminals. [4, 5] MEA 1.0 sensors are 200 by 300 μm in size and they cannot be made smaller without substantial modification of the fabrication technique since the thickness of a silicon oxide wafer is 200 μm.

MEAs of generation 2.0 were smaller in size and they can be implanted into the rat's brain without damage of the adjacent dopaminergic terminals. The backside etching was used to thin the MEA 2.0 sensor down to 15-25 μm. The microelectrodes were located vertically on the dagger-shaped probe which was 35 μm wide near the tip and 100 μm wide above the sensing elements. More details about fabrication and characterization in flow cell of the MEA 2.0 can be found in literature. [21]

Electrically evoked dopamine release was detected with all four electrodes of MEA 2.0 sensors implanted in striatum of anesthetized rat (**Figure 4.5A**). Intraperitonial injection of raclopride (D2 autoreceptor antagonist) caused expected increase in stimulated dopamine release ranging from 138% to 256% (**Figure 4.5B**). Application of cocaine (dopamine transporter inhibitor) further increased the release from 713% to 1357% (**Figure 4.5C**). The effect of these drugs on the signals on all four electrodes confirms that the analyte measured on all four channels is dopamine.

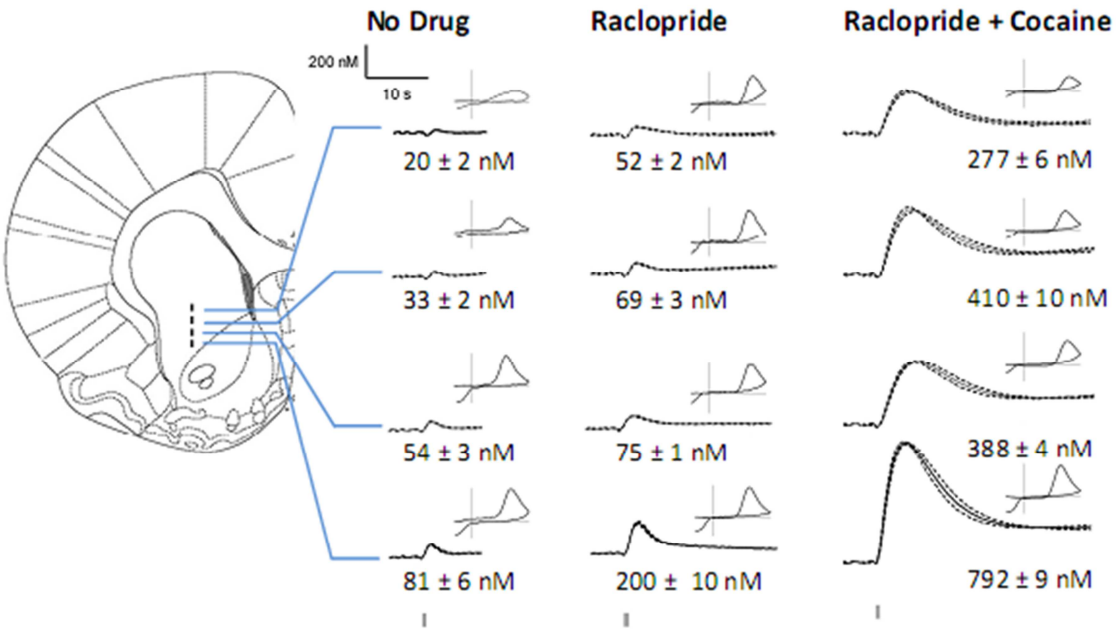


**Figure 4.5.** Simultaneous monitoring of electrically excited dopamine release in vivo.

Each trace is an average of five trials (4 min between trials) with the dashed lines indicating the standard error of these measurements. (Insets) Cyclic voltammograms of electrically stimulated dopamine release (scaled to the highest release per experiment). Grey bars indicate stimulus start and duration (60 Hz biphasic VTA stimulation: 60 pulses, 2 ms, ±150 µA).

MEA 2.0 is the first FSCV compatible probe that was able to measure dopamine release in vivo. However, it has several issues that need to be investigated and addressed in future generation of the devices. First, cyclic voltammograms for dopamine have recognizable shape but the voltammetric peaks are shifted by as much as 300 mV. As it was discovered later the reason for this peak shift is Ohmic loss associated with resistivity of PPF connections that go from the microelectrodes to the pads. This problem can be fixed by making PPF connections wider. Second, dopamine signal does not come back to zero within 15 seconds after stimulation while it typically decays to zero when measured with carbon-fiber microelectrodes. [36] This discrepancy should be investigated. The possible explanation is hindered dopamine diffusion from the microelectrode due to big size of the probe.

## CONCLUSIONS

This chapter describes microfabricated PPF microelectrode arrays of two generations designed for FSCV detection of electrochemically active analytes, particularly dopamine, in the brain. Microelectrodes in the array were independently controlled which made it possible to use several advanced detection schemes. Simultaneous measurement of dopamine concentration on four microelectrodes spaced 100 μm apart allows monitoring longitudinal difference in dopamine concentration. Simultaneous detection with voltammetry and amperometry combines advantages of selectivity with fast time resolution. Application of tailored waveforms to separate microelectrodes in the array permits decoupled FSCV detection of dopamine and oxygen with enhanced sensitivity for both analytes.

MEAs of first generation were too large for implantation in brain and they were characterized in flow cell. Improved MEAs 2.0 of smaller size were successfully used for

detection of electrically stimulated dopamine release in brain of anesthetized rat. Pharmacological manipulation with raclopride (D2 autoreceptor antagonist) and cocaine (dopamine transporter blocker) confirmed identity of the signal and showed that MEAs is valuable tool for characterization of dopamine release in vivo.

## REFERENCES


1. Robinson, D. L.; Hermans, A.; Seipel, A. T.; Wightman, R. M., Monitoring rapid chemical communication in the brain. *Chemical Reviews* 2008, 108, (7), 2554-2584.

2. Michael, A. C.; Borland, L. M., *Electrochemical methods for neuroscience*. CRC Press/Taylor & Francis: Boca Raton, 2007; p 512 , [8] of plates.

3. Kita, J. M.; Wightman, R. M., Microelectrodes for studying neurobiology. *Current Opinion in Chemical Biology* 2008, 12, (5), 491-496.

4. Khan, A. S.; Michael, A. C., Invasive consequences of using micro-electrodes and microdialysis probes in the brain. *Trac-Trends in Analytical Chemistry* 2003, 22, (9), 503-508.

5. Jaquins-Gerstl, A.; Michael, A. C., Comparison of the brain penetration injury associated with microdialysis and voltammetry. *Journal of Neuroscience Methods* 2009, 183, (2), 127-135.

6. Takmakov, P.; Zachek, M. K.; Keithley, R. B.; Walsh, P. L.; Donley, C.; McCarty, G. S.; Wightman, R. M., Carbon Microelectrodes with a Renewable Surface. *Analytical Chemistry* 2010, 82, (5), 2020-2028.

7. Bath, B. D.; Michael, D. J.; Trafton, B. J.; Joseph, J. D.; Runnels, P. L.; Wightman, R. M., Subsecond adsorption and desorption of dopamine at carbon-fiber microelectrodes. *Analytical Chemistry* 2000, 72, (24), 5994-6002.

8. Madou, M. J., *Fundamentals of microfabrication : the science of miniaturization*. 2nd ed.; CRC Press: Boca Raton, 2002; p 723 p.

9. Cheung, K. C.; Renaud, P.; Tanila, H.; Djupsund, K., Flexible polyimide microelectrode array for in vivo recordings and current source density analysis. *Biosensors & Bioelectronics* 2007, 22, (8), 1783-1790.

10. Burmeister, J. J.; Pomerleau, F.; Huettl, P.; Gash, C. R.; Wemer, C. E.; Bruno, J. P.; Gerhardt, G. A., Ceramic-based multisite microelectrode arrays for simultaneous measures of choline and acetylcholine in CNS. *Biosensors & Bioelectronics* 2008, 23, (9), 1382-1389.

11. Zachek, M. K.; Hermans, A.; Wightman, R. M.; McCarty, G. S., Electrochemical dopamine detection: Comparing gold and carbon fiber microelectrodes using background subtracted fast scan cyclic voltammetry. *Journal of Electroanalytical Chemistry* 2008, 614, (1-2), 113-120.

12. Ranganathan, S.; McCreery, R.; Majji, S. M.; Madou, M., Photoresist-derived carbon for microelectromechanical systems and electrochemical applications. *Journal of the Electrochemical Society* 2000, 147, (1), 277-282.

13. Hebert, N. E.; Snyder, B.; McCreery, R. L.; Kuhr, W. G.; Brazill, S. A., Performance of pyrolyzed photoresist carbon films in a microchip capillary electrophoresis device with sinusoidal voltammetric detection. *Analytical Chemistry* 2003, 75, (16), 4265-4271.

14. Kim, J.; Song, X.; Kinoshita, K.; Madou, M.; White, B., Electrochemical studies of carbon films from pyrolyzed photoresist. *Journal of the Electrochemical Society* 1998, 145, (7), 2314-2319.

15. Hermans, A.; Wightman, R. M., Conical tungsten tips as substrates for the preparation of ultramicroelectrodes. *Langmuir* 2006, 22, (25), 10348-10353.

16. Kostecki, R.; Song, X.; Kinoshita, K., Electrochemical analysis of carbon interdigitated microelectrodes. *Electrochemical and Solid State Letters* 1999, 2, (9), 465-467.

17. Fletcher, S.; Horne, M. D., Random assemblies of microelectrodes (RAM (TM) electrodes) for electrochemical studies. *Electrochemistry Communications* 1999, 1, (10), 502-512.

18. Johnson, M. D.; Franklin, R. K.; Gibson, M. D.; Brown, R. B.; Kipke, D. R., Implantable microelectrode arrays for simultaneous electrophysiological and neurochemical recordings. *Journal of Neuroscience Methods* 2008, 174, (1), 62-70.

19. Zhang, B.; Adams, K. L.; Luber, S. J.; Eves, D. J.; Heien, M. L.; Ewing, A. G., Spatially and temporally resolved single-cell exocytosis utilizing individually addressable carbon microelectrode arrays. *Analytical Chemistry* 2008, 80, (5), 1394-1400.

20. Zachek, M. K.; Takmakov, P.; Moody, B.; Wightman, R. M.; McCarty, G. S., Simultaneous Decoupled Detection of Dopamine and Oxygen Using Pyrolyzed Carbon Microarrays and Fast-Scan Cyclic Voltammetry. *Analytical Chemistry* 2009, 81, (15), 6258-6265.

21. Zachek, M. K.; Park, J.; Takmakov, P.; Wightman, R. M.; McCarty, G. S., Microfabricated FSCV-compatible microelectrode array for real-time monitoring of heterogeneous dopamine release. *Analyst* 2010, 135, (7), 1556-1563.

22. Zimmerman, J. B.; Wightman, R. M., Simultaneous Electrochemical Measurements of Oxygen and Dopamine Invivo. *Analytical Chemistry* 1991, 63, (1), 24-28.

23. Kristensen, E. W.; Wilson, R. L.; Wightman, R. M., Dispersion in Flow-Injection Analysis Measured with Microvoltammetric Electrodes. *Analytical Chemistry* 1986, 58, (4), 986-988.

24. Paxinos, G.; Watson, C., *The rat brain in stereotaxic coordinates*. Compact 3rd ed.; Academic Press: San Diego, 1997; p xxxiii, [78] p.

25. Robinson, D. L.; Phillips, P. E. M.; Budygin, E. A.; Trafton, B. J.; Garris, P. A.; Wightman, R. M., Sub-second changes in accumbal dopamine during sexual behavior in male rats. *Neuroreport* 2001, 12, (11), 2549-2552.

26. Compton, R. G.; Banks, C. E., *Understanding voltammetry*. World scientific publishing: Singapore, 2007; p 371 p.

27. Gerhardt, G.; Adams, R. N., Determination of Diffusion-Coefficients by Flow-Injection Analysis. *Analytical Chemistry* 1982, 54, (14), 2618-2620.

28. Ranganathan, S.; McCreery, R. L., Electroanalytical performance of carbon films with near-atomic flatness. *Analytical Chemistry* 2001, 73, (5), 893-900.

29. Heien, M. L. A. V.; Phillips, P. E. M.; Stuber, G. D.; Seipel, A. T.; Wightman, R. M., Overoxidation of carbon-fiber microelectrodes enhances dopamine adsorption and increases sensitivity. *Analyst* 2003, 128, (12), 1413-1419.

30. Heien, M. L. A. V.; Johnson, M. A.; Wightman, R. M., Resolving neurotransmitters detected by fast-scan cyclic voltammetry. *Analytical Chemistry* 2004, 76, (19), 5697-5704.

31. Wightman, R. M.; Jankowski, J. A.; Kennedy, R. T.; Kawagoe, K. T.; Schroeder, T. J.; Leszczyszyn, D. J.; Near, J. A.; Diliberto, E. J.; Viveros, O. H., Temporally Resolved Catecholamine Spikes Correspond to Single Vesicle Release from Individual Chromaffin Cells. *Proceedings of the National Academy of Sciences of the United States of America* 1991, 88, (23), 10754-10758.

32. Chow, R. H.; Vonruden, L.; Neher, E., Delay in Vesicle Fusion Revealed by Electrochemical Monitoring of Single Secretory Events in Adrenal Chromaffin Cells. *Nature* 1992, 356, (6364), 60-63.

33. Venton, B. J.; Zhang, H.; Garris, P. A.; Phillips, P. E. M.; Sulzer, D.; Wightman, R. M., Real-time decoding of dopamine concentration changes in the caudate-putamen during tonic and phasic firing. *Journal of Neurochemistry* 2003, 87, (5), 1284-1295.

34. Parikh, V.; Kozak, R.; Martinez, V.; Sarter, M., Prefrontal acetylcholine release controls cue detection on multiple timescales. *Neuron* 2007, 56, (1), 141-154.

35. Venton, B. J.; Michael, D. J.; Wightman, R. M., Correlation of local changes in extracellular oxygen and pH that accompany dopaminergic terminal activity in the rat caudate-putamen. *Journal of Neurochemistry* 2003, 84, (2), 373-381.

36. Park, J.; Kile, B. M.; Wightman, R. M., In vivo voltammetric monitoring of norepinephrine release in the rat ventral bed nucleus of the stria terminalis and anteroventral thalamic nucleus. *European Journal of Neuroscience* 2009, 30, (11), 2121-2133.

# Chapter 5

# Instrumentation for Fast-Scan Cyclic Voltammetry Combined with Electrophysiology for Behavioral Experiments in Freely Moving Animals.

## INTRODUCTION

In vivo fast-scan cyclic voltammetry (FSCV) is a powerful technique that allows real time measurement of electrochemically active biomolecules in both slices and the intact animal brain with nanomolar sensitivity. [1] Initially it was developed for the detection of biogenic amines, specifically dopamine, with carbon-fiber microelectrodes. However, in the last decade, the field has witnessed significant growth in the number of analytes that can be measured with FSCV. Detection of adenosine, [2] norepinephrine, [3] oxygen, [4] pH [5] and serotonin [6] in brain *in vivo* have been demonstrated.

Dopaminergic neurons are involved in control of motor activity, learning and motivation. FSCV has been used to detect dopamine release at the terminal fields of dopaminergic neurons in the striatum during such behaviors. [1] Technical advances in the construction of miniaturized and highly sensitive electronics as well as improvement in chemical sensitivity of the microelectrodes [7, 8] has made it possible to measure endogenous dopamine release in freely moving animals routinely, allowing the study of behavior associated with this release.

While electrochemical detection of neurotransmitter release in behaving animals is a relatively new invention, the recording of single-units, which was pioneered in the

early 1950s, is a more traditional method for investigation of brain function in real time. [9] This method is based on recording changes in extracellular potential induced by the firing of single neurons. Sharp microelectrodes, with megaohm resistance made of either glass pipettes, insulated metal wires or carbon-fiber microelectrodes are traditionally used for these recordings. [10] Multiple cells can be recorded with a single microelectrode. Today, single-unit recording is used in behaving animals and with microelectrode arrays that allow for recording of ensembles of hundreds of neurons. [11]

About thirty years ago, Julian Millar and coworkers developed instrumentation to perform FSCV and single-unit measurements simultaneously in brain preparations using a single carbon-fiber microelectrode. [12, 13] Several advantages result from the use of a single electrode for both measurements instead of separate electrodes, [14] including the ability to measure action potentials from the same cells that are being influenced by local neurotransmitter release and the minimization of brain tissue damage. The combined electrochemical/electrophysiological technique (Echem/Ephys) allows the investigation of both presynaptic and postsynaptic events simultaneously. However, the early experiments were restricted to brain slices and anesthetized animals. The original instrumentation was unsuitable for experiments in behaving animals.

In the ensuing twenty years there has been considerable refinement of electronic components pertinent to these experiments, including miniaturized electronic components and custom printed-circuit-board technology. We have taken advantage of these advancements to design a combined Echem/Ephys instrument for behavioral experiments in freely moving rats. Miniature headstages have been designed that can be mounted directly on the rat's head. Also, the traditional 3-electrode potentiostat has been reduced to a simpler 2-electrode potentiostat. Unique insight into brain processing

during behavior has been obtained with this instruments as described in prior publications. [15, 16]

## DESIGN

### Overview of Setup for Combined Behavioral Experiments.

A block diagram of the overall system is shown in **Figure 5.1**. Typically, a rat (not shown) is placed in a behavioral chamber (Med Associates Inc, St Albans, VT) with levers, house lights and an audio speaker that are used as behavioral cues during experiments. The operant box is located inside of a Faraday cage which shields the animal and sensitive components from extraneous electric fields. A set of rotating contacts (slip rings) contained in a swivel (Crist Instrument Co Inc, Hagerstown, MD) is fixed on the top of the behavioral chamber. It allows all of the electrical signals to be passed to and from a tethered headstage located on the animal's head and allows the animal free movement throughout the box. The swivel also provides one fluid port that can be used for administration of drugs. The headstage connects through the swivel to a modular Universal Electrochemical Instrument (UEI) mainframe which contains ancillary circuitry for headstage operation and processing.

Before the experiment, surgery is performed on the rat under general anesthesia. Holes are drilled in the skull to allow electrode placement in specific brain regions according to stereotaxic coordinates. [17] For dopamine measurements, a bipolar stimulating electrode is implanted in the ventral tegmental area or medial forebrain bundle, allowing stimulation of dopaminergic neurons. A guide cannula for the carbon-fiber microelectrode is implanted above the nucleus accumbens, the site of dopaminergic terminals. A Ag/AgCl reference electrode is implanted contralaterally. The animal is allowed to recover for at least three days before experiments.

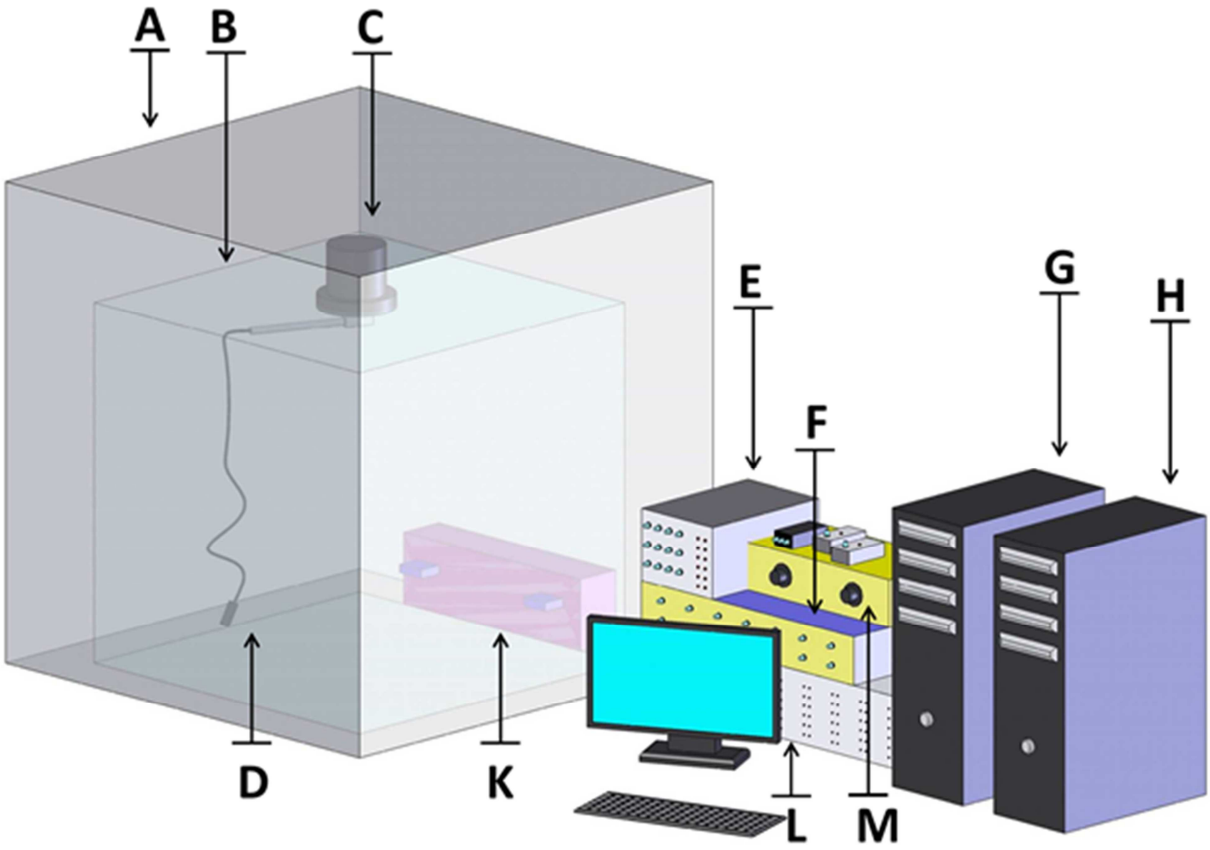


**Figure 5.1.** Setup for combined freely moving Echem/Ephys experiments.

The behavioral chamber (B) is located inside grounded Faraday cage (A). Headstage (D) is fixed on rat's head and connected through a rotating swivel (C) with the UEI potentiostat (E). The UEI is interfaced with breakout box (F) though front panel BNC connectors. The voltammetric part of the experiment is controlled by a PC (G) with NI cards that are connected to the breakout box. The electrophysiological signal is high-pass filtered (M) and sampled with NI card on the separate PC (H). The interface of the behavioral chamber components (levers, lights and tones,K) is controlled with Med Associates control module (L) that is connected to a third computer (not shown).

During recording, the carbon-fiber microelectrode is lowered into the nucleus accumbens of an awake animal. A triangular voltage excursion of -0.4 V to 1.3 V at a scan rate of 400 V/sec is applied at regular frequency for cyclic voltammogram generation. For electrochemical experiments, the triangular wave is repeated at 10 Hz, termed the CV frequency (CVF), and voltammograms are acquired in ~ 10 ms. In the combined Ephys/Echem mode, the CV frequency is 5 Hz. The 200 ms delay between cyclic voltammograms is implemented for two reasons. First, it increases the sampling window for electrophysiological data. Second, a longer holding period between cyclic voltammograms facilitates dopamine adsorption, promoting sensitivity. [7] Note that in the combined mode the potential of the carbon-fiber microelectrode is allowed to float. The voltammetric experiment, as well as delivery of electrical stimulations, is controlled by a computer running a locally written LabVIEW based program along with three National Instruments PCI DAQ cards (National Instruments, Austin, TX). The cards employed are the NI-6251 (updated version of NI-6052E), which is used for generation of the voltammetric ramp and data acquisition; the NI-6711, which is used for the output of the main clock (CVF), synchronization and generation of stimulation pulses; and the NI-6601, which is used to acquire digital signals associated with the behavior from Med Associates SmartCtrl module (Med Associates Inc, St Albans, VT).

The UEI has a switching module that uses the CVF clock to alternate between Echem and Ephys modes of operation (**Figure 5.2**). There are five CMOS switches with a total of four switches located in the switching module and one switch located on the headstage.

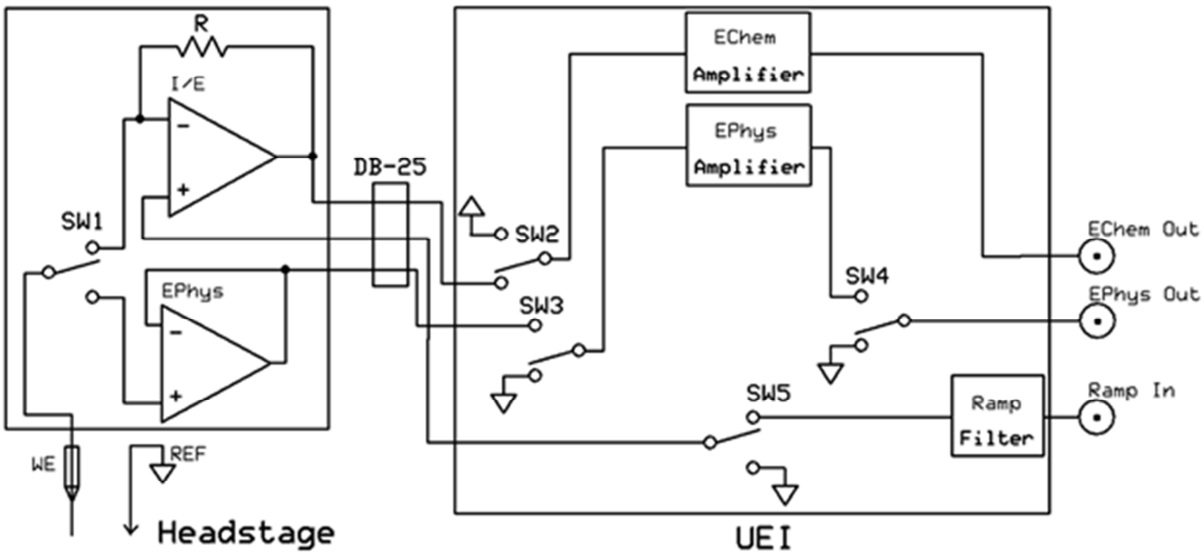


**Figure 5.2.** Block diagram of UEI potentiostat and headstage.

Left portion is the headstage that is connected via a DB-25 connector to the UEI chassis (right panel). The reference electrode (REF) is connected to ground. The output from the working electrode (WE) alternates between FSCV (Echem) and electrophys (Ephys) preamplifiers with the switch (SW1). Afterwards, signals are sent to a switching module where in Echem mode SW2 is used to connect the headstage to the Echem Amplifier. Switch SW3 grounds input to the Ephys amplifier and switch SW4 grounds the output from the Ephys amplifier to prevent overload. SW5 is used to ground the non-inverting input of the I/E converter when the system operates in Ephys mode. Headstage is connected to UEI via DB-25 cable.

The electrophysiology signal from the UEI is fed to a Grass model AM 10 high-pass filter and an audio speaker (Grass Product Group, Astro-Med Inc, West Warwick, RI) to provide audio output of neuronal activity. The same signal is also filtered using a Dual Channel Butterworth/Bessel Model 3382 8-pole filter (Krohn-Hite Corportation, Brockton, MA) and is fed to a computer equipped with an NI-6040 DAQ card and Plexon software (Plexon Inc, Dallas, TX) for unit recording and analysis.

**Design of Potentiostat for In Vivo Voltammetry.**

For FSCV measurements, 2-electrode circuitry is used. In this configuration, a voltage ramp is applied between a pair of electrodes and the resulting current is measured. This differs from the traditional 3-electrode design, in which oxidation/reduction takes place at the working electrode according to the voltage applied to the auxiliary electrode. In some systems where the resistance of the media is high, there can be a substantial difference between the desired voltage and the voltage that appears at the working electrode (due to the iR drop in the solution). Therefore, a third reference electrode is utilized to sense the actual voltage in proximity to the working electrode and, through feedback circuitry, to increase the voltage applied to the auxiliary electrode to offset the iR drop. [18] However, in this application the 2-electrode scheme is advantageous. First, the hazard of accidental electrical shocks to the experimental animal from the auxiliary electrode is avoided. Second, the 3-electrode scheme is unnecessary for compensating iR drop with microelectrodes. The resistance of the electrochemical cell with a cylindrical microelectrode is proportional to the logarithm of the distance between the working and auxiliary electrodes. [19, 20] This means that the majority of the potential drop occurs immediately adjacent to the microelectrode making it difficult to place a reference electrode in close proximity without causing damage in the measurement region. In addition, brain tissue has a relatively high conductivity (ionic

strength is greater than 0.1M), so the iR drop for microelectrodes is small and does not significantly affect the value of the applied potential. This small error can be further reduced by in vitro calibration in solution with resistivity similar to that of the brain microenvironment. [21] Additionally, as the triangular wave scan rate increases, the auxiliary electrode introduces complex impedance to the circuitry. This affects the gain and phase margins of potentiostatic circuitry which can cause stability problems leading to undesirable oscillations. [22]

In both the 3-electrode and 2-electrode potentiostatic methods, the Ag/AgCl electrode is referred to as the "reference electrode". However, it actually serves different functions in each method. In the 3-electrode scheme, the reference electrode is used to sense the potential near the working electrode, and because it is followed by a high input impedance amplifier, no current flows through the reference electrode. Current flow is from the auxiliary electrode to the working electrode in the 3-electrode method. In the 2-electrode method, current flows from the working electrode to the reference electrode which is at ground potential, so the "reference electrode" is really performing the duty of the auxiliary electrode. However, to preserve consistency with the literature, the Ag/AgCl will be called "reference electrode" throughout this manuscript.

Normally, two-electrode measurements employ an operational amplifier (op-amp) as a current to voltage (I-E) converter with the non-inverting input at ground potential and the inverting input connected to the working electrode. The ramp signal is inverted and then applied directly to the reference electrode and the current is measured by the I-E converter. This design is used in EI-400 potentiostat (ESA Biosciences Inc, Chelmsford, MA). The main drawback of this approach is that it makes it difficult to use additional current sources and sinks in the same preparation because their current will flow to the working electrode. Also, the working electrode is held at ground potential

instead of at the desired potential due to the virtual ground present at the input of the op-amp.

In the UEI, the headstage consists of an operational amplifier in I-E mode with the ramp signal applied to the non-inverting input while the working electrode is connected to the inverting input. In this case, the voltage at the microelectrode follows the voltage applied to the non-inverting input of the amplifier. At the same time, the current that flows between the working and the reference electrodes (as a result of the applied voltage) is summed at the inverting input and adds to the voltage seen at the output of the amplifier. The output voltage then becomes:

$$V_O = -\left(I_{IN} \times R_F\right) + V_R \qquad (5.1)$$

where $V_o$ is output voltage, $I_{IN}$ is input current, $R_F$ is feedback resistor and $V_R$ is ramp voltage. Since the output $V_o$ has the added ramp voltage, $V_R$, and it should be subtracted in hardware or software to produce a signal related to the voltammetric current.

The realization of this 2-electrode approach proved to be beneficial since it allowed for a number of experimental setups that are complimentary with traditional FSCV experiments in animals. For example, iontophoresis which is quantitative drug delivery technique [23] is compatible with presented potentiostat design because introduction of extra current source in iontophoretic barrel does not disturb measuring of electrochemical current on the working electrode (**Figure 5.3A**). All of the currents (electrochemical and iontophoretic) flow to the reference electrode.

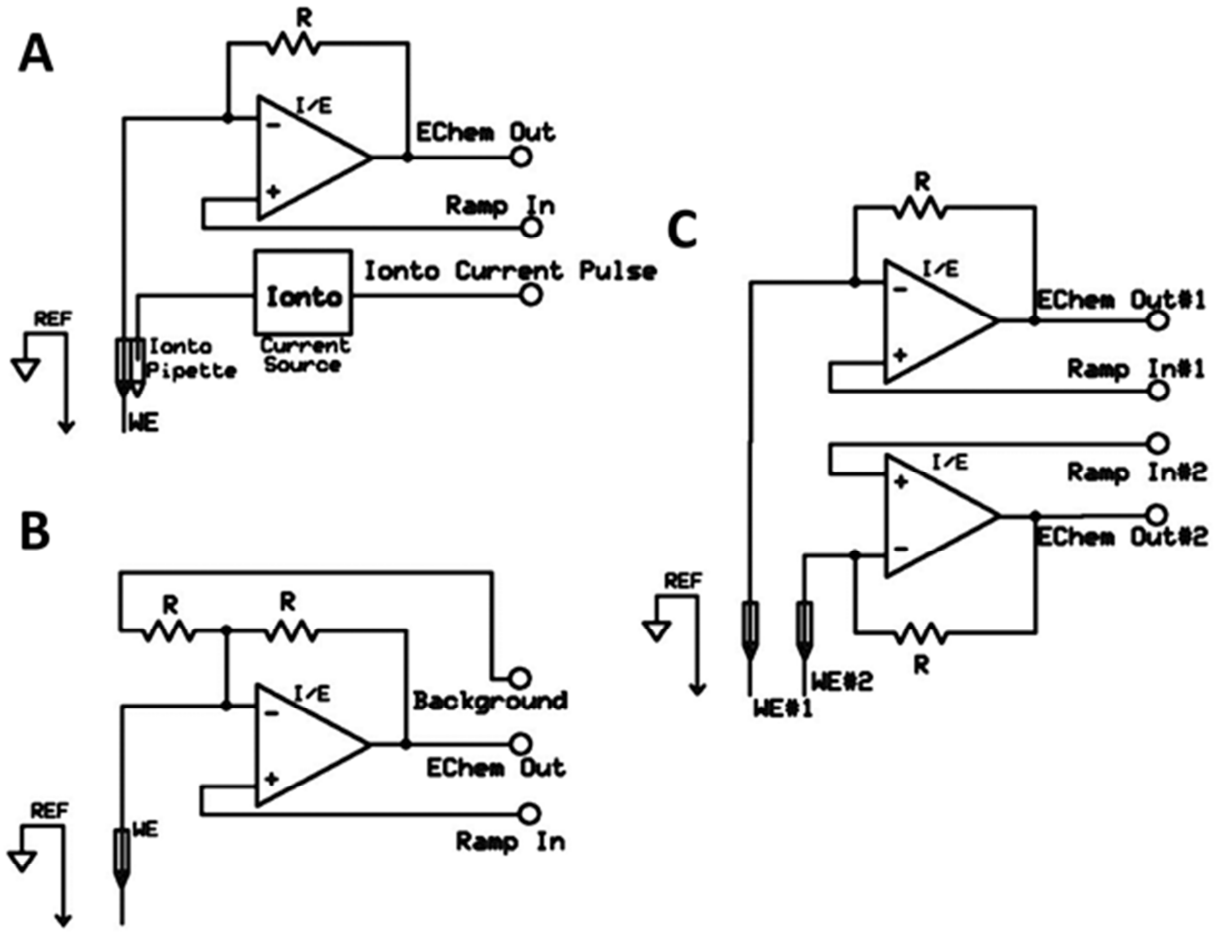


**Figure 5.3.** Schematic circuitries for headstages with iontophoresis, analog background subtraction and multiple electrodes recordings.

For the iontophoretic setup, an additional current source for drug ejection is added to the circuitry (A). For analog-background subtraction, an additional input through the gain resistor is added to the summing point of the amplifier (B). Recordings with multiple independent microelectrodes can be performed by using a separate amplifier for each microelectrode (C).

The use of fast scan rates leads to high background currents which are significantly higher than the current for oxidation of the analyte (i.e. dopamine). Traditionally, numerical background subtraction in software is used to remove this current. However, analog-background subtraction is possible and it has number of advantages such as an increase in amplifier dynamic range, a decrease in digitization noise and compensation for background drift. Recently, analog background subtraction was realized by a simple modification to the headstage circuitry. [24] An additional input for inverted background current was added to the summing point of the amplifier (**Figure 5.3B**). The background current is recorded in the absence of analyte and stored in the computer. During measurements, a DAC is used to generate the inverted background current which is sent through the second gain resistor and subtracted from the current flowing from the working electrode.

Another important advantage of the UEI is the ability to execute measurements with multiple independently controlled microelectrodes. In this setup multiple operational amplifiers can be used with a separate amplifier for each microelectrode and the same grounded reference (**Figure 5.3C**). The same voltammetric ramp can be applied to all microelectrodes [25, 26] to sample dopamine in different brain regions simultaneously. Alternatively, different voltammetric ramps can be applied to each electrode each of which is suited for specific analyte such as dopamine and oxygen [27] or 5-hydroxytryptamine. [6]

**Headstage Design for Combined FSCV and Electrophysiological Measurements in Freely Moving Animals**

Typical stand-alone electrophysiological measurement of single-unit impulses is carried out with a simple voltage follower amplifier which outputs the potential between a pair of electrodes. In our case, the measurement is between the same electrodes as

that used for FSCV, that is, between the carbon fiber microelectrode and the Ag/AgCl electrode. Because the input impedance of the buffer amplifier is extremely high, the signal amplitude is unaffected by relatively high impedance of the electrodes.

To perform simultaneous measurements in freely moving animals, a miniaturized headstage has been designed (**Figure 5.4**). The headstage is designed to fit on the rat's head without affecting its behavior and it weighs just 2.5 grams. A DB-25 connector attaches to the swivel in the behavioral chamber which, in turn, connects to the UEI mainframe. The main feature of the headstage is the surface-mount OPA 2604AU (Texas Instruments, Dallas, TX) dual operational amplifier (**Figure 5.5**). One amplifier on this chip (U2a) functions as a high gain current transducer. The other one (U2b) is arranged as a voltage follower for the electrophys signal. The system flips between Ephys and Echem mode by CMOS analog switch (SW1) MAX 319CSA (Texas Instruments, Dallas, TX) that is triggered by a digital "Relay In" signal. Particular care has been taken to select CMOS switches that have been optimized for low leakage, low charge transfer, low and matched input capacitance, and low noise. Because typical I-E converter transconductance gains vary from 1V/μA to 1V/10 nA ($R_F$ values of 1 MOhm to 100 MOhm) depending on the application, and because the redox currents are on the order of nanoamperes or less, leakage currents for the CMOS switches in the off state must be far below these levels. We chose the MAX 319CSA CMOS switch for the use on the headstage. It has leakage current 250 pA and open resistance below 20 Ohm. Charge transfer from the CMOS switch control line into the inputs and outputs must also be low in order to avoid amplifier saturation during switching. The CMOS switch open and closed terminal capacitances need to be low and relatively well matched to minimize excess charging currents during the switching process. For MAX 319CSA, on and off capacitances match and are equal to 8 pF. In addition, the analog path noise of the

CMOS switch is of concern since the switches work on the input side of the amplifier and therefore contribute directly to the total circuit noise.

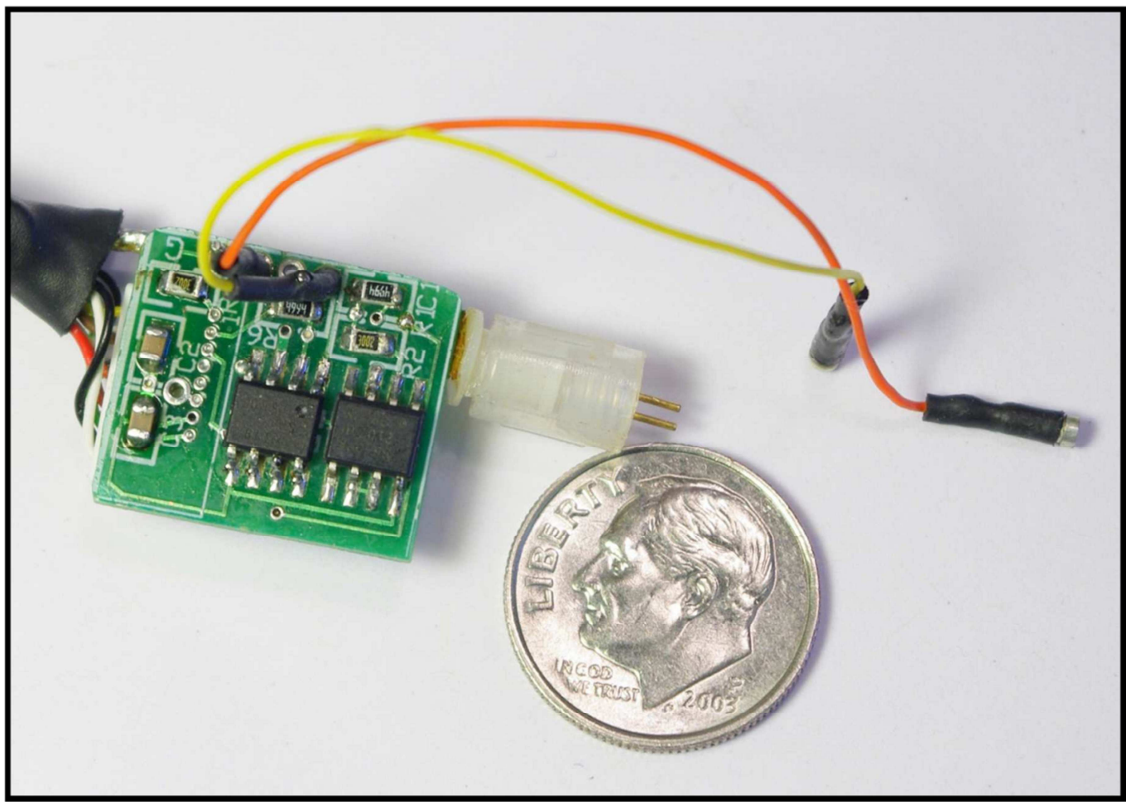


**Figure 5.4.** Photo of miniaturized headstage used for combined Echem/Ephys freely moving experiments adjacent to a U.S dime.

The orange and yellow connecting wires are for reference and working electrodes. The copper connectors on the right are for bipolar stimulating electrode. One of the SO chips is the analog switch and the other is the op amps. The cable on the left of the printed circuit board leads to a DB-25 connector.

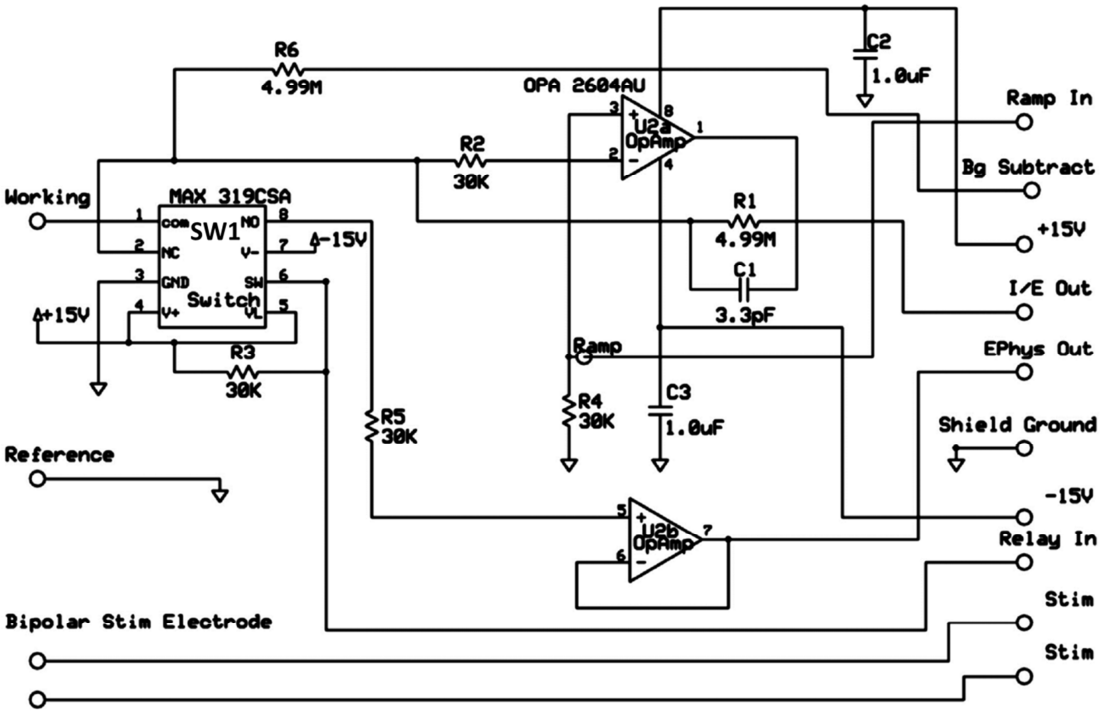


**Figure 5.5.** Circuitry for headstage used for combined Echem/Ephys freely moving experiments.

The operational amplifiers, switch, resistors and capacitors are all on a single printed circuit board (Figure 4). The outputs and inputs on the right hand side of the diagram are interfaced through a DB-25 connector.

**Design of the UEI Chassis.**

The supporting electronics for the headstage reside in the main UEI chassis. In present models, a low noise linear regulated power supply for all of the circuitry needed for FSCV and electrophysiological measurements is housed in a separate chassis. This separate chassis is located at a distance from the mainframe in order to reduce electromagnetic noise coupled from the transformer to sensitive circuitry. The UEI mainframe has a backplane for inserting various support modules. This allows for maximum flexibility in construction of multi-channel systems, addition of filtering hardware, and addition of future enhancements. In the simplest case, two plug-in modules are used. One module contains additional variable post-amplification for both the electrochemical and the electrophysiological signals and routes signals to and from the headstage. The second module is used for analog low pass filtering of the digitized triangular signal before it is directed to the headstage. The filter removes the staircase transitions from the ADC output which can noise due to unwanted C*dV/dt charging of the electrode capacitance at each transition. Other plug-in modules consist of a video text module that synchronizes real-time video with the control software and multi-channel FSCV modules.

Electronic Design for Switching Control Module.

The switching control modules alternate between the Ephys and Echem mode of operation (**Figure 5.6**). Switching is triggered by a “Relay In” signal that is received from the computer via a BNC on the front panel of the UEI instrument. Analog CMOS switches U5 (SW2 and SW5) and U2 (SW3 and SW4) are MAX 314 CMOS switches (DIP, Maxim, Sunnyvale, CA), that have a rapid (> 1 μS) switching time with low (10 Ω) on-resistance.

In Echem mode, the I/E signal received from the headstage is sent to the electrochemical amplifier. The triangular wave (Ramp In) is computer generated and received from BNC connector on UEI front panel and sent to the headstage (Ramp Out). In Echem mode, the “Ephys In” signal from the headstage, the output to the spike amplifier (Ephys Out to Amp), and the “Ephys Out” to UEI front panel are all grounded. In Ephys mode, the “Ephys In” signal received from the headstage is sent to the spike amplifier. Afterwards, it is sent out on front panel BNC “Ephys Out”. Voltammetric ramp (Ramp In), electrochemical input from the headstage (I/E In) and input to electrochemical amplifier (I/E Out to Amp) are disconnected. A “RELAY IN” LED on the front panel notifies the user whenever the system switches to the Ephys state and it is controlled by circuitry shown on the right bottom corner (**Figure 5.6**).

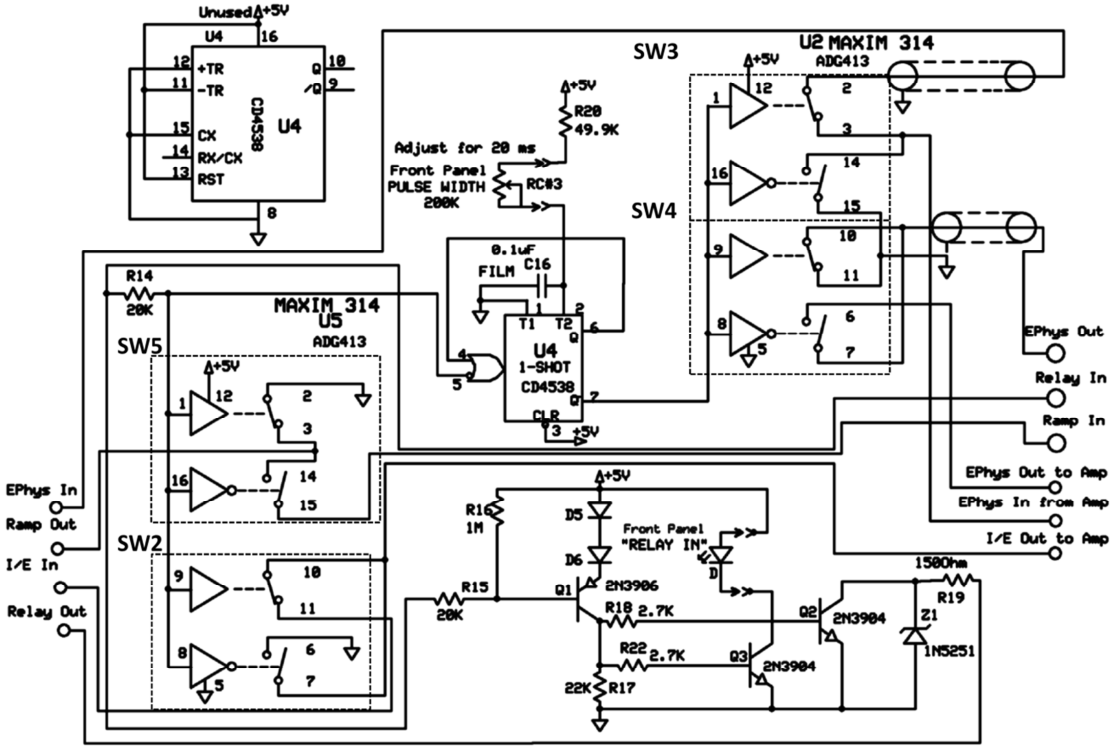


**Figure 5.6.** Circuitry for switching control module.

Switching control module is housed in the UEI and it consists of SW2, SW3, SW4 and SW 5 switches. They alternate between Echem and Ephys modes of operation.

Electronic Design of the Electrochemical Amplifier with Variable Gain.

The voltammetric signal is received from the switching control model after being amplified on the headstage and it is further amplified with variable gain (**Figure 5.7**). The main amplifier U2a is based on dual low noise LT1113 chip (Linear Technology, Milpitas, CA). The gain of this amplifier can be chosen using push buttons on UEI front panel (K3, K4 and K5) and can be set to X1, X2, X5 and X10 multiplies of the headstage gain. Front panel LEDs mark the gain selected. A CD4017 (National instruments, Austin, TX) counter chip is used to control the LEDs and switch the gain.

To notify the user about overload in I/E signal, an overload detector is constructed with U5a and U5b which are LM393 low power low voltage dual comparator (National Semiconductors, Santa Clara, CA). In a case of an overload, a red LED on the front panel illuminates when the I/E current exceeds the amplifier output limit. The LED "on" time is controlled with dual precision monostable CD4538 (National Semiconductors, Santa Clara, CA). After being processed through the first amplifier, the I/E signal is buffered through the second LT1113 chip (U2b) and sent out through a BNC connector on UEI front panel.

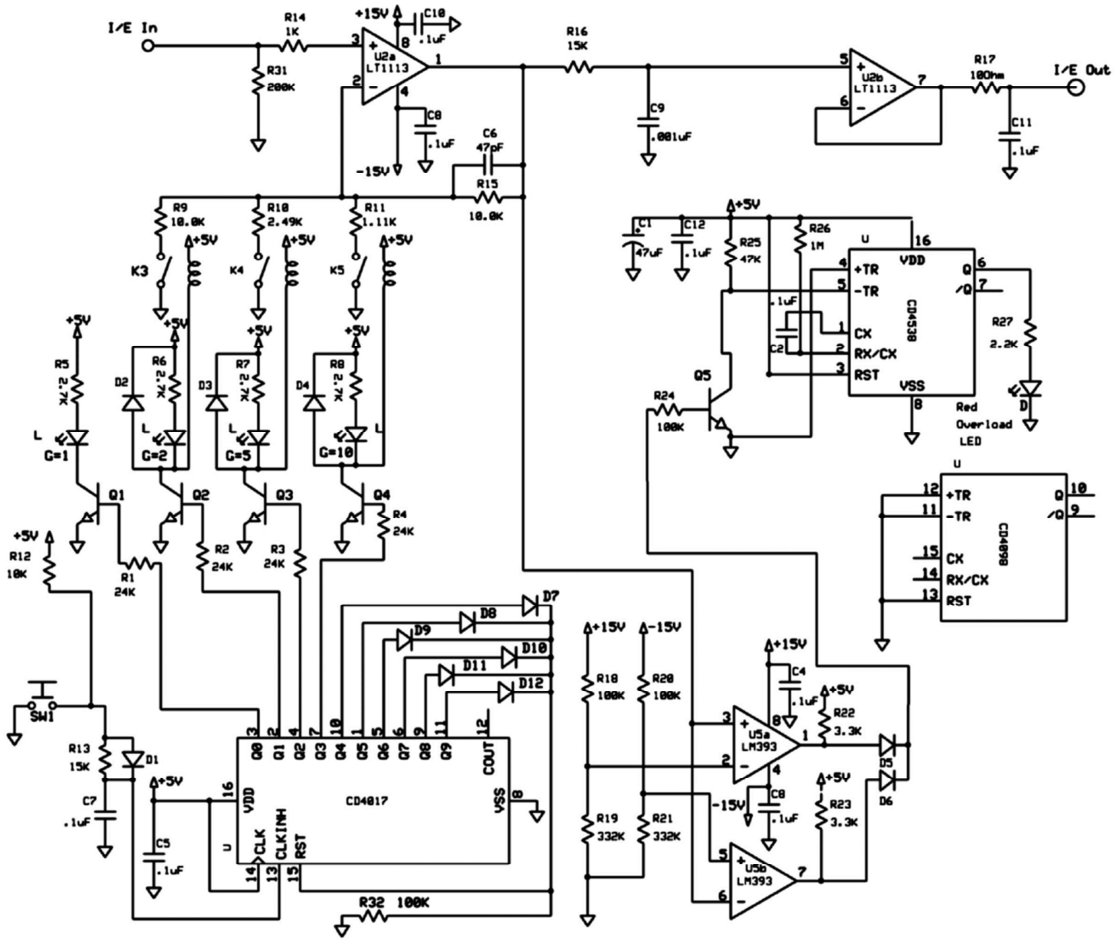


**Figure 5.7.** Circuitry for electrochemical amplifier with variable gain.

Electronic Design of the Spike Amplifier.

The electrophysiological signal from neurons (spikes) is received from the switching control module. Amplification of this Ephys signal is done by an OP27 (Analog Devices, Norwood, MA) low-noise precision operational amplifier (**Figure 5.8**). The signal is amplified by two amplifiers with high gain, U1 and U2 (resistors R5, R12 and capacitors C3, C4). Adjustable high pass filtering is employed to remove the DC component ("Front Panel RC"). Overload can latch amplifiers used with high gain. To prevent it, diode pairs (D1, D2, D3 and D4) are used to limit the maximum input voltage to ±0.6 V. After being processed through the second U2 amplifier, the Ephys signal is sent back to switching control module. Switching is utilized on the Ephys signal because active gating is not always available on the various third party hardware used for spike processing (i.e., Plexon).

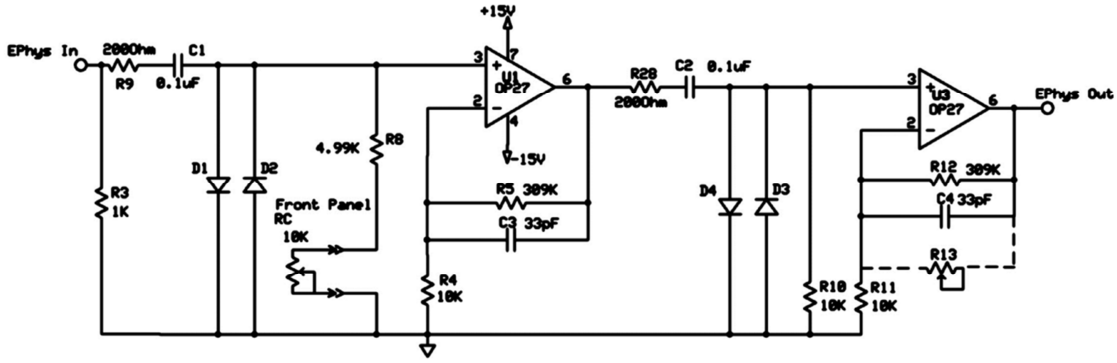


**Figure 5.8.** Circuitry for the neural spike amplifier.

## CONCLUSIONS.

FSCV combined with single-unit electrophysiology is a powerful technique for studying the dopaminergic system on both the presynaptic and post-synaptic side. The instrument allows chemical and electrical information to be obtained at a single location within the brain. Application of this technique in behaving animals is of particular interest.

## REFERENCES


1. Robinson, D. L.; Hermans, A.; Seipel, A. T.; Wightman, R. M., Monitoring rapid chemical communication in the brain. *Chemical Reviews* 2008, 108, (7), 2554-2584.

2. Swamy, B. E. K.; Venton, B. J., Subsecond detection of physiological adenosine concentrations using fast-scan cyclic voltammetry. *Analytical Chemistry* 2007, 79, (2), 744-750.

3. Park, J.; Kile, B. M.; Wightman, R. M., In vivo voltammetric monitoring of norepinephrine release in the rat ventral bed nucleus of the stria terminalis and anteroventral thalamic nucleus. *European Journal of Neuroscience* 2009, 30, (11), 2121-2133.

4. Venton, B. J.; Michael, D. J.; Wightman, R. M., Correlation of local changes in extracellular oxygen and pH that accompany dopaminergic terminal activity in the rat caudate-putamen. *Journal of Neurochemistry* 2003, 84, (2), 373-381.

5. Takmakov, P.; Zachek, M. K.; Keithley, R. B.; Bucher, E. S.; McCarty, G. S.; Wightman, R. M., Characterization of Local pH Changes in Brain Using Fast-Scan Cyclic Voltammetry with Carbon Microelectrodes. *Analytical Chemistry* 2010, 82, (23), 9892-9900.

6. Hashemi, P.; Dankoski, E. C.; Petrovic, J.; Keithley, R. B.; Wightman, R. M., Voltammetric detection of 5-hydroxytryptamine release in the rat brain. *Anal Chem* 2009, 81, (22), 9462-71.

7. Heien, M. L. A. V.; Phillips, P. E. M.; Stuber, G. D.; Seipel, A. T.; Wightman, R. M., Overoxidation of carbon-fiber microelectrodes enhances dopamine adsorption and increases sensitivity. *Analyst* 2003, 128, (12), 1413-1419.

8. Takmakov, P.; Zachek, M. K.; Keithley, R. B.; Walsh, P. L.; Donley, C.; McCarty, G. S.; Wightman, R. M., Carbon Microelectrodes with a Renewable Surface. *Analytical Chemistry* 2010, 82, (5), 2020-2028.

9. Lemon, R.; Prochazka, A., *Methods for neuronal recording in conscious animals*. Wiley: Chichester [West Sussex] ; New York, 1984; p xii, 162 p.

10. Humphrey, D. R.; Schmidt, E. M., *Extracellular single-unit recording methods*. Humana Press: Clifton, N.J., 1991; Vol. 15, p 391.

11. Nicolelis, M. A. L., *Methods for neural ensemble recordings*. 2nd ed.; CRC Press: Boca Raton, 2008; p xx, 269 p., [16] p. of plates.

12. Millar, J.; Barnett, T. G., Basic Instrumentation for Fast Cyclic Voltammetry. *Journal of Neuroscience Methods* 1988, 25, (2), 91-95.

13. Stamford, J. A.; Palij, P.; Davidson, C.; Jorm, C. M.; Millar, J., Simultaneous Real-Time Electrochemical and Electrophysiological Recording in Brain-Slices

with a Single Carbon-Fiber Microelectrode. *Journal of Neuroscience Methods* 1993, 50, (3), 279-290.

14. Su, M. T.; Dunwiddie, T. V.; Gerhardt, G. A., Combined Electrochemical and Electrophysiological Studies of Monoamine Overflow in Rat Hippocampal Slices. *Brain Research* 1990, 518, (1-2), 149-158.

15. Cheer, J. F.; Heien, M. L. A. V.; Garris, P. A.; Carelli, R. M.; Wightman, R. M., Simultaneous dopamine and single-unit recordings reveal accumbens GABAergic responses: Implications for intracranial self-stimulation. *Proceedings of the National Academy of Sciences of the United States of America* 2005, 102, (52), 19150-19155.

16. Owesson-White, C. A.; Ariansen, J.; Stuber, G. D.; Cleaveland, N. A.; Cheer, J. F.; Wightman, R. M.; Carelli, R. M., Neural encoding of cocaine-seeking behavior is coincident with phasic dopamine release in the accumbens core and shell. *European Journal of Neuroscience* 2009, 30, (6), 1117-1127.

17. Paxinos, G.; Watson, C., *The rat brain in stereotaxic coordinates*. 5th ed.; Elsevier Academic Press: Amsterdam ; Boston, 2005; p xliii, [166] p.

18. Kissinger, P. T.; Heineman, W. R., *Laboratory Techniques in Electroanalytical Chemistry*. Marcel Dekker Inc: 1996.

19. Robinson, R. S.; Mccurdy, C. W.; Mccreery, R. L., Microsecond Spectroelectrochemistry by External Reflection from Cylindrical Microelectrodes. *Analytical Chemistry* 1982, 54, (13), 2356-2361.

20. Wightman, R. M.; Wipf, D. O., Voltammetry at Ultramicroelectrodes. In *Electroanalytical chemistry: a series of advances*, Bard, A. J., Ed. Marcel Dekker: 1989; Vol. 15, pp 267-353.

21. Kristensen, E. W.; Wilson, R. L.; Wightman, R. M., Dispersion in Flow-Injection Analysis Measured with Microvoltammetric Electrodes. *Analytical Chemistry* 1986, 58, (4), 986-988.

22. Amatore, C.; Maisonhaute, E., When voltammetry reaches nanoseconds. *Analytical Chemistry* 2005, 77, (15), 303a-311a.

23. Herr, N. R.; Kile, B. M.; Carelli, R. M.; Wightman, R. M., Electroosmotic flow and its contribution to iontophoretic delivery. *Anal Chem* 2008, 80, (22), 8635-41.

24. Hermans, A.; Keithley, R. B.; Kita, J. M.; Sombers, L. A.; Wightman, R. M., Dopamine detection with fast-scan cyclic voltammetry used with analog background subtraction. *Anal Chem* 2008, 80, (11), 4040-8.

25. Zachek, M. K.; Park, J.; Takmakov, P.; Wightman, R. M.; McCarty, G. S., Microfabricated FSCV-compatible microelectrode array for real-time monitoring of heterogeneous dopamine release. *Analyst* 2010, 135, (7), 1556-63.

26. Zachek, M. K.; Takmakov, P.; Park, J.; Wightman, R. M.; McCarty, G. S., Simultaneous monitoring of dopamine concentration at spatially different brain locations in vivo. *Biosens Bioelectron* 2010, 25, (5), 1179-85.

27. Zachek, M. K.; Takmakov, P.; Moody, B.; Wightman, R. M.; McCarty, G. S., Simultaneous decoupled detection of dopamine and oxygen using pyrolyzed carbon microarrays and fast-scan cyclic voltammetry. *Anal Chem* 2009, 81, (15), 6258-65.

# Chapter 6

# Evidence of Contralateral Synchronization of Transient Dopamine Release in Nucleus Accumbens In Vivo.

## INTRODUCTION

The brain is a very complex and precisely interconnected organ. Its major cellular components are neurons and glia cells. Neurons are differ from other types of cells as they can extend over large distances and send their axons to remote locations. This architectural feature implies the importance of communication between different brain regions and suggests that a full understanding of cerebral functions can be achieved only by integral investigation of the brain as an intact organ.

Establishing flows of information between brain regions and revealing the structural organization of the brain is sometimes declared as a major goal for neuroscience. [1] New language was developed to describe this focus. The complex matrix of interconnections of the human brain is referred to as "connectome" [2] in analogy to such terms as genome, proteome and metabolome that are more familiar for analytical chemists. From a scientific point of view, the connectome is the most complex system to study and it requires multidisciplinary approach that recruits experimental innovations from different fields.

Understanding of the connectome has a number of practical challenges including the requisite to use noninvasive or minimally invasive techniques since the dynamic communication between regions in the functioning brain is an object of the research and

violation of brain integrity jeopardizes validity of the findings. Integral investigation of the brain is currently done using functional resonance imaging (fMRI) in humans. [3] Also, electrophysiological recordings with implantable microelectrode arrays are used in primates and rodents. [4]

Both fMRI and electrophysiological recordings are very powerful techniques but they suffer from a common limitation. fMRI provides information about transport of chemical markers with the blood flow in the brain which has little or no specificity to the type of participating neurons in the area of interest. [5] Identification of specific neurons with electrophysiological recording is possible in certain cases due to the nature of neural firing and by the shape and dynamic characteristics of the transient changes in electrical field but it is not completely specific. It is especially problematic for recordings of dopaminergic neurons. [6, 7] Overall, neither of fMRI or electrophysiological recordings can provide sufficient information to establish unequivocally the identity of the neurons that were sampled.

Spatially resolved sampling of chemical evidence of neural activity in real time is an excellent tool to study brain connectome since chemical identity of the released neurotransmitters in many cases allows for unequivocal identification of participating neurons. There are very few reliable techniques that can sample neural activity in multiple brain regions simultaneously with the desired precision. Fast-scan cyclic voltammetry (FSCV) has been used to detect release of catecholamines in brain in real time. [8] Recent progress in fabrication of carbon microelectrode arrays compatible with fast-scan cyclic voltammetry in vivo provides a route to investigate brain connectome using chemical sampling. [9-11] In this chapter, this approach was employed for the investigation of synchronization of dopaminergic neurotransmission in different brain regions.

Dopaminergic neurons are involved in learning, memory and initiation of movement. Dysfunctions of dopaminergic system are associated with a number of debilitating diseases such as substance abuse, schizophrenia and Parkinson's disease. [12] Dopaminergic neurons are pacemaking neurons and they usually fire in a regular pattern. Understanding of this pacemaking activity might help to shed further light on the functions associated with dopaminergic neurotransmission. [13, 14]

Slow oscillations of neuronal activity (<1 Hz) are observed in the brain during deep sleep and under general anesthesia. [15] These oscillations are known to synchronize neuronal activity across large areas of the brain including the entire cortex. Cortical neurons modulate dopaminergic neurons [16] and cortical input goes to medium spiny neurons of nucleus accumbens, [17] the target of dopaminergic neurons. Medium spiny neurons in turn have projections that feedback to dopaminergic neurons in the ventral tegmental area (VTA). Since slow oscillations during sleep and anesthesia involve global synchronization, it is interesting to investigate whether they reflected in synchronization of activity of dopaminergic neurons during sleep. Slow oscillations in electrical activity of dopaminergic neurons in anesthetized animals have been reported. [18, 19] These oscillations were enhanced after application of raclopride in combination with psychostimulants (cocaine and amphetamines). Furthermore, forebrain transection from the VTA leads to elimination of oscillations, which suggests that they are controlled by inputs from the cortex. [19]

Previously we reported the observation of dopamine concentration transients in urethane anesthetized animals after combined application of certain drugs. The combinations were haloperidol with nomifensine [20] and raclopride with cocaine. [21] Haloperidol and raclopride are D2 dopamine receptor antagonists. The D2 dopamine receptor is an inhibitory receptor that functions as an autoreceptor that is expressed

presynaptically on dopaminergic terminals. After dopamine binding and activation of the receptor, it provides negative feedback to dopaminergic neurons and inhibits their firing and decreases dopamine release. The antagonists turn off this feedback by occupying D2 receptors. [22] Nomifensine and cocaine are dopaminergic transporter (DAT) inhibitors. DAT works as a pump that removes dopamine from the extracellular space after it was released from the synaptic terminal. DAT blockers bind to the DAT and inhibit its function. [23] Analogous to the DAT blockers, there are some psychostimulant drugs that effectively reverse the activity of the DAT that causes the DAT to pump dopamine out of the neuron. In both cases, dopamine stays longer in the extracellular space and diffuses further away from the release site.

The transients observed in anesthetized rat after these drug cocktails occurred in a regular pattern with a frequency of ~ 0.25 Hz, similar to the frequency of slow oscillations occurring in the cortex during sleep. In this work we investigated whether this activity of dopaminergic neurons is synchronous in both hemispheres.

## MATERIALS AND METHODS

### Chemicals and Drugs

All chemicals and drugs were reagent-quality and were used as received from Sigma-Aldrich (St. Louis, MO, USA). Raclopride (3 mg/kg), cocaine (15 mg/kg), amphetamine (3 mg/kg), methamphetamine (3 mg/kg) and methylphenidate (10 mg/kg) were dissolved in saline. GBR-12909 hydrochloride (15 mg/kg) was dissolved in double distilled water and then diluted with saline. All drugs were injected intraperitoneally (i.p.). Post calibration of carbon-fiber microelectrodes was performed in a PBS buffer solution (140 mM NaCl, 3 mM KCl, 10 mM $NaH_2PO_4$, pH 7.4) prepared with double distilled water.

**Fast-Scan Cyclic Voltammetry**

Glass-encased cylindrical carbon-fiber and Ag/AgCl reference electrodes were prepared as described earlier. [24] T-650 carbon fibers (Thornel, Amoco Corp., Greenville, SC) with an exposed length of 100 µm and 6 µm in nominal diameter were used. The experimental setup for dual measurement has been described previously. [9, 10] A modified version of TH1- software (ESA Inc, Chelmsford, MA, USA) was used with Quad UEI instruments with four independent potentiostats (University of North Carolina Department of Chemistry Electronic Shop) operated in two electrode mode. FSCV experiments were performed using triangular waveform from - 0.4 to + 1.3 V and back to - 0.4 V with scan rate of 400V/s that was repeated every 100 ms. The waveform was low-pass filtered at 2 kHz and applied to both carbon-fiber microelectrodes. Background-subtracted cyclic voltammograms were obtained by digitally subtracting voltammograms collected during baseline recording from those collected during electrical stimulation event. Data were digitized and processed using NI-6711 and NI-6251 DAC/ADC cards and TH-1 software.

**Experiments in Animals**

Adult male Sprague-Dawley rats weighing between 300-400 g were purchased from Charles Rivers (Wilmington, MA) and housed in temperature and humidity controlled rooms with a 12 hour light-dark cycle. Food and water were available ad libitum. All procedures for handling and caring for the laboratory animals were in accordance with the Guide for Care and Use of Laboratory Animals and were approved by the Institutional Animal Care and Use Committee of the University of North Carolina at Chapel Hill.

Rats were anesthetized with urethane (1.5 g/kg) and immobilized in a stereotaxic frame (David Kopf Instruments, Tujunga, CA). The holes were drilled for the reference

(Ag/AgCl) electrode and the carbon-fiber microelectrodes. Anteroposterior (AP), mediolateral (ML) and dorsoventral (DV) positions were referenced from bregma. All coordinates were obtained from the rat brain atlas. [25] The pia mater was punctured, removed and two carbon-fiber microelectrodes were implanted vertically into right and left nuclei accumbens (AP + 1.8 mm, ML + 1.2 mm, DV from - 6.5 to - 7.5 mm). Microelectrode placement is shown on **Figure 6.1A**. An Ag/AgCl reference electrode was placed in the contralateral cortex and fixed with dental cement on the skull for all measurements.

Simultaneous measurement of transient dopamine release induced by the drug cocktail in caudate putamen of the left hemisphere and nucleus accumbens of the right was performed to prove that there is no electronic cross talk between the electrodes and that the correlation of dopamine transients has biological relevance (**Figure 6.1B-C**).

Experiment with electrical stimulation was done by placing a bipolar stainless steel stimulating electrode (0.2 mm diameter, Plastics One, Roanoke, VA, USA) in the pathway of axons of dopaminergic neurons in medial forebrain bundle (MFB) of the right hemisphere (AP – 2.8 mm, ML -1.7 mm, DV from - 8.0 to - 9.0 mm). Bipolar stimulation train pulses were generated with TH-1 software (60 Hz, 40 pulses, 2 ms wide) and applied through current to voltage converters (NL 800A, Neurolog, Medical Systems Corp, Great Neck, NY, USA) with output current of 300 µA for each phase of the pulse.

**Data Analysis.**

Voltammetric data are presented in a form of color plots where abscissa represents time, ordinate represents potential and current is encoded in false color. [26] Raw data were low-path filtered and smoothed with TH-1 software. Cross correlation analysis and fast Fourier transforms were performed with MATLAB (MathWorks Inc,

Natick, MA, USA). Plots were created using Graphpad Prizm (GraphPad Software, San Diego, CA, USA).

All data presented here are representative single experiments.

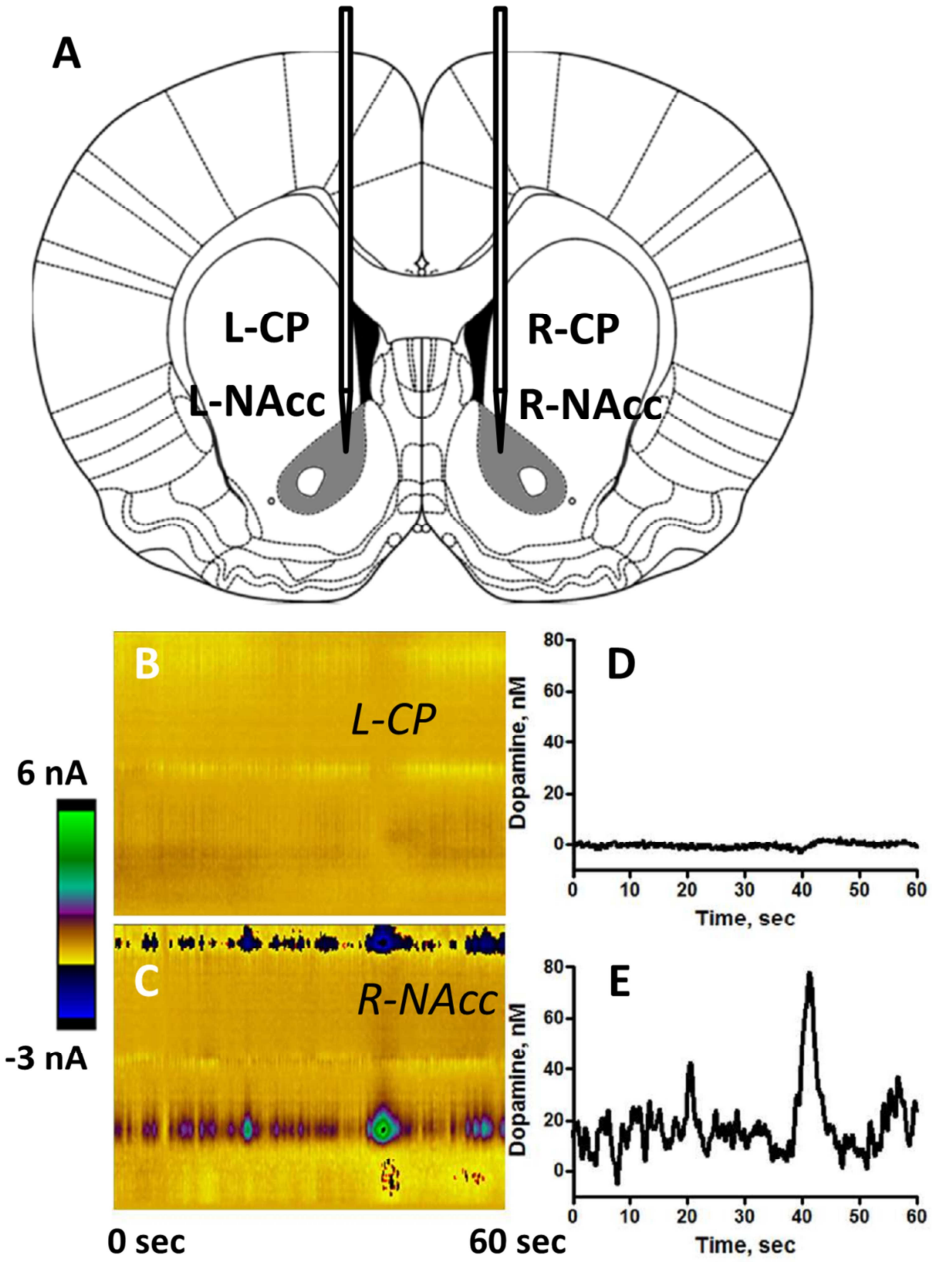


**Figure 6.1.** Carbon-fiber microelectrodes placement for dual contralateral recordings.

Carbon-fiber microelectrodes were implanted in each nucleus accumbens (core) of both hemispheres contralaterally to each other. Recordings were done at depth of 6.5 – 7.0 mm (dorsal-ventral). Nuclei accumbens (core) are shown as gray areas (A). Simultaneous sampling of dopamine transients between caudate-putamen (L-CP) and nucleus accumbens (R-NAcc) after application of raclopride (3 mg/kg) with ritalin (10 mg/kg) showed no transients in the left caudate-putamen (B - color plot, D – concentration trace), but robust transient dopamine release in the right nucleus accumbens (C - color plot, E – concentration trace).

## RESULTS AND DISCUSSION

### Evidence of Connection between Dopaminergic Systems of Left and Right Hemispheres.

Most of the neural circuits are symmetrical and some of them such as optical and motor neurons decussate (cross over to the opposite side). [27] In this arrangement, neurons from the right hemisphere sent projections to their targets in the left hemisphere and vice versa. Anatomical studies involving tracers demonstrated that less than 5% of dopaminergic neurons decussate [28]. Dopamine neurons whose cell bodies are located in the VTA of one hemisphere project their axons to the nucleus accumbens in the same hemisphere. However, it is known that neurons in frontal cortex and thalamus decussate and both hemispheres of the brain communicate with each other through these connections.

To investigate connection between dopaminergic neurons in opposite hemispheres, contralateral stimulation of dopaminergic neurons was used. It was observed that stimulation of the MFB pathway in the left hemisphere elicited robust dopamine release in the nucleus accumbens of the right hemisphere (**Figure 6.2**). This observation provides evidence that there is a connection between dopaminergic systems in right and left hemispheres, but, it must involve additional pathways besides dopamine neurons.

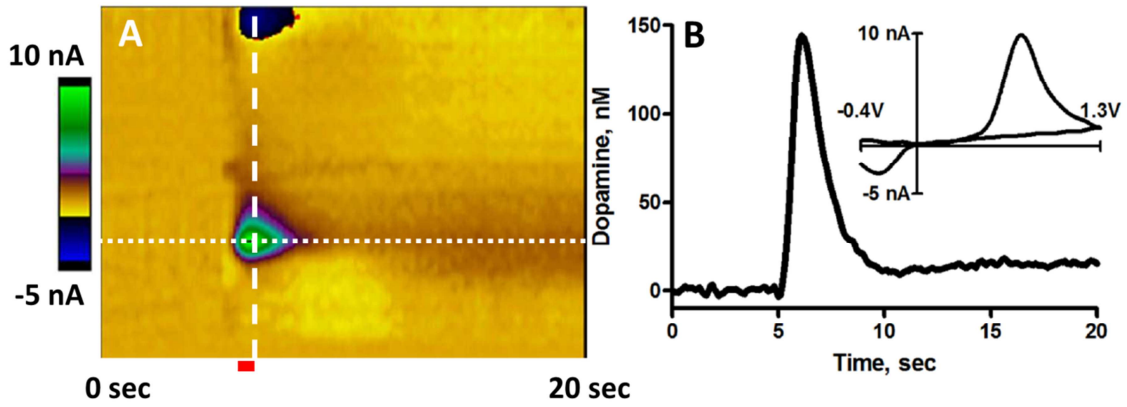


**Figure 6.2.** Contralateral stimulation induces dopamine release in nucleus accumbens.

The stimulating electrode was placed in the MFB of the left hemisphere and the recording carbon-fiber microelectrode was placed in nucleus accumbens in the right hemisphere. Train of stimulation pulses applied to MFB in left hemisphere (60 Hz, 40 pulses, 2 ms width, 300 µA in amplitude) elicited robust dopamine release in the contralateral nucleus accumbens in the right hemisphere (color plot, A). Red bar shows stimulation train; dashed and dotted lines represent cyclic voltammogram and current versus time traces extracted from the two-dimensional array of color-plot data (B).

**Synchronization of Endogenous Dopamine Transients between Hemispheres in Anesthetized Rat.**

In prior work, dopamine transients in anesthetized rats were observed only following application of the drug cocktail. However, these experiments were done using the 1.0 V waveform which is less sensitive than the 1.3 V waveform that was adapted later. [29, 30] In this work, spontaneous dopamine transients were observed in the nuclei accumbens (core) of both hemispheres with the 1.3 V waveform. Apparently, the increase in electrode sensitivity made it possible to detect dopamine transients in anesthetized rat without application of any drugs. However, transients were very rare and small with a maximum amplitude less than 50 nM (**Figure 6.3**).

Curiously, dopamine transients appear to be synchronized in time between hemispheres. Two transients, at 20 sec and at 53 sec can be clearly seen on **Figure 6.3** and their coincidence on both electrodes in two hemispheres is apparent. However, due to the infrequent occurrence of naturally occurring transients in anesthetized rats it was difficult to collect relevant statistics to make convincing argument about their synchronization. Instead, several drug cocktails that can induce more transients were used to investigate synchronization in firing of dopaminergic neurons.

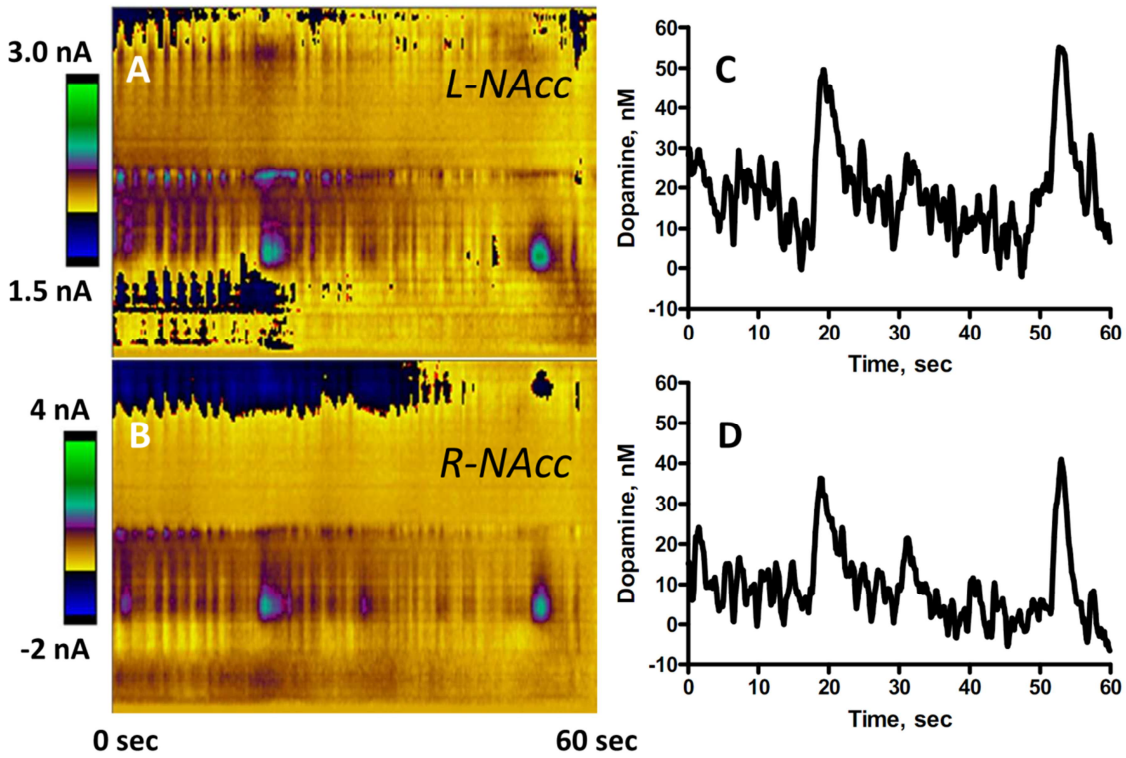


**Figure 6.3.** Recording of dopamine transients in nucleus accumbens core in the left and right hemispheres.

Dopamine transients acquire in urethane anesthetized rat without pharmacological intervention. Transients are very rare but they are synchronized in time. There are two transients, at 20 sec and 53 s that are simultaneously observed at both microelectrodes.

**Synchronization of Pharmacologically Induced Dopamine Transients between Hemispheres in Anesthetized Rat.**

Application of the D2 autoreceptor antagonist, raclopride, alone led to appearance of abundant dopamine transients (**Figure 6.4A**). The transients in both hemispheres were temporally synchronous (**Figure 6.4A**, concentration traces). Cross correlation analysis was used to quantify synchronization of dopamine transients (**Figure 6.5A**). The correlation coefficient of 0.802 for the main peak at lag of zero seconds suggests strong synchronization between both traces.

Use of raclopride with GBR-12909, which is a selective DAT blocker like nomifensine, also induced synchronous transients (**Figure 6.4B**). Similar synchrony of dopamine release was also observed following raclopride and cocaine, a nonselective DAT blocker (**Figure 6.4C**). Cross correlation analysis reveals presence of major correlation peak at lag of -0.1 sec. The correlation coefficient is lower for GBR-12909 and lag is insignificantly different from zero presumably due to the presence of interferences in signal that was acquired in the right hemisphere.

In addition to DAT blockers, drugs that cause reverse transport at the DAT were used. There are no reports on the ability of these drugs to induce transients when applied with raclopride. However, mechanism of their action on DAT as well as evidence that they can induce slow oscillations in firing of dopaminergic neurons [19] makes it plausible to expect dopamine transients after these drugs. Thus, application of raclopride with either methylphenidate (**Figure 6.4D**); amphetamine (**Figure 6.4E**) or methamphetamine (**Figure 6.4F**) caused abundant dopamine transients that were synchronous in time between hemispheres (**Figure 6.5D-F**).

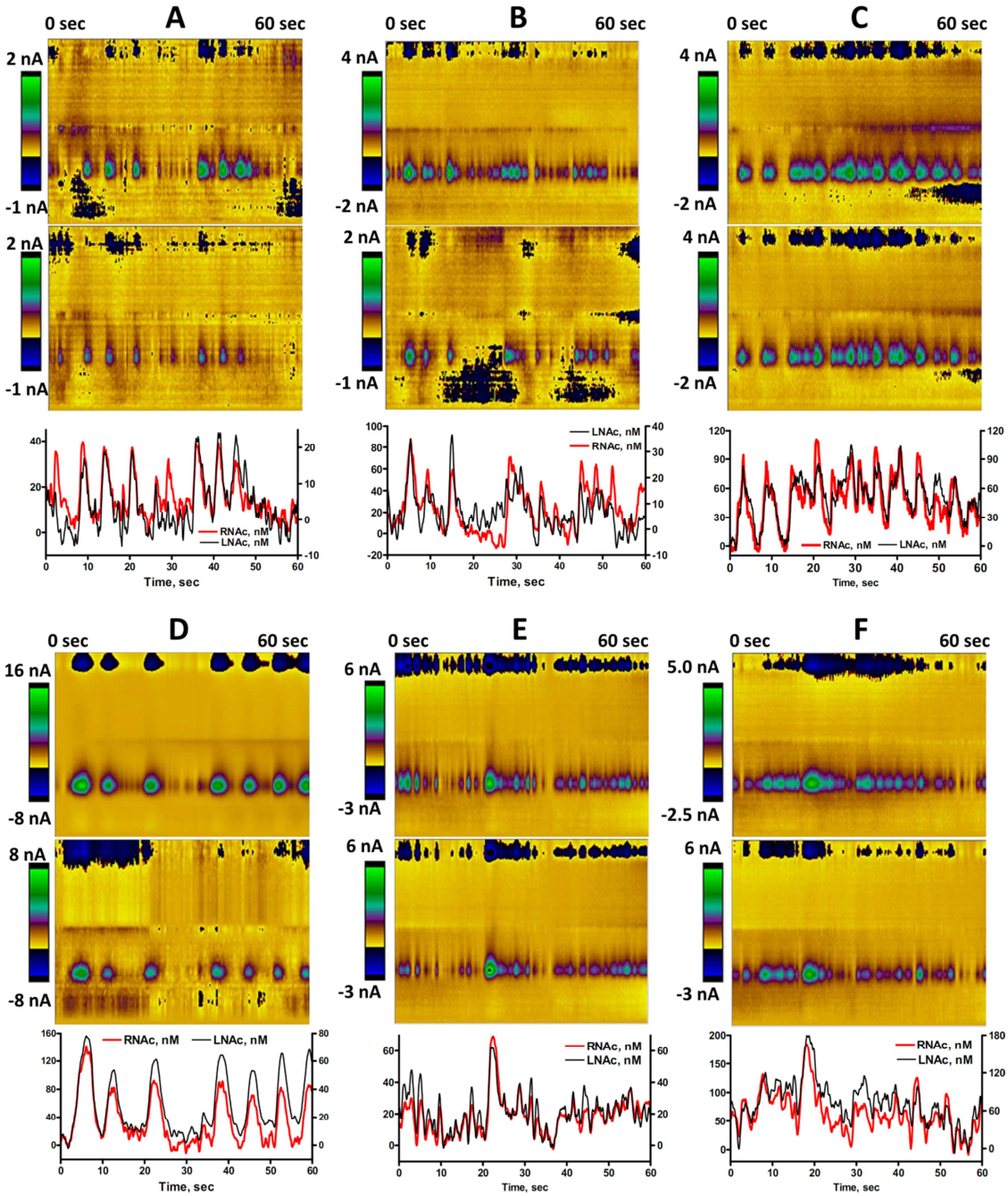


**Figure 6.4.** Dopamine transients in the nucleus accumbens core in left and right hemispheres.

Abundant dopamine transients were observed after raclopride alone (A); raclopride + GBR-12909 (B); raclopride + cocaine (C); raclopride + ritalin (D); raclopride + amphetamine (E); raclopride + methamphetamine (F). Color plots are shown for both left and right hemispheres (top and bottom panel in each figure). Concentration traces are shown below the color plots in each figure.

The series of well pronounced peaks in the cross correlation of the concentration time traces from different hemispheres after drugs implies that there is periodicity or rhythmic oscillations in dopamine transients. The peaks are present for raclopride (**Figure 6.5A**); raclopride with cocaine (**Figure 6.5C**) and raclopride with methylphenidate (**Figure 6.5D**). Fourier transform of these concentration traces shows that the major frequency of oscillations is around 0.2 Hz. (**Figure 6.5G-K**) Frequency of slow oscillations in firing of dopaminergic neurons that was observed with electrophysiology after application of similar drug cocktails was around 0.8 Hz., [19] faster than the frequency of dopamine transients. If these slow oscillations are related to the dopamine transients, than either the electrophysiological activity is averaged and encoded in a slower neurotransmitter release or that not every oscillation in firing of dopaminergic neurons leads to dopamine release in the nucleus accumbens. Additional experiments that involve simultaneous electrophysiological measurements of dopaminergic neurons activity in VTA combined with FSCV recording of dopamine release in nucleus accumbens would allow establishing relationship between slow oscillations and dopamine transients.

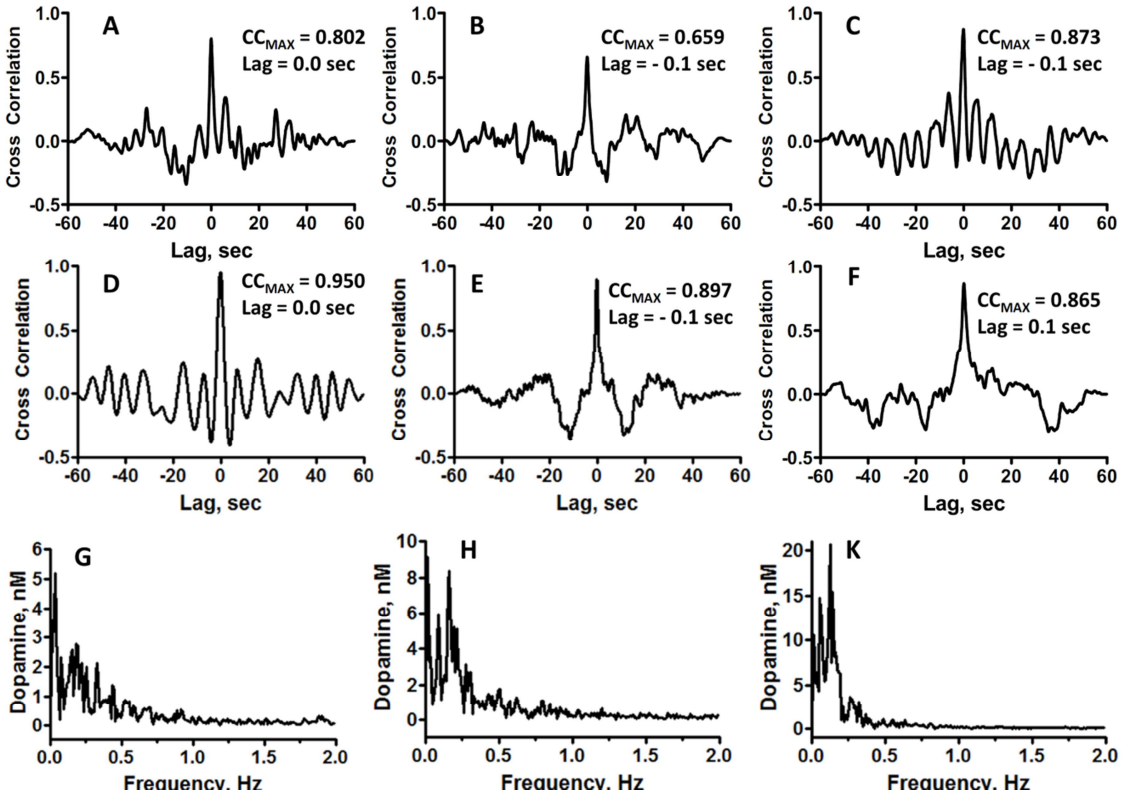


**Figure 6.5** Spectral analysis of the dopamine transients.

Cross correlation function for dopamine concentration traces in the left and right hemispheres after raclopride alone (A); raclopride + GBR-12909 (B); raclopride + cocaine (C); raclopride + ritalin (D); raclopride + amphetamine (E); raclopride + methamphetamine (F). Cross correlation values and lags are shown for the dominant peak in each case. Fast Fourier transforms of transients after application of raclopride alone (G); raclopride with cocaine (H); and raclopride with ritalin (K).

## CONCLUSIONS

In this chapter, dual electrode recordings in nuclei accumbens (core) of urethane anesthetized rats were used to characterize naturally acquiring and pharmacologically induced dopamine transients. Endogenous dopamine transients were observed even without application of drugs. Also, application of raclopride alone and raclopride with DAT blockers and psychostimulants induced transients in nuclei accumbens of both hemispheres. Furthermore, both endogenous and pharmacologically induced transients were synchronized in the time between hemispheres. It is likely, that these rhythmic dopamine transients are reflections of slow oscillations that exist in the cortex during sleep. They are slow than the oscillations in rhythmic firing of dopaminergic neurons that were observed under similar conditions using electrophysiological recordings. Additional investigation that involves simultaneous chemical sampling of dopamine release and electrophysiological measurements is necessary to establish the relationship between them.

These experiments provide an introduction to the integral understanding of dopaminergic signaling and a pathway for multielectrode voltammetric recordings in freely moving animals that can address challenging questions related to role of dopaminergic system in animal behavior.

## REFERENCES


1. DeFelipe, J., From the Connectome to the Synaptome: An Epic Love Story. *Science* 2010, 330, (6008), 1198-1201.

2. Sporns, O.; Tononi, G.; Kotter, R., The human connectome: A structural description of the human brain. *Plos Computational Biology* 2005, 1, (4), 245-251.

3. Biswal, B. B.; Mennes, M.; Zuo, X. N.; Gohel, S.; Kelly, C.; Smith, S. M.; Beckmann, C. F.; Adelstein, J. S.; Buckner, R. L.; Colcombe, S.; Dogonowski, A. M.; Ernst, M.; Fair, D.; Hampson, M.; Hoptman, M. J.; Hyde, J. S.; Kiviniemi, V. J.; Kotter, R.; Li, S. J.; Lin, C. P.; Lowe, M. J.; Mackay, C.; Madden, D. J.; Madsen, K. H.; Margulies, D. S.; Mayberg, H. S.; McMahon, K.; Monk, C. S.; Mostofsky, S. H.; Nagel, B. J.; Pekar, J. J.; Peltier, S. J.; Petersen, S. E.; Riedl, V.; Rombouts, S. A. R. B.; Rypma, B.; Schlaggar, B. L.; Schmidt, S.; Seidler, R. D.; Siegle, G. J.; Sorg, C.; Teng, G. J.; Veijola, J.; Villringer, A.; Walter, M.; Wang, L. H.; Weng, X. C.; Whitfield-Gabrieli, S.; Williamson, P.; Windischberger, C.; Zang, Y. F.; Zhang, H. Y.; Castellanos, F. X.; Milham, M. P., Toward discovery science of human brain function. *Proceedings of the National Academy of Sciences of the United States of America* 2010, 107, (10), 4734-4739.

4. Nicolelis, M. A. L., *Methods for neural ensemble recordings*. 2nd ed.; CRC Press: Boca Raton, 2008.

5. deCharms, C. R., Applications of real-time fMRI. *Nat Rev Neurosci* 2008, 9, (9), 720-729.

6. Cameron, D. L.; Wessendorf, M. W.; Williams, J. T., A subset of ventral tegmental area neurons is inhibited by dopamine, 5-hydroxytryptamine and opioids. *Neuroscience* 1997, 77, (1), 155-166.

7. Ungless, M. A.; Magill, P. J.; Bolam, J. P., Uniform inhibition of dopamine neurons in the ventral tegmental area by aversive stimuli.(Reports). *Science* 2004, 303, (5666), 2040(3).

8. Robinson, D. L.; Hermans, A.; Seipel, A. T.; Wightman, R. M., Monitoring Rapid Chemical Communication in the Brain. *Chemical Reviews* 2008, 108, (7), 2554-2584.

9. Zachek, M. K.; Takmakov, P.; Moody, B.; Wightman, R. M.; McCarty, G. S., Simultaneous Decoupled Detection of Dopamine and Oxygen Using Pyrolyzed Carbon Microarrays and Fast-Scan Cyclic Voltammetry. *Analytical Chemistry* 2009, 81, (15), 6258-6265.

10. Zachek, M. K.; Takmakov, P.; Park, J.; Wightman, R. M.; McCarty, G. S., Simultaneous monitoring of dopamine concentration at spatially different brain locations in vivo. *Biosensors & Bioelectronics* 2010, 25, (5), 1179-1185.

11. Zachek, M. K.; Park, J.; Takmakov, P.; Wightman, R. M.; McCarty, G. S., Microfabricated FSCV-compatible microelectrode array for real-time monitoring of heterogeneous dopamine release. *Analyst* 2010, 135, (7), 1556-1563.

12. Iversen, L. L.; Iversen, S.; Dunnett, S.; Bjorklund, A., *Dopamine Handbook*. Oxford University Press: 2009.

13. Guzman, J. N.; SÃ¡nchez-Padilla, J.; Chan, C. S.; Surmeier, D. J., Robust Pacemaking in Substantia Nigra Dopaminergic Neurons. *The Journal of Neuroscience* 2009, 29, (35), 11011-11019.

14. Surmeier, D. J.; Guzman, J. N.; Sanchez-Padilla, J., Calcium, cellular aging, and selective neuronal vulnerability in Parkinson's disease. *Cell Calcium* 2010, 47, (2), 175-182.

15. Steriade, M.; McCormick, D. A.; Sejnowski, T. J., Thalamocortical Oscillations in the Sleeping and Aroused Brain. *Science* 1993, 262, (5134), 679-685.

16. Sesack, S. R.; Grace, A. A., Cortico-Basal Ganglia Reward Network: Microcircuitry. *Neuropsychopharmacology* 2009, 35, (1), 27-47.

17. Murer, M. G.; Tseng, K. Y.; Kasanetz, F.; Belluscio, M.; Riquelme, L. A., Brain Oscillations, Medium Spiny Neurons, and Dopamine. *Cellular and Molecular Neurobiology* 2002, 22, (5), 611-632.

18. Shi, W.-X., Slow Oscillatory Firing: A Major Firing Pattern of Dopamine Neurons in the Ventral Tegmental Area. *Journal of Neurophysiology* 2005, 94, (5), 3516-3522.

19. Shi, W.-X.; Pun, C.-L.; Zhou, Y., Psychostimulants Induce Low-Frequency Oscillations in the Firing Activity of Dopamine Neurons. *Neuropsychopharmacology* 2004, 29, (12), 2160-2167.

20. Venton, B. J.; Wightman, R. M., Pharmacologically induced, subsecond dopamine transients in the caudate–putamen of the anesthetized rat. *Synapse* 2007, 61, (1), 37-39.

21. Park, J.; Aragona, B. J.; Kile, B. M.; Carelli, R. M.; Wightman, R. M., In Vivo Voltammetric Monitoring of Catecholamine Release in Subterritories of the Nucleus Accumbens Shell. *Neuroscience* 2010, 169, (1), 132-142.

22. Neve, K. A.; Neve, R. L., *The dopamine receptors*. Humana Press: 1997.

23. Cragg, S. J.; Rice, M. E., DAncing past the DAT at a DA synapse. *Trends in Neurosciences* 2004, 27, (5), 270-277.

24. Cahill, P. S.; Wightman, R. M., Simultaneous Amperometric Measurement of Ascorbate and Catecholamine Secretion from Individual Bovine Adrenal-Medullary Cells. *Analytical Chemistry* 1995, 67, (15), 2599-2605.

25. Paxinos, G.; Watson, C., *The rat brain in stereotaxic coordinates*. Academic Press/Elsevier: Amsterdam; Boston, 2007.

26. Michael, D. J.; Joseph, J. D.; Kilpatrick, M. R.; Travis, E. R.; Wightman, R. M., Improving data acquisition for fast scan cyclic voltammetry. *Analytical Chemistry* 1999, 71, (18), 3941-3947.

27. Kandel, E. R.; Schwartz, J. H.; Jessell, T. M., *Principles of neural science*. McGraw-Hill, Health Professions Division: 2000.

28. Pritzel, M.; Sarter, M.; Morgan, S.; Huston, J. P., Interhemispheric nigrostriatal projections in the rat: Bifurcating nigral projections and loci of crossing in the diencephalon. *Brain Research Bulletin* 1983, 10, (3), 385-390.

29. Heien, M. L. A. V.; Phillips, P. E. M.; Stuber, G. D.; Seipel, A. T.; Wightman, R. M., Overoxidation of carbon-fiber microelectrodes enhances dopamine adsorption and increases sensitivity. *Analyst* 2003, 128, (12), 1413-1419.

30. Takmakov, P.; Zachek, M. K.; Keithley, R. B.; Walsh, P. L.; Donley, C.; McCarty, G. S.; Wightman, R. M., Carbon Microelectrodes with a Renewable Surface. *Analytical Chemistry* 2010, 82, (5), 2020-2028.